Circular organic economy through insect biorefineries: Utilisation of organic compounds from *Hermetia Illucens* larvae for biomedical applications

YANTI BINTI PADLI

B.Eng., M.Eng.Sc (Malaya)

A thesis submitted to fulfil requirements for the degree of
Doctor of Philosophy

The research reported in this thesis was supported by the award of
a Research Training Program scholarship to the PhD candidate

School of Chemical and Biomolecular Engineering
Faculty of Engineering
The University of Sydney
Australia

2024

Originality Statement

I hereby declare that this thesis is presented to the School of Chemical and Biomolecular Engineering, Faculty of Engineering, The University of Sydney, to meet the requirements for the Doctor of Philosophy degree.

I affirm that, to the best of my knowledge, the content of this thesis is the result of my independent research. I confirm that the intellectual content presented in this thesis is my original own work with conceptualisation and supervision by my supervisor Prof Ali Abbas, and I have duly acknowledged all the assistance and sources utilised during its preparation.

Chapter 2 has been prepared as a manuscript for publication.

Parts of Chapter 3 and Chapter 4 have been filed for patent protection (Australian Provisional Patent Application Filed, reference number 2023903776, filed on 23 November 2023), and a draft manuscript stemming primarily from Chapter 4 has been prepared for publication.

Yanti Binti Padli

Authorship Attribution Statements

Parts of Chapter 3 and Chapter 4 have been filed for patent protection (Australian Provisional Patent Application Filed, reference number **2023903776**, filed on 23 November 2023), and a draft manuscript stemming primary from Chapter 4 has been prepared for publication.

For this patent submission, I co-designed the study, conducted the experiment, analyzed and interpreted the data with project supervisor Prof Ali Abbas. I drafted the manuscript and patent specification. The supervisor reviewed and edited the draft manuscript and the specification of the patent. Additionally, Dr. Gustavo Fimbres Weihs also reviewed the manuscript and patent specification.

Yanti Binti Padli

July 2024

As a supervisor for the candidature upon which this thesis is based, I can confirm that the authorship attribution statements above are correct.

Professor Ali Abbas

July 2024

Acknowledgement

In the name of Allah, The Most Gracious and The Most Merciful. Alhamdulillah, upon the completion of this research, I convey my deepest appreciation to the Almighty Allah. It is through His divine will and permission that I have successfully concluded this work.

Foremost, I extend my sincere gratitude to Professor Ali Abbas, my supervisor, for his unwavering support and continuous guidance throughout my doctoral study. I am also profoundly thankful to Dr. Gustavo Fimbres Weihs, whose invaluable advice, guidance, and feedback significantly contributed to the completion of this thesis. Without their steadfast support, this achievement would not have been possible.

I extend my gratitude to my lab colleague, Zachary Cohn, for his assistance in the early stages of my study and continuous support throughout my research, including handling BSFL, providing suggestions on various parts of my thesis, and offering technical support during my doctoral study. Then, to Sergio Londono, who assisted me in troubleshooting the SC-CO2 extractor machine and provided technical support during my doctoral study.

Special thanks to Dr. Nicholas Proschogo for his assistance in performing GCMS analysis and providing technical support and meaningful advice in data analysis. I also express my appreciation to Dr Helen Wang, technical officer of the Solid State & Elemental Analysis Unit at Mark Wainwright Analytical Centre, for their assistance in sample analysis. Additionally, I would like to thank Dr Samuel Duyker, a professional officer in powder diffraction from Sydney Analytical, for his assistance in the XRD sample analysis. Thank you for dedicating your time and efforts to support me in data analysis.

Gratitude is extended to Dr. Yogambha Ramaswamy for her instrumental assistance in designing experiments for cell culture and analysing my data. I offer immense thanks to Dr. Aklima Nasrin for her training and guidance in familiarising myself with the cell culture

experiment, and to Dr. Md Hassan for advice and suggestions related to the cell culture study.

I had the pleasure of being part of the School of Chemical and Biomolecular Engineering at the University of Sydney. A special thanks to Elizabeth Dobrinsky for helping me with any procurement item, Dr Rachel Xia Zhong, Dr Tino Kausmann, Nancy and to all the beautiful colleagues I met throughout my PhD years.

Special appreciation goes to Amira Farzana Samat, my lab buddy, for constantly listening to my daily thoughts and concerns and helping me with some of my work lab. Words cannot express my gratitude for your attentiveness and thoughtfulness. Your unwavering support throughout this journey has been inspiring, and I wish you all the best in your future endeavours. I would also like to express my thanks to Hawra Elhossaini, Shymma Rahem, Dr Ivan Kristianto, Dr Mona Hamad, Phebe Kristania Samrani and Zhe Gong (George), as well as all my friends, for their supportive presence throughout this challenging journey. My heartfelt thanks are extended to everyone who contributed directly and indirectly to the success of this project.

Finally, and of utmost significance, I extend profound gratitude to my family, particularly in memory of my late mother and my cherished husband, T M Indra Mahlia, along with my beloved children, Cut Alya and Itzhak. Their unwavering support and understanding throughout this doctoral study have been indispensable. Without their love and blessings, all endeavours would have been futile. This study was conducted under the Engineering Research Scholarship (ERS) from the Faculty of Engineering at The University of Sydney.

Abstract

Food waste is a critical global issue contributing significantly to methane emissions, which is a potent greenhouse gas. Addressing this issue requires innovative solutions, such as adopting a circular economy approach to valorise food waste. This thesis evaluates the use of Black Soldier Fly larvae (BSFL) for the bioconversion and valorisation of organic waste. BSFL can efficiently convert low-value organic waste into high-quality lipids, proteins, and chitin. It focuses on the use of supercritical carbon dioxide (SC-CO2) for extracting valuable products like BSFL oil and chitin and investigates potential biomedical applications for these products. An in vitro test is conducted to assess the cytotoxicity of BSFL lipid for biomedical applications. Chitin and chitosan are obtained from the defatted BSFL using SC-CO2, followed by hydrolysis to remove minerals and proteins. Additionally, a chitosan-based hydrogel has been synthesized to demonstrate its potential application in biomedicine.

SC-CO2 is used to extract high-value oils from BSFL, and this method is compared against traditional solvent extraction. A response surface modelling (RSM) approach is used to optimise the SC-CO2 extraction conditions by examining the effect of temperature (30 – 50 °C), pressure (150 – 400 bar), and extraction time (1 – 3 hours) on larval oil recovery (lipid yield %), fatty acid composition (mainly lauric acid), and the ratio of saturated fatty acids (SFA). The SC-CO2 extraction is found to outperform conventional solvent extraction across all measured responses, significantly improving the SFA concentration ratio.

When maximising larval oil recovery, the SC-CO2 extraction method achieves a recovery of 35.6%, which is 5.6% higher than solvent extraction, when extracting for 2.2 hours at 366 bar and 43 °C. Moreover, a multi-objective optimisation leads to a combined maximum larval oil recovery of 30.1%, maximum lauric acid content of 52.0 g/100g, and a minimum

SFA ratio concentration of 5.0, achieved under SC-CO2 conditions of 400 bar, 46.8 °C, and 1.4 hours of extraction time. This optimisation method can also target extraction of fatty acids from BSFL, achieving a better SFA ratio by manipulating SC-CO2 process conditions.

Lipids extracted from BSFL using SC-CO2 are rich in lauric acid, beneficial for cell migration, wound healing, and antibacterial applications. These lipids are safe, non-cytotoxic, and valuable within the circular economy. BSFL is also a source of biopolymers, chitin and chitosan, with alpha chitin forming about 5% of the dry matter of the BSFL and being biodegradable. This study highlights the use of BSFL-derived chitosan for hydrogels, exhibiting unique properties. Hydrogels with higher gelatin content have a 288% swelling ratio and degrade significantly, while those with more chitosan degrade slower and have a 137% swelling ratio. These chitosan-based hydrogels are promising for wound dressings, tissue scaffolds, and drug delivery.

This thesis shows that SC-CO2 extraction is a promising method for enhancing the conversion of low-value waste to high-value biomedical resources. This SC-CO2 method can also be scaled up for industrial use, enhancing the circular economy performance of organic waste resources and creating new businesses and markets for BSFL products and by-products. By utilising innovative SC-CO2 extraction techniques, this study offers an environmentally friendly solution for mitigating food waste and producing valuable resources. Integrating BSFL into waste management fills an important gap in resource recovery systems and contributes to a more sustainable and circular future. This offers a model for circular economies globally that could revolutionise food waste management.

Table of Contents

List of Figures

List of Tables

CHAPTER 1: INTRODUCTION

Food production, or more specifically, food waste generated from daily human requirements, has had a negative effect on the environment. According to the United Nations, food, energy, and water are the building elements of sustainability. The need for all three has risen rapidly as the world's population has grown, which is directly proportional to the quantity of food, clean water, and energy used. Traditional methods of energy production also require significant amounts of fresh water. Nonetheless, the agricultural sector has been identified as a potential interconnected energy source [1].

All countries can take more positive environmental measures to address the problem of food waste by reducing, reusing, and recycling using a circular economy model. These approaches can enable new business models to generate financial advantages while contributing to a better world. Agriculture is responsible for almost a quarter (26%) of worldwide greenhouse gas emissions, approximately half of the world's liveable land, 70% of the world's freshwater use and, ultimately, much of the worldwide ocean and freshwater eutrophication pollution [2, 3]. In light of this, food and agriculture significantly contribute to environmental impacts and require special attention. The circular economy has become a trend today to replace the conventional linear economy that has created enormous amounts of waste and is harmful to the environment. Recently, the circular economy has been suggested as a solution to adverse environmental impacts by utilising the biological cycle of food waste.

It is believed that food system activities, such as producing food, transporting food, and storing or dumping wasted food in landfills, produce greenhouse gases that cause climate change [4]. The cost of managing waste has become an enigma for some municipalities worldwide. While food waste is one of the most significant challenges, the exact amount of

food wasted by retailers and individual consumers is yet to be quantified. There are many aspects of relevance within the circular economy's biological and technical cycles. One of the biological cycles of a circular economy is organic waste valorisation by Black Soldier Fly Larvae (BSFL), as shown in **Fig. 1.1**.

Fig. 1.1: Business as usual vs. circular economy for organic waste by BSFL utilisation.

Many technological solutions have been developed to address this issue, with insect bioconversion of side streams as one of the most inventive technologies for waste management, particularly for food waste [5]. Among the proven ways is to use insects to process food waste into something useful, one of the popular candidate species is Hermetia illucens, more commonly known as the Black Soldier Fly (BSF) [6]. This insect has spread all over the world from its native habitat in the Neotropical realm. BSF is found across Europe, the United States, and the Krasnodar Territory on Russia's Black Sea coast [7-9]. It can also be found in the Afrotropical, Australasian, East Palaearctic, Nearctic, North African, Southern African, and Indomalayan realms [10-14]. BSF is a mimetic fly, in size, colour,

and appearance, very similar to the wasp dauber and its family. The BSF Larvae (BSFL) may be distinguished from the larvae of speckled flies by a fine grey-black band on their posterior extremities. Based on the food given to the larvae, the larvae stage may last somewhere from 18 to 36 days [15], and the post-feeding (pre-pupal) stage lasts about 7 days [16]. The pupal phase lasts between one and two weeks [17]. If given water and sustenance, such as nectar in the wild or sugar in captivity, adults may survive for 47 to 73 days on average [15, 18], or 8 to 10 days on accumulated fat stores during the larvae stage if water is available [17]. One of the most significant benefits of utilising BSFL as a waste bio converter is that, they do not feed as adult flies, which means there's no danger of disease transmission [19]. Therefore, there are many patented innovations reported in the use of BSFL in food or agricultural waste, and the value-added products from this process, specifically in the World Intellectual Property Organization (WIPO) database. These innovations guide the objectives of this thesis.

1.1.Background

Scientists have worked on identifying edible insect species with (i) straightforward rearing processes, (ii) availability in regular supplies and no/minimal risk of overexploitation with farming, (iii) high sustainability, (iv) economically friendly costs so consumers would be encouraged to purchase in place of other meats, and (v) desirable taste and texture. One insect of high interest is the BSF, *Hermetia illucens*, a true fly (Diptera) of the Stratiomyidae family [20]. Based on the new market research by Meticulous Research, the global BSFL market will develop at a 33.3% compound annual growth rate from 2019 to 2030, reaching US$2.57 billion in a decade.

This is why BSFLs are ideal for use in the organic circular economy, and this research aims to learn more about patent innovation and technological advancements related to the end product of this fascinating species. The chemical and enzymatic extraction and their various products of BSFL are tabulated in **Table 1.1**. The example of the implementation of the circular economy for organic waste via BSFL utilisation is presented in **Fig. 1.2** (modified from [21]). The economic assessment of BSFL conversion to valuable resources is given in Table 1.2. [22]

Table 1.1: Type of extractions and various products of BSFL.

Feeding Substrate	**Extraction**	**Protein***	**Lipid***	**Chitin***	**Refs.**
Unknown	Chemical	32%	37%	9%	[6]
Bread, fish & mussels	Chemical	34%	37%	-	[23]
Unknown	Enzymatic	-	7%.	-	[24]
Unknown	Enzymatic	42%	21%	7%	[25]
Fruit & vegetable	Chemical	37%	33%	-	[26]
Waste coconut	Chemical	53%	19%	-	[27]
Fermented waste Coconut	Chemical	58%	15%	-	[28]
Soybean curd residue	Chemical	53%	26%	-	[29]
Unknown	Enzymatic	-	10%	3%	[6]
Unknown	Enzymatic	67%	10%	-	[30]

*Average

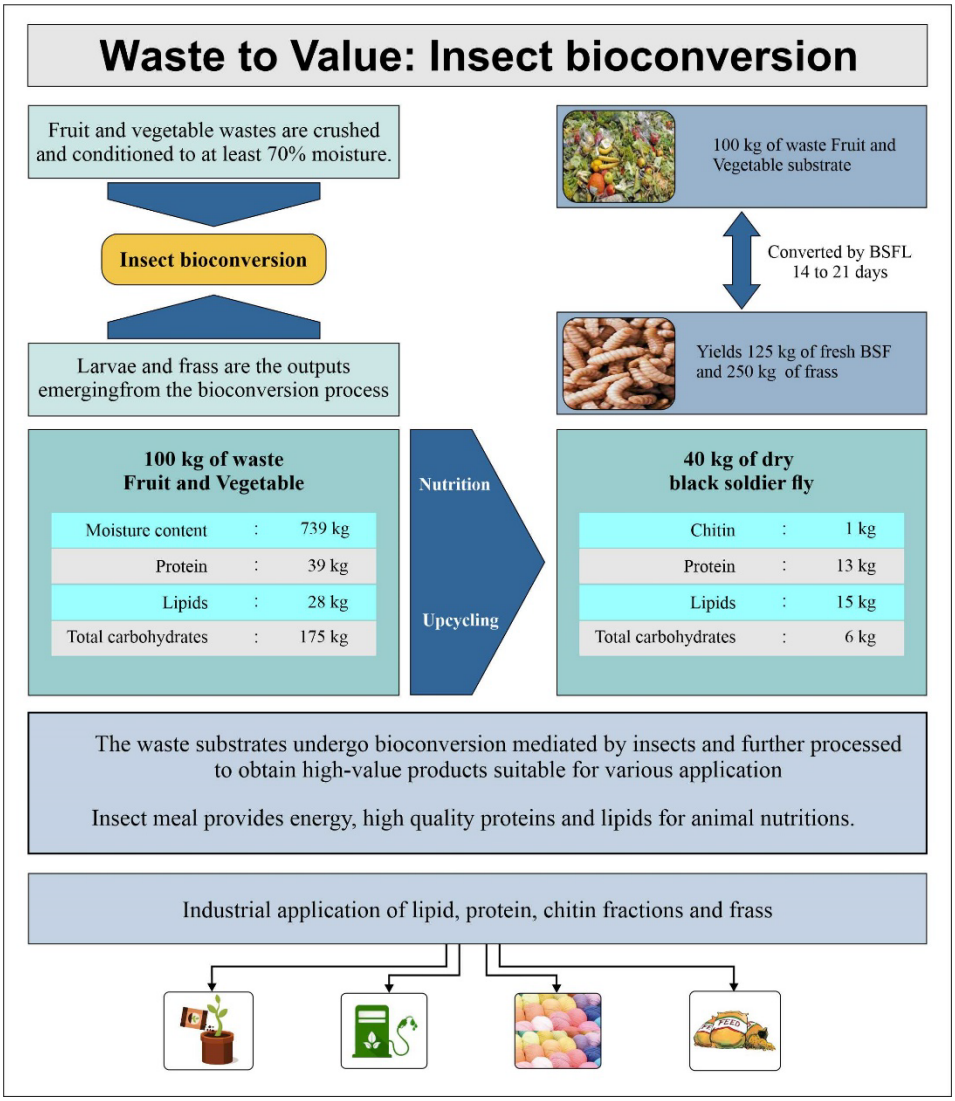

Fig. 1.2: Material balance of utilisation of BSFL to convert waste to valuable resources.

Table 1.2: The economic assessment of BSFL conversion to valuable resources [22].

Descriptions	Amount (kg)	Price per Unit (AU$/kg)	Total Cost/Revenue (AUD)
Inputs			
Waste Fruit and Vegetables	100	0.15	15
Outputs			
Fresh BSFL (converted to dry BSFL)	40	37.50	1500
Frass (insect manure)	250	0.075	18.75
Chitin	1	75	75
Protein	13	7.50	97.50
Lipids	15	45	675
Total Revenue			*2,366.25*
Costs			
Waste Fruit and Vegetables	100	0.1	15
Processing and Labor	-	-	300
Total Costs			*315*
Net Profit			*2,051.25*

*The prices are converted from GB£ to AU$

Due to the commercial feasibility of SC-CO2 extraction, this technique is extensively utilised by various industries, such as food and beverage industries, to decaffeinate coffee and extract essential oils from spices, due to the high quality and efficiency of the result it produces [31]. Other commercial uses are to extract bio-reactive compounds from herbal and other natural sources in pharmaceutical industries, as well as high-purity fragrances and flavours [32]. In the cosmetics industry, this method is utilised to produce a fine purity of ingredients of cosmetics substances like antioxidants, oil and waxes from plants and other natural resources. These are some benefits compared to conventional methods; it's non-toxicity and the ability to preserve the initial profile of the substances being extracted. This continuing technological development, combined with the high market demand for pure and high-quality substances, can create economic feasibility for SC-CO2 extraction.

Several research projects have extensively examined the use of supercritical carbon dioxide (SC-CO2) to extract useful components from insects. The thoroughly analysed parameters, including pressures, temperatures, extraction periods, flow rates, and the major discoveries linked with SC-CO2 extraction for a selected insect species, are tabulated in Table 1.3.

1.2.Research gap

Municipalities in various countries worldwide are concerned about increasing waste generation due to population growth and unsustainable consumption patterns. Waste production has risen tenfold in the past century and is projected to double by 2025 [33]. To reduce the problem, the bioconversion of side streams by insects is one of the most creative waste management technologies, particularly for food waste [5]. BSFL, also known as *Hermetia illucens* larvae, can convert trash into biomass while maintaining a healthy environment. One of the most significant benefits of employing BSFL as waste bio-converters is that adult flies do not feed, thus there's no danger of disease transmission [19]. BSFL has been proven to be a good resource of nutrients, such as protein, lipids, and minerals. The BSFL comprise 32% protein, 37% lipids, 19% minerals, and 9% chitin, as measured by dry weight [6]. BSFL have been utilised as a feed component for various animals, including chicken, fish, and pet food, due to their high protein content. Furthermore, some scientists recently experimented with larvae fat to replace butter in waffles, cakes and cookies, claiming the fat from insects is more sustainable and environmentally friendly than the dairy version, and taste testers cannot tell the differences [34].

Large amounts of fat in the larvae have also been exploited to produce biodiesel from the BSFL biomass [35-37]. The other compound constituting BSFL's dry weight is chitin, which, after cellulose, is the second most prevalent biopolymer on the planet. Because of its

intriguing characteristics and prospective uses, chitin and its primary derivative, chitosan, have considerable commercial worth. Numerous utilisation of chitosan have been identified, for example, in biomedical areas used for wound healing and tissue regeneration, agriculture, food safety, cosmetics, papermaking, textiles, and wastewater treatment are just a few of the industries that use chitin and chitosan [38].

The method for extracting lipids has been established in the past, and it typically involves large amounts of organic solvents and lengthy extraction processes, which often result in the thermal destruction of discarded molecules and poor product quality [39]. Moreover, using organic solvents will raise concerns about environmental pollution, health safety, and product contamination with solvent residue [39, 40]. Thus, using environmentally benign methods to extract lipids from BSFL is critical for promoting long-term customer desire for healthy and sustainable living.

Supercritical carbon dioxide extraction (SC-CO2), deemed a 'green' process, is a favourable technique to the environment and can be an alternative for effective extraction of the natural bioactive compound from natural matter such as lipids or oil. Carbon dioxide is cheap and non-toxic, non-explosive, easily obtain at high purity, easily removed from the extracted product, and offers various solvent properties at different pressures and temperatures [41]. The SC-CO2 critical temperature and pressure are relatively low, at 31.1°C and 7.2 bar. It is an excellent solvent for extracting thermally sensitive compounds since extraction is feasible at ambient temperature [41].

Response surface modelling (RSM) has been used to optimise experimental conditions and study crucial process factors with fewer experimental trials because it offers an efficient statistical approach [42]. Optimisation of extracted yields from insects using RSM was reported recently but only for sorghum bug and silkworm species and at ideal circumstances

[43]. For the BSFL oil product, there is still no information regarding the SC-CO2 extraction parameters, composition, or physicochemical characteristics, nor is there an analysis of fatty acids compared to the oil yield and composition of insects and vice versa.

Table 1.3: Lipid extraction of some insects using the SC-CO2.

Insects	SC-CO2 Condition				Method/Solvent	Fat/Lipid Content	Lipid Characteristic	Refs.
	Temp	Pressure	Time	CO2 Flowrate				
Black Soldier Fly larvae	35°C	350 bar	6 hours	26 l CO2/h.	Hot water treatment	Defatting almost 95% of total fat from the BSF Larvae	7 fatty acids composition which is palmitic acid, stearic acid, oleic acid, linoleic acid, linolenic acid, arachidic acid and docosanoic acid	[44]
Mealworm Beetle Larvae	45°C	400/250 bar	105 mins	20 kg/h	Hexane	Defatting almost 95% of total fat from the TML	Unsaturated fatty acid (72%) and Oleic acid (42%) of total FAME in the fat contents	[43]
Oak Silkworm pupae	35 °C	280 bar	1.83 hours	20 L/h	N/A	Total fat is 26.18%	8 fatty acids, unsaturated fatty acids (77.29%) alpha-linolenic (ALA) (34.27%)	[45]
Crickets	50 °C	250 bar	45 mins	1.0 kg/h	Methanol	The dry weight fat is 12%	Unsaturated fatty acids: 60-80% (e.g., oleic acid 20-30%, linoleic acid 15-25%, alpha-linolenic acid 1-5%) Saturated fatty acids: 10-20% (e.g., palmitic acid)	[46]
Termites	47	290 bar	75 mins	1.7 kg/h	Ethanol	The dry weight fat is 17%	Unsaturated fatty acids: 40-60% (e.g., linoleic, oleic, and alpha-linolenic acids) Saturated fatty acids: 30-40% (e.g., palmitic and stearic acids)	[47]

Therefore, this study attempts to fill in the knowledge gaps in investigating the optimisation of BSFL oil extraction using the response surface modelling (RSM) method for SC-CO2 extraction. The objectives include enhancing the yield of larvae oil, optimising the fatty acid composition, and controlling the concentration of saturated fats. Overall, these objectives highlight the study's contributions to closing current research gaps in the areas of developing new materials for diverse industrial and biological applications, extracting and exploiting valuable by-products, and using BSFL for the sustainable management of organic waste as follows:

- Evaluating BSFL in Organic Circular Economy: This study explores BSFL use in reducing the environmental impact of food waste, contributing to the organic circular economy. It addresses the lack of thorough research on BSFL in waste management and their role in a closed-loop biological cycle.
- Comparative Study of Extraction Techniques: This study examines the efficiency and environmental impacts of chemical versus enzymatic extraction methods for BSFL-derived products, providing clarity on the best approach regarding environmental friendliness, cost, and efficacy.
- Patent Trends and Innovation in BSFL Technology: A comprehensive analysis of patents related to BSFL in waste management is conducted. This thesis assesses these patents' geographic distribution and subject matter, and notes trends in patent publications.
- Optimising SC-CO2 Extraction for BSFL Products: The thesis contributes to optimising SC-CO2 extraction parameters for BSFL oil recovery and compares its effectiveness with conventional solvent extraction.

- Analysing BSFLO's Cytotoxicity: Research into the cytotoxic effects and potential applications of BSFL Oil (BSFLO), especially in regenerative medicine, was conducted. The study tested BSFLO on 3T3 cells for its wound healing potential.
- Chitin and Chitosan Characterisation and Comparison: This research fills the gap in the comprehensive characterisation and comparison of chitin and chitosan from BSFL with traditional sources, like prawn chitosan.
- Creation of Chitosan-based Hydrogels: This study explores the development of chitosan-based hydrogels using chitosan derived from BSFL, examining their properties and potential biomedical applications.

1.3.Objectives of the study

The main objective of this study is to develop the circular organic economy through insect biorefinery - Utilisation of organic compounds from *Hermetia Illucens* larvae, focusing on the circular technical basis of transforming waste into a valuable and high-quality product, which leads to economic analysis. Meanwhile, the comprehensive objectives of the study are summarised as follows:

- To analyse patented innovations related to utilising BSFL in food or agricultural waste and examine the resulting value-added products using the World Intellectual Property Organization (WIPO) database.
- To extract and optimise the yield, fatty acid composition, and concentration of saturated fats in BSFL oil through SC-CO2 extraction using response surface modelling (RSM).
- To assess the cytotoxicity of BSFL oil through in-vitro testing, specifically focusing on its high lauric acid content and potential applications in wound healing and cosmetic.

- To investigate the impact of SC-CO2 extraction on the isolation of chitin and chitosan from BSFL and characterise these biopolymers.
- To examine the synthesis of a chitosan-based hydrogel extracted from BSFL, incorporating gelatine and crosslinking it with glutaraldehyde for biodegradable and biomedical purposes.

1.4.Contribution of the research

The research contributes significantly to sustainable waste management and resource recovery by exploring the use of BSFL in the context of a circular economy. Key contributions include:

- Developing a sustainable solution for food waste management using BSFL, reducing methane emissions and recovering valuable resources.
- Advancing green extraction methods, particularly SC-CO2 extraction, outperforming conventional methods in recovering larval oil with a better saturated fatty acid ratio.
- Optimising SC-CO2 extraction parameters through response surface modelling, improving the efficiency of valuable component recovery like lauric acid.
- Analysing patent technology in BSFL applications, providing insights into global innovation trends, including submitting part of this research for an Australian Provisional Patent under application number 2023903776.
- Exploring the biomedical potential of lipids and chitin from BSFL, especially in wound healing, offers a sustainable medical material source.
- Developing chitosan-based hydrogels from BSFL for potential use in wound dressings and tissue engineering.

- Supporting the circular economy by integrating BSFL into waste management, reducing food waste's environmental impact and enabling resource recovery.
- Addressing economic and environmental concerns related to food waste, proposing a solution with economic and ecological benefits.

In summary, the research presents a comprehensive study that addresses a significant environmental issue and offers practical, sustainable solutions with potential for wide-ranging applications in waste management and resource recovery.

1.5.Thesis Structure

The thesis is structured into eight chapters, each serving a distinct purpose: Chapter 1 provides an introduction, Chapter 2 conducts a comprehensive literature review, Chapter 3 outlines the research methodology employed, Chapters 4, 5, 6 and 7 present the results and corresponding discussions, and finally, Chapter 8 offers the conclusion and recommendations. The detail of every chapter as follows:

Chapter 1 introduction begins with a background, outlining the study's context and its significance. Next, showing unknown areas in the body of existing literature indicates the research gap. The study's goals are outlined in the objectives, flowing from research contribution, and outlining how the study advances the field's understanding or contributes new perspectives. The thesis structure is finally described, giving a quick rundown of the topics and arrangements of the ensuing chapters.

Chapter 2 presents a literature review, starting with an introduction to the circular organic economy and the role of BSFL in waste bioconversion. It examines food waste management and its ecological implications. The chapter then examines the use of black soldier passes for waste conversion, including the biology and life cycle of the larvae. Various products

derived from the larvae, such as lipids, lauric acid, proteins, chitin, chitosan, and minerals, are explored for their properties and applications. The chapter concludes with a discussion on extraction methods, comparing chemical and enzymatic techniques. This section sets a foundational understanding of the study's focus on sustainable waste management using BSFL as well as patent search and review.

Chapter 3 presents the materials and methods of the study. It includes details on SC-CO2 extraction, cell culture, chitin and chitosan extraction materials, and hydrogel synthesis. The procedures cover lipid extraction and optimisation, cell culture tests, chitin and chitosan isolation, their characterisation using techniques like FTIR and SEM, and hydrogel synthesis and analysis. The chapter also emphasises the importance of rigorous statistical analysis to validate the research findings.

Chapter 4 examines the extraction and optimisation of lipids from BSFL using supercritical carbon dioxide (SC-CO2) extraction. It starts with an overview of the materials and methods used. The chapter then presents results and discussions on various aspects: it analyses solvent extraction effectiveness, delves into response surface analysis for parameter interactions, and discusses the optimisation of SC-CO2 extraction parameters. The chapter compares SC-CO2 with solvent extraction, focusing on efficiency and lipid quality, and assesses the impact of SC-CO2 on fatty acid composition. It also explores how SC-CO2 conditions can be adjusted for specific fatty acid extraction. This chapter provides a comprehensive study of lipid extraction from BSFL, highlighting the efficiency and benefits of using SC-CO2 extraction.

Chapter 5 This chapter encompasses the characterisation of BSFLO, emphasising its lauric acid and 2-monolaurin content, known for promoting cell growth and repair. Beginning with the assessment of acid value and free fatty acid content, the research employs Fourier-

Transform Infrared (FT-IR) analysis to unveil the molecular composition of BSFLO. The investigation then shifts to identifying optimal BSFLO concentrations for cell activity, considering pH changes in the culture media and potential cytotoxic effects. Delving into the dynamics of cell growth, the study explores the influence of different BSFLO concentrations on 3T3 cell proliferation over time. Furthermore, it examines the presence of a lipid layer in the culture media and its impact on cellular respiration. Finally, the research extends to practical applications, assessing BSFLO's potential in wound healing through a scratch test. This comprehensive approach aims to unravel the multifaceted impact of BSFLO, contributing insights for its integration into diverse industries.

Chapter 6 covers the isolation and characterisation of chitin and chitosan from BSFL. It outlines the extraction process and presents results on the quality and yield of the compounds. The chapter includes analyses using Fourier Transform Infrared (FTIR) spectroscopy, elemental analysis, and determination of the degree of acetylation. Thermogravimetric analysis (TGA) assesses their thermal stability, and Scanning Electron Microscopy (SEM) and X-Ray Diffraction (XRD) provide insights into their morphology and crystallinity. This chapter offers a detailed examination of the properties and potential of chitin and chitosan from BSFL.

Chapter 7 discusses creating and evaluating a novel chitosan-based hydrogel for biomedical uses. It begins with the methodology of hydrogel preparation and then details its characterisation, including structure and composition. The chapter includes an FTIR analysis for chemical understanding, examines the hydrogel's thermal properties for stability, and conducts swelling and biodegradation tests to assess its suitability for biomedical applications, such as drug delivery and wound healing. This chapter offers a concise yet comprehensive insight into the potential of this chitosan-based hydrogel in medical contexts.

Chapter 8 summarises the thesis concisely, covering the efficient SC-CO2 lipid extraction from BSFL, the safety of BSFL oil, and the properties of chitin and chitosan extracted from BSFL. It also highlights the potential biomedical uses of chitosan-based hydrogel. The chapter concludes with recommendations for further research in BSFL-derived products and their applications.

CHAPTER 2: LITERATURE REVIEW

2.1. Introduction

The global demand for proteins, lipids, and chitin, essential for nutrition, biodiesel production, and various medical applications, is rapidly increasing. Organic waste, particularly food waste, presents a potential resource to meet this demand [48]. However, the environmental impact of food production and the resultant waste is a significant concern. Human activities, including those related to food production, are major contributors to climate change, which is already affecting numerous nations [49]. Food production processes are highly water-intensive, contributing to environmental stress [50]. Agriculture alone accounts for about 26% of worldwide greenhouse gas emissions, amounting to 13.7 billion tonnes of CO2 annually. It also utilises 50% of the planet's habitable land and 70% of its freshwater resources while contributing to 78% of eutrophication in oceans and freshwater quantities [51]. Given this, food and agriculture play a significant environmental impact and need particular attention. The impact of food and agriculture on the environment can be seen in more detail in **Fig. 2.1** and **Fig. 2.2** depicts the worldwide greenhouse gas emissions associated with food production (draw based on [2]).

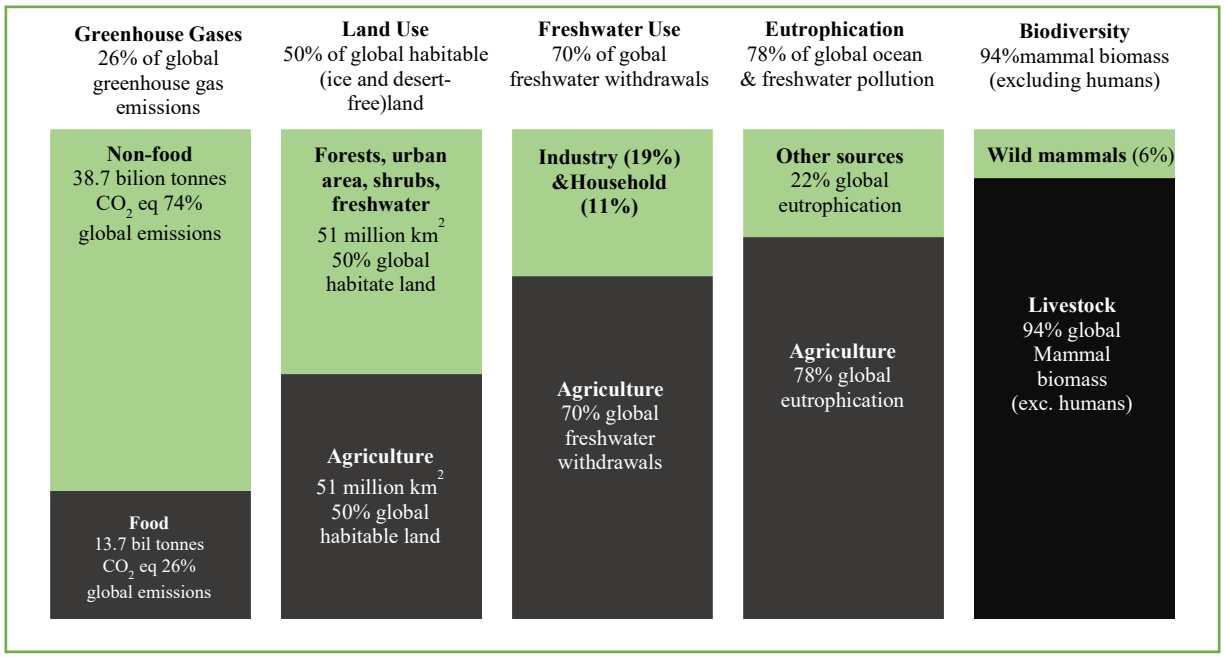

Fig. 2.1: Effects of food and agriculture on the environment.

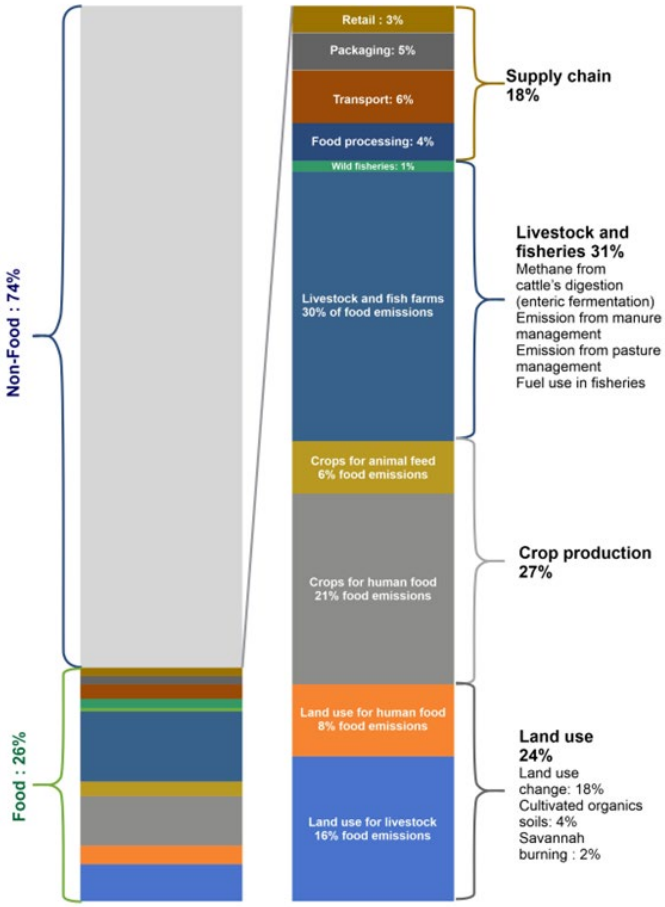

Fig. 2.2: Greenhouse gas emissions in food production worldwide.

Several scientists are looking closer at the link between food production and climate change [52-55]. Food system operations, such as food production, transportation, and storage or disposal of wasted food in landfills, emit greenhouse gases that contribute to climate change. As a result, the food industry is at the crucial initiatives to fight climate change, decrease water shortage, minimise pollution, restore forest or grassland regions, and conserve biodiversity throughout the globe [4].

Rapid population growth has contributed to a substantial increase in waste production globally. In the last century, waste generation has escalated tenfold and is projected to quadruple by 2025 [33]. This surge has significantly escalated waste management costs, posing challenges for many communities worldwide. Food waste represents one of the most critical waste categories. By 2050, global calorie waste is expected to nearly triple, with per capita food waste rising by 72%, equivalent to 812 kcal per year [56]. In response to this issue, innovative technological solutions have been developed, notably the bioconversion of waste by insects. This approach is particularly revolutionary in managing food waste [5]. It enhances the environmental appeal of products and positively impacts the economy by creating new business opportunities. Implementing a circular economy in the food sector could generate substantial economic benefits, yielding up to US$2.7 trillion annually [57]. This is achieved through reducing food waste, developing value-added by-products, and fostering health and environmental benefits.

2.2.Circular organic economy

For billions of years, living systems have survived without the creation of landfills. Instead, species feed on one another’s waste, 'dead' material returns to the earth, and the cycle continues [58]. Conversely, humans have adapted a more linear economic model for mass industrial production of food and other consumables: the "take-make-use-dispose"

paradigm. This implies that raw materials are gathered, processed, used, and discarded, creating a landfill. With each production procedure, humans are not only using up *finite* natural resources, but are also creating environmental pollution: water, soil, and air pollution, loss of biodiversity, and agricultural land depletion [59]. Therefore, the circular economy (CE) concept is a new and trending paradigm of sustainability that replaces the linear economy of "take-make-use-dispose" by using materials in a closed-loop system. According to the Ellen Macarthur Foundation, which has done significant work in this field, the CE is a structured economic process that benefits all stakeholders: humanity, companies and manufacturers, and the environment [60]. However, there remains ambiguity around correctly defining a CE, such that it needs to be more clearly distinguished from recycling, as illustrated in **Fig. 2.3** [61].

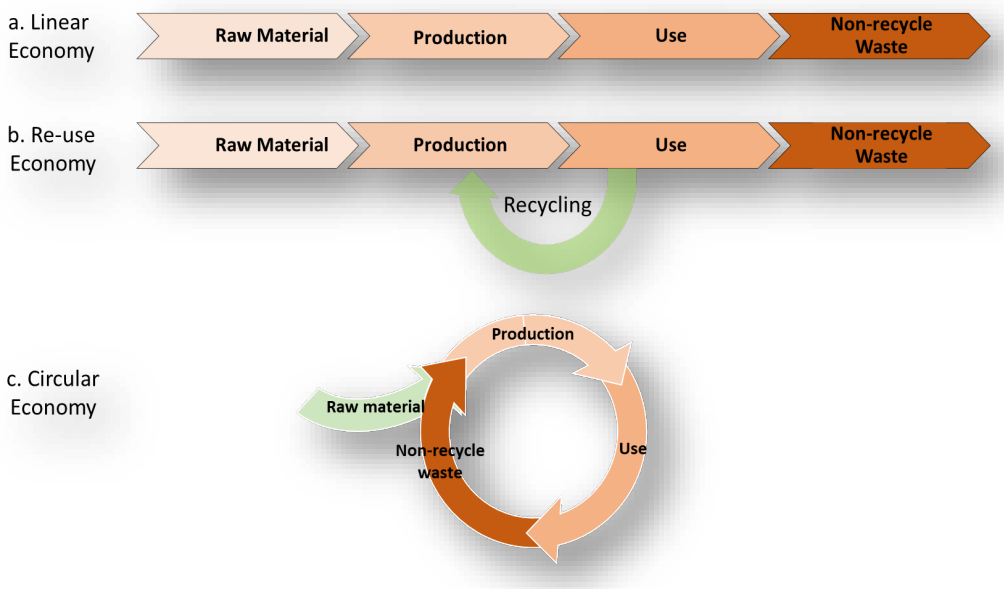

Fig. 2.3: From linear towards circular economy (**a**) Linear economy: raw materials are extracted from the earth, used, and discarded: "take-make-waste" (**b**) Re-use economy: many non-recycled materials reused again (cascading, repair/maintenance, remanufacturing, recycling) (**c**) Circular economy: Raw materials are never depleted [61].

Recycling is the process of either: (i) recycling raw material into the same raw material (e.g. a glass bottle is recycled into a glass bottle over and over), (ii) the downcycling of raw materials into a lower grade raw material where reuse in any form is no longer possible, (iii) the upcycling of raw materials so that the end product is of higher quality and value than the original [62]. Mechanical and chemical recycling provide many advantages for the environment, such as the decrease of raw material and agricultural land exploitation, the reduction of greenhouse gas emissions due to less energy requires, the decline in the amount of incinerated waste, and it also creates employment opportunities [62]. Nevertheless, this process is still finite and depends entirely on raw materials being used in the first place, Many materials cannot be recycled at all, and most recycled materials are downgraded during the process [63]. The solution is adopting a CE principal where the source of the material itself is sustainable.

The circular economy concept is now trending and, although not new, it has more recently come into the spotlight. Researchers believe the correct meaning has been blurred, and it now holds several classifications; a study analysed a then-existing 114 definitions to the circular economy concept [64]. Their findings show that CE is typically portrayed as a collection of activities like reduce, reuse, and recycle. The definitions analysed also reveal few specific connections between the circular economy and sustainable development, according to the authors. They conclude that the circular economy's primary goal is economic development with environmental quality while having an impact on social equality. By doing so, the world's limited resources can be conserved, and the negative environmental effect of manufacturers would potentially be reduced. This study specifically focuses on food waste, where a closed-loop biological system of organic waste

bioconversion using BSFL can be achieved. The circular economy for organic waste via BSFL is depicted in **Fig. 2.4**.

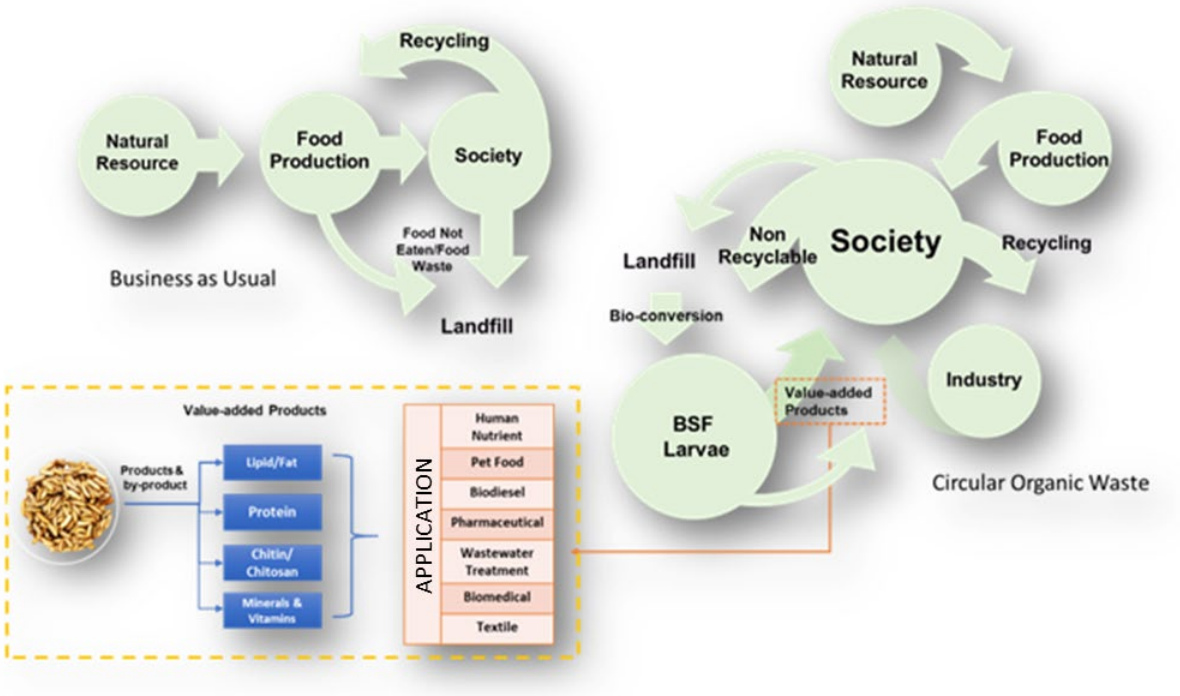

Fig. 2.4: Circular economy for organic waste by BSFL utilisation.

2.3.Food waste

Food waste is defined as food that has been prepared for human consumption but has not been eaten [65]. The actual amount of food lost by merchants and individual customers is still unknown, but it is estimated that 1.3 billion tonnes of food is lost from primary production to final consumption and that food production accounts for almost a quarter (26%) of greenhouse gas emissions of world [66, 67]. Approximately one-quarter of all calories generated on the planet are squandered, discarded in supply networks, or thrown away by retailers, restaurants, and consumers [68]. Most developing nations only utilise a

handful of ways to dispose of food waste, such as landfills, incineration, composting, anaerobic digestion, and animal feed [69-73]. Dumping or landfilling are the most common methods of food disposal in cities worldwide. Food waste disposed of in landfills is understood to decompose under anaerobic circumstances, releasing methane, a powerful greenhouse gas. Compared to CO_2, methane generated by food waste in landfills has a 28-fold effect on global warming [74]. The entire amount of waste generated in 2016 and estimated increases by 2030 and 2050 are presented in **Fig. 2.5** [75]. The share of waste compositions generated worldwide is illustrated in **Fig. 2.6** [75]**,** and the causes of food waste are shown in **Fig. 2.7** [76].

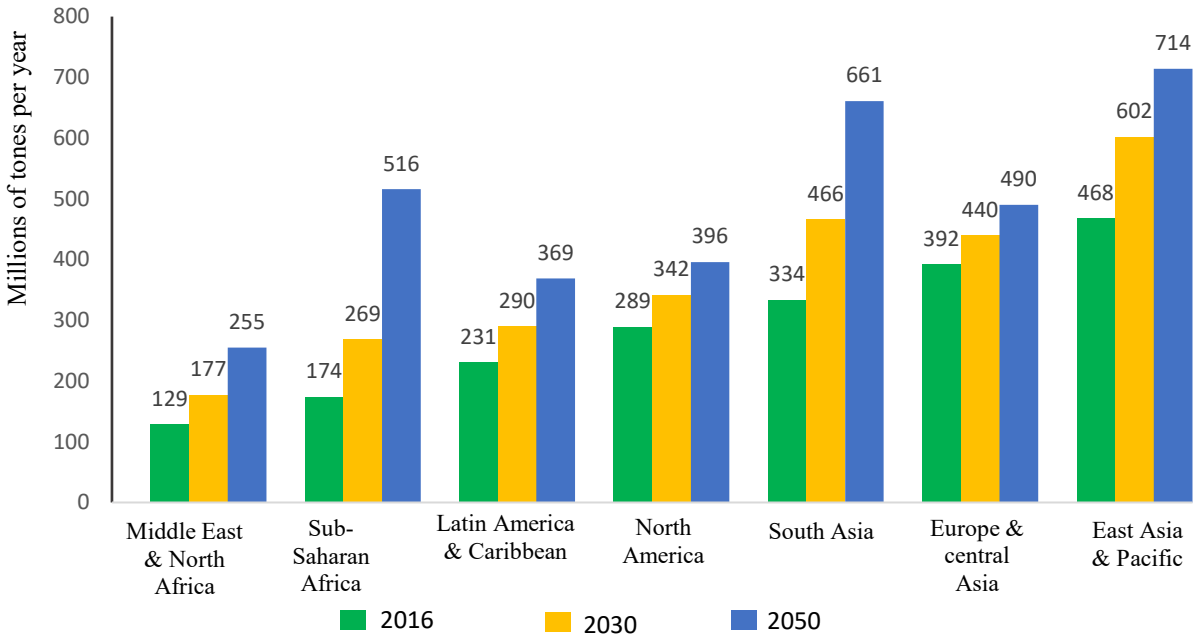

Fig. 2.5: The amount of waste generated in 2016 relative to the increased estimates in 2030 and 2050 [75].

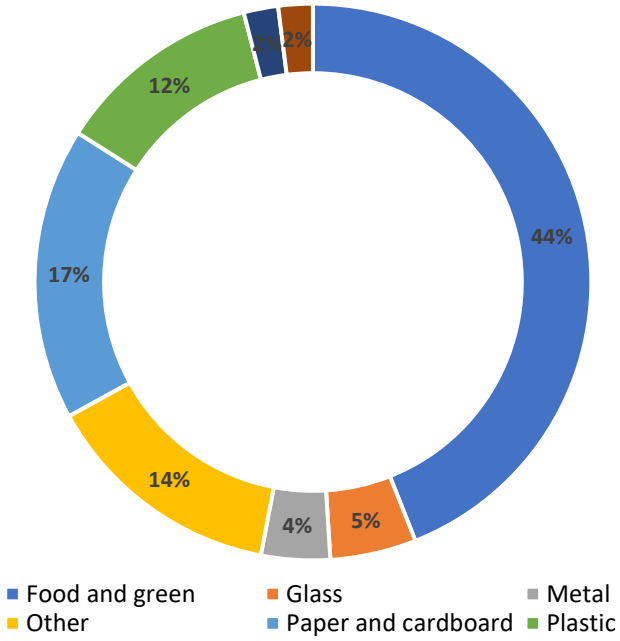

.

Fig. 2.6: Share of waste compositions generated worldwide [75].

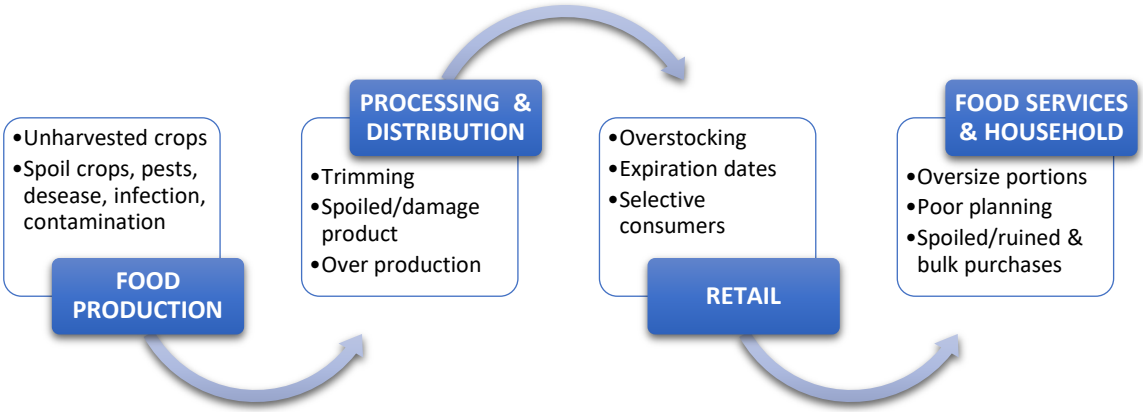

Fig. 2.7: Causes of food waste [76].

Replacing landfills with ecologically sound technologies is essential to mitigate greenhouse gas emissions and enhance environmental sustainability. Composting is one of the most environmentally beneficial methods, compared to landfilling and incineration, since it generates by-products that may be utilised as soil nutrients [77]. Organic waste streams from food production are often used as animal feed, particularly when produced close to local

farms [78]. Yet, using these streams as animal feed doesn't eliminate them from waste management, especially considering certain limitations. For instance, the presence of anti-nutritional factors such as pesticides, tannins, and other contaminants can restrict their use in feed blends [79]. This method is illegal in some countries due to the risk of disease transmission [80]. A promising alternative to these traditional methods is the bioconversion of food waste using BSFL. This technique offers a viable pathway for transforming food waste into commercially valuable products, aligning with sustainable waste management practices [81-84].

2.4. Entomology and bioconversion of waste using black soldier fly

Using insects to reduce greenhouse gas emissions and enhance the environment is the most potential solution supporting the circular economy hypothesis [85]. BSF, also known as *Hermetia illucens Linnaeus*, is one of the most significant species suggested as an organic waste converter [6] alongside other edible insects. Human consumption of insects, or entomophagy, is not a new concept. Humans have consumed insects for centuries, and it has been practised in numerous countries, though it is not such a mainstream practice in developed countries such as Europe and North America. The number of edible insect species eaten by 3,071 ethnic groups was calculated to be around 2,000 varieties [86]. Hence, discussing incorporating insects into modern food culture has become significant [20]. Even individuals without established customs/traditions of entomophagy are paying greater attention to insects as a food source. They are becoming more aware of the nutritional benefits they provide over other, more conventional foods [87-90]. More so, quite a few cookbooks have been dedicated to insects, and several international conferences have been held discussing this topic [91-95]. Interest in entomophagy has reached levels where insect suppliers are now finding it challenging to meet the increased demand, and a few species are

at risk of overexploitation [20]. Insects have comparable nutritional value to traditional animal food sources, including similar protein amounts, vitamin levels, and saturated/unsaturated fat concentrations [96]. Furthermore, insects are incredibly easy to raise due to their fast reproduction rate. BSFL are potential edible insects that can substitute conventional animal food sources and have other remarkable environmental benefits, such as being bio-converters of organic waste. This means there are two promising approaches to implementing circular economy principles in the context of food waste: to work upstream by (i) reducing the food waste from occurring in the first place and (ii) meeting the high demand for the food itself by using environmentally friendly food sources: insects. This approach makes achieving a circular economy in the food industry potentially possible.

The International Platform of Insects for Food and Feed (IPIFF) has issued many guidelines, recommendations, and regulation papers on insect processing. The IPIFF, for example, has published guidance on acceptable sanitary standards for European Union insect producers for food and feed, which member institutions are urged to follow [97]. **Fig. 2.8** illustrates the guideline utility of BSFL-based products for animals and aquafeed [21, 97] (redrawn from the IPIFF information website).

Prohibited BSF Feed Substrate	Authorised BSF Feed Substrate
• Unprocessed former foodstuff (fish, meat and poultry) • Manure (human and animal) • Restaurant waste and slaughter house products	• Fruit and vegetable • Agri-crop biomass • Unprocessed former foodstuff (dairy, eggs and honey) • Fruit and vegetable industrial by-products

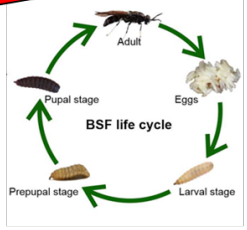

Animal	Black soldier fly (BSF)		
	Live	Protein	Fat
	Yes	Yes	Yes
	Yes	No	Yes
	Yes	No	Yes
	Yes	Yes	Yes
Nutrient for Animal			

Fig. 2.8: Guidelines on appropriate hygienic standards for European Union producers of insects for food and feed.

Considering the restrictions on BSFL feeds outlined in **Fig. 2.8**, pre-consumer waste streams offer significant potential for BSFL cultivation. This fact opens up a broader spectrum of target markets, with BSFL meals suited for diverse animal species. **Table 2.1** highlights facilities that are significant point sources of pre-consumer organic wastes amenable for BSFL feed. Moreover, supermarket waste also contributes to the available organic waste pool. For instance, in Australia, in the 2014-15 financial year, approximately half of all Woolworths supermarket stores had a farmer donation program, resulting in 40,000 tonnes of food being diverted from waste [78]. Similarly, other supermarkets like Coles and Aldi have donation schemes, albeit store-by-store.

Table 2.1: Significant point sources of pre-consumer organic wastes eligible for BSFL feed.

No	Facility Type	Dominant organic waste types produced
1	Almonds	Shells, hulls
2	Bakery	Baked products, flour, bread
3	Breweries	Brewers grains, trub, yeast
4	Canola and other oilseeds processing	Shells, hulls, kernel fragments
5	Cotton ginning	Cotton trash (cotton fibre, leaves, sticks, dirt)
6	Feed mills	Grain waste (non-endosperm), off-spec batches, oilseed waste
7	Food processing	Off-spec products, ingredients, off cuts
8	Fruit and vegetable production	Fruit and veg off-cuts
9	Grain milling	Bran, mill mix/middlings, grain dust, germ, pollard, screenings
10	Grain storage and distribution (including rice)	Spilled grains, dust
11	Malt processing	Culms, dust, screenings
12	Sugar milling and refining	Molasses, clarifying agents, filter cake/mud,
13	Wineries	Grape marc, lees

Insects have advantages over other animal meat sources, entomophagy is more sustainable due to its higher feed-to-protein conversion ratio when compared to both cattle and swine [98, 99]. Hence, insects pose a less significant impact on the environment and their rearing yields through (i) lower greenhouse gases and (ii) less ammonia production than any typical livestock [99-101]. Another significant benefit is that insect farming needs much less water and land, to the point that insects may even be cultivated on organic waste streams, decreasing pollution and turning organic waste into high-protein food sources [93]. This also suggests that BSFL bioconversion supports the circular economy.

2.5. Black soldier fly larvae (BSFL)

Scientists have worked on identifying edible insect species with (i) straightforward rearing processes, (ii) availability in regular supplies and no/minimal risk of overexploitation with

farming, (iii) high sustainability, (iv) economically friendly costs so consumers would be encouraged to purchase in place of other meats, and (v) desirable taste and texture. For this study, only the BSFL, *Hermetia illucens* is discussed. This species is a true fly (Diptera) of the Stratiomyidae family [20]. According to new market research by Meticulous Research, the global BSFL market is expected to grow at an annual rate of 33.3% from 2019 to 2030, reaching US$2.57 billion within a decade. This species is native to the neotropical region but has spread across all continents in recent decades, becoming virtually worldwide [102]. BSFL may be found in the US, Europe, and Russia's Krasnodar Territory [7-9]. It also exists in the Afrotropical, Australasian, East Palaearctic, Nearctic, North African, Southern African, and Indo-Malayan realms [10-14].

Adult BSFs are approximately 16 mm long, with primarily black bodies featuring metallic reflections ranging from blue to green on the breast and a scarlet tip on the abdomen [103]. The Latin term for the second abdominal target comes from the presence of translucid zones. The eyes are well-developed, and the head is big. The antennae are about twice as long as the head. The tarsus is white, and the legs are blackish. The wings look like membranes and are folded horizontally across the abdomen when not in use [11]. BSFL is a mimetic fly that resembles the Dauber wasp and its family in size, colour, and appearance. The fly appears to have a slender "wasp waist" due to its wasp-like antennae, pale hind tarsi, and two small transparent windows in the basal abdominal segments [11]. A fine grey-black stripe on the BSFL's posterior extremities distinguishes them from the larvae of speckled flies [102]. The life cycle and phases of BSFL development, as well as the average length of each stage, are shown in **Fig. 2.9**.

Fig. 2.9: The life cycle and phases of BSFL development, as well as the average length of each stage.

A mature female may lay anywhere from 206 to 639 eggs[17], often placing them in cracks or on surfaces above or near decaying materials like dung or compost. The eggs hatch in about four days [19]. Newly emerged larvae grow to a length of 2.5 mm and a weight of 0.10 to 0.22 grams by the end of the larval stage [11], which can last anywhere from 18 to 36 days, depending on the dietary substrates provided [15]. The pre-pupal (post-feeding) stage lasts approximately 7 days. Under low temperatures or in the absence of food, the larval stage may extend for several months. The pupal stage lasts from one to two weeks. Adults can live for 47 to 73 days if given water and food, such as sugar in captivity or nectar in the wild [15, 18]. Adult flies do not eat, which eliminates the risk of disease transmission when using BSFL as a waste bio converter [19]. Adult flies survive by feeding on nectar in their adult stage, while the larvae consume waste as food during their development.

2.6.Product of black soldier fly, properties, and application

BSFL are of particular interest in managing organic waste, the larvae can convert this waste into a variety of materials that are valuable for humans. BSFL have been reported to feed on various organic waste substrates such as manure [104], food waste [105], faecal sludge [106], animal offal, kitchen waste, and others [107-112]. Consequently, BSFL has proved to have great potential for industrial waste and by-product treatment, biorefining, and agroindustry waste bioconversion owing to this great diversity of materials they can process with greater efficiency relative to any other materials other fly species [20, 113]. BSFLs themselves are also edible and non-toxic. They are so high in lipids that their conversion into biodiesel has been closely discussed [114-116]. More advantages associated with BSFL rearing include: (i) their frass is nitrogen-rich and suitable for use as fertiliser, (ii) longer larval phase relative to other flies, meaning they can feed for longer on more significant substrate amounts and grow to larger sizes, (iii) they self-harvest, i.e. they migrate from the 'waste' location to higher and cleaner places instinctively, thus creating a less labour intensive farming process [20, 117, 118]. In this study will specifically discuss potential BSFL by-products in terms of their (i) properties and composition, (ii) industrial applications mainly as food sources, and other applications (iii) downstream harvesting, and extraction methods for use.

Protein, lipids, minerals, and certain vitamins are abundant in BSFL. By dry weight, BSFL comprises 32% protein, 37% lipids, 19% minerals, and 9% chitin [6]. They have the capability to transform low-value organic waste, estimated at around 1.3 billion tonnes annually, into high-value protein [119]. A Krona chart revealing BSFL's proximate elements is depicted in **Fig. 2.10** [21, 120]. Meanwhile, a summary of the extraction of lipids, proteins, and chitin from BSFL, prepupae, and pupae in a sequential manner is illustrated in **Fig. 2.11,**

redrawn from Ref. [121]. The proximate composition of larvae, prepupae, and pupae of BSFL is tabulated in **Table 2.2.**

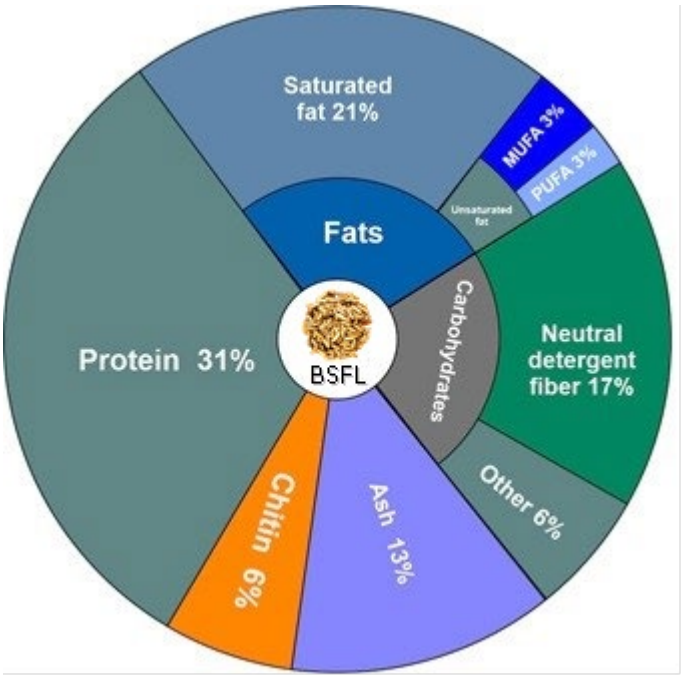

Fig. 2.10: Krona chart showing BSFL's proximate elements.

Table 2.2: Proximate composition of BSFL, prepupae, and pupae [121].

Substances	Dry matter†	Lipids‡	Protein‡	Chitin‡	Ash‡
Larvae	27.74 ± 0.57	40.96 ± 0.93	38.86 ± 1.70	3.85 ± 0.24	9.56 ± 0.49
Prepupae	35.67 ± 0.41	47.65 ± 0.92	31.81 ± 1.26	4.72 ± 0.76	8.83 ± 0.27
Pupae	39.95 ± 0.25	39.85 ± 0.86	31.27 ± 0.92	6.31 ± 0.41	9.24 ± 0.14

† g/100 g as is
‡ g/100 g dry matter

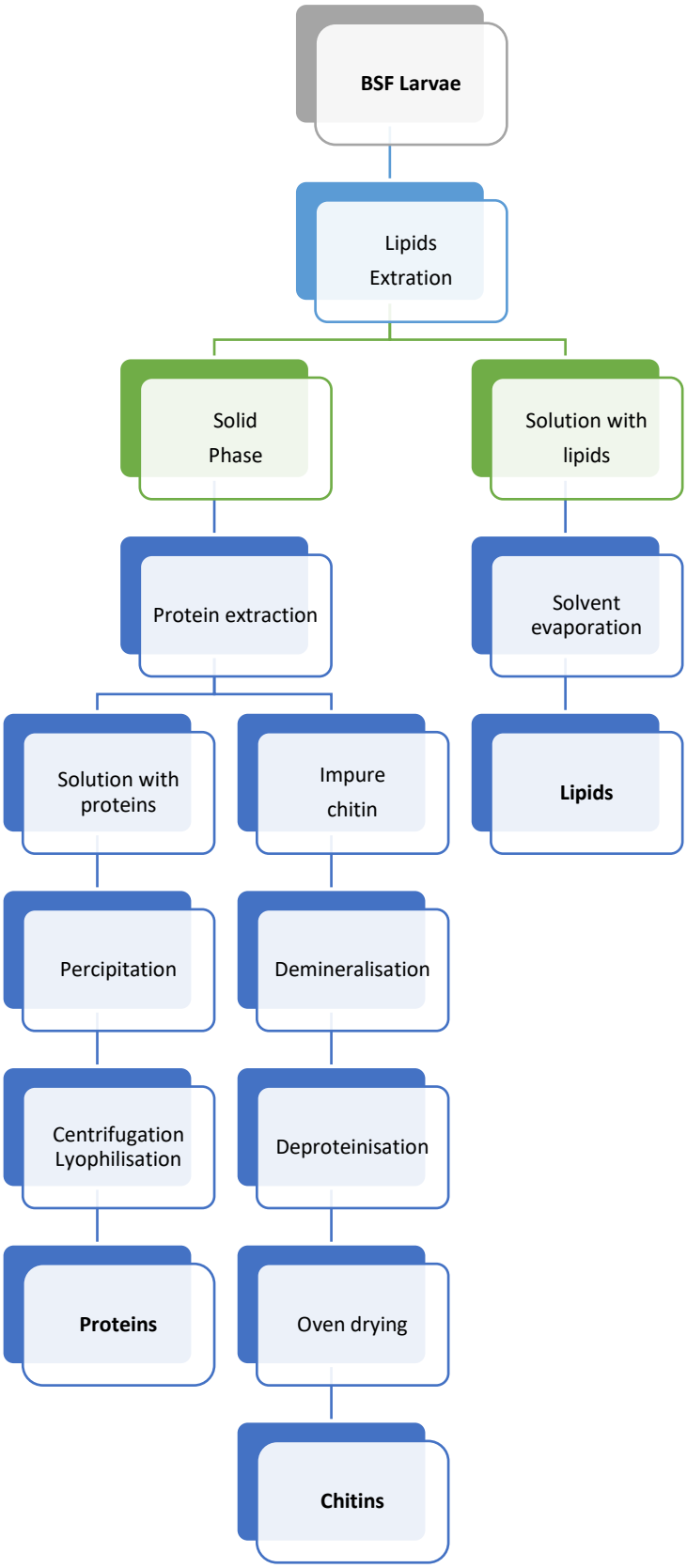

Fig. 2.11: Chronological extraction of lipids, proteins, and chitin from BSFL.

2.6.1. Lipids

Previously, significant levels of lipids or fat, particularly in the form of saturated fatty acids (SFA), were observed in BSFL [23, 121]; the primary fatty acids being lauric acid (C12:0), oleic acid (C18:1 n-9), palmitic acid (C16:0) and linoleic acid (C18:2 n-6) [122-126]. The fatty acid profile varied based on feeding frequency or diet, and some studies attempted to alter the fatty acid profile of BSFL by employing an enriched feed formulation [127-130]. Triglycerides are the most abundant lipid type in BSFL oil [131-133]. Storage lipids, which provide the energy source for metabolic activities, are found in the larvae stage of BSF and not in the adult phase[21]. Due to the high lipid content of the larvae, they are used for biodiesel production [36]. Biodiesel synthesis using enzyme-assisted lipid extraction from BSFL is shown in **Fig. 2.12**. The fatty acid composition of mature BSFL is provided in **Table 2.3**.

Table 2.3: The fatty acid composition of mature BSFL [134].

Ref.	C12:0 (%)	C14:0 (%)	C16:0 (%)	C18:0 (%)	C18:1 (%)	C18:2 (%)	Feeding Substrate
[135]	57.35	7.34	9.65	1.36	7.54	11.55	Chicken Feed
	57.56	7.14	10.29	0.98	7.97	7.83	Food Waste
	60.89	9.48	8.70	1.11	5.66	4.52	Fruit and Vegetable Waste
[136]	63.10	13.50	8.20	-	8.30	2.00	Waste Coconut Endosperm + Mixed-Bacteria Powder
[84]	66.00	14.40	6.60	0.40	5.60	2.30	Waste Coconut Endosperm + *S. cerevisiae*
[27]	28.52	0.87	4.66	6.24	26.43	-	Waste Coconut Endosperm + SCR (1:4 of Waste Coconut Endosperm: SCR)
	0.35	8.80	0.73	1.80	40.81	-	Waste Coconut Endosperm + SCR (3:2 of Waste Coconut Endosperm:SCR)
	0.90	4.78	0.37	0.98	54.03	-	Waste Coconut Endosperm
[29]	39.60	6.50	13.10	2.10	11.50	17.50	Soybean Curd Residue + *L. buchneri*
	36.90	5.90	13.20	1.70	12.10	17.00	Soybean Curd Residue

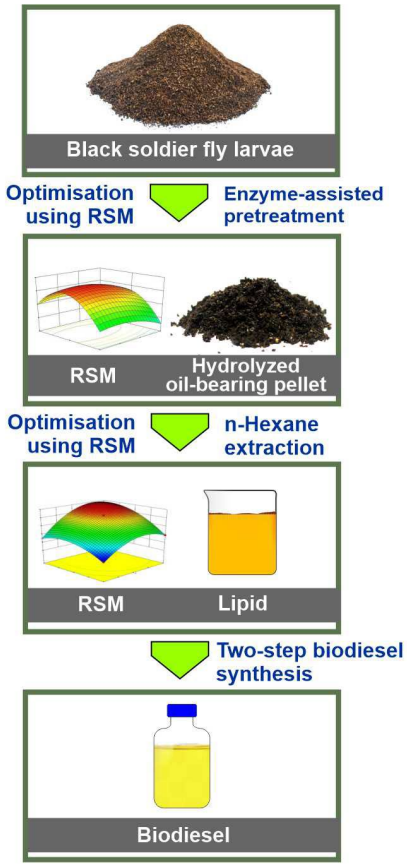

Fig. 2.12: Biodiesel synthesis using enzyme-assisted lipid extraction from BSFL.

2.6.2. Lauric Acid

Lauric acid is a saturated fat-containing medium-chain fatty acid (MCFA) or medium-chain triglyceride (MCT) found in palm kernel and coconut oil. It has been recently determined that the lauric acid composition in the BSFL oil (BSFLO) is similar to those two oils, around 45-47 % of the total saturated fat [133]. The chemical structure is composed of 12 carbon (C), 24 hydrogens (H), and 2 oxygen (O) atoms with the molecular formula of $C_{12}H_{24}O_2$. Lauric acid is a white solid with a melting point of 43–44 ºC and a molecular weight of 200.32 g mol–1 [137]. Several studies have tried manipulating the fatty acid profile using an enriched feed formulation [127-130]. A recent study found that dietary BSFLO enhances feed conversion ratio, boosts the absorption of medium-chain fatty acids into the abdominal

fat pad, and raises serum antioxidant capacity in broiler chickens.[138]. Furthermore, dietary BSFLO has demonstrated to be an acceptable alternative lipid source in rainbow trout diets without negatively impacting growth performance, feed efficiency, nutrient retention, and survival [139].

In the human body, the lipase enzyme digests lauric acid into monolaurin, a monoester composed of glycerol and lauric acid. According to a reference, the majority of ingested lauric acid is carried directly to the liver, where it is converted to energy and other metabolites rather than stored as fat [140]. Lauric acid and other fatty acids primarily function as structural components of cell membranes and contribute to a variety of physiological activities in the body. Lauric acid and monolaurin are antibacterial and anti-inflammatory agents that can effectively treat skin problems. Furthermore, they can also accelerate the process of epithelialisation, which involves the upward migration of epithelial cells to repair damaged areas. This is due to their capacity to enhance the proliferation and migration of cells. During the wound healing process, the cells near the wound's borders grow and expand, resulting in re-epithelialisation of the wound surface [137, 141].

2.6.3. Protein

BSFL has been used in the diet of various animals due to their high protein content, including chicken, fish, and pet food [142-144]. It is one of many bug species approved for use as aquaculture food by an EU commission [75]. Humans can also consume BSFL. They are very efficient protein conversion and contain about 42% protein, high calcium, and high amino acid concentrations. On a dry matter basis, the calcium content in BSFL can range from 5-8% or even higher in some cases. A study conducted found that the calcium (Ca)

is the most abundant and ranges from 1.2 g/kg to 35.7 g/kg [145]. 1 gramme of BSF eggs yields 2.4 kilos of protein every 432 hours, implying that 1 gramme contains almost 45,000 eggs [102]. The proteins' nutritional quality is defined by their essential amino acid content and BSFL lipid extraction. Because lipids do not affect protein extraction, the larvae may enhance protein recovery [21]. The schematic diagram in **Fig. 2.13** depicts the process of BSFL treatment for the extraction of protein sources for animals [146].

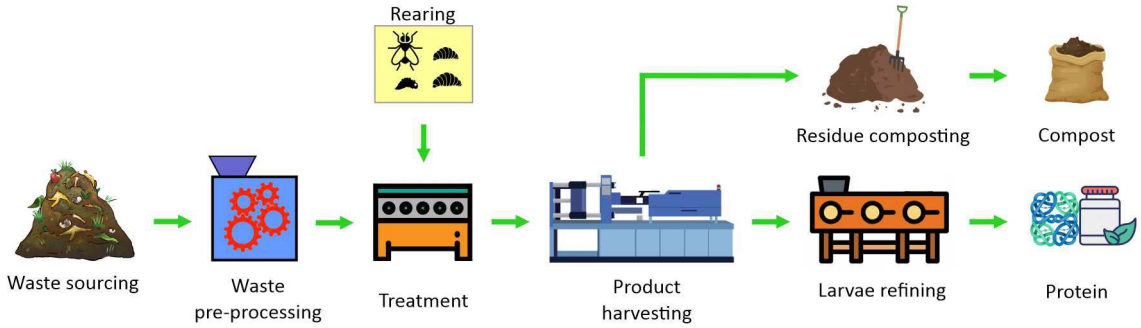

Fig. 2.13: Schematic diagram of the treatment of BSFL for protein extraction.

Lysine, valine, arginine, and proline are essential amino acids, while glutamic amino acids and aspartic amino acids are non-essential amino acids [147]. When BSFL fed on four distinct diets, including chicken feed, vegetable waste, biogas digester, and restaurant waste, they exhibited comparable amino acid profiles despite the fact that the amino acid content of the diet varied significantly. This led to the finding that their food unaffected BSFL's amino acid composition [135]. Unlike other dietary proteins, BSF prepupae's entire amino acid content is provided in g/100 DM, and essential amino acids are also represented in mg/g of crude protein. Compared to other dietary proteins and the FAO/WHO standard protein, the total amino acid composition of BSF prepupae is tabulated in **Table 2.4** [6, 148]. Similarly, the 5 amino acid profiles for the different substrates are presented in **Table 2.5**.

Table 2.4: Total amino acid content in BSF prepupae relative to other food proteins and the FAO/WHO protein standard [6, 148].

Descriptions	BSFL Protein (g/100 g DM)	Protein (mg/g protein)	FAO/WHO 1985 Reference (mg/g protein)
AminoAcid			
Histidine	1.17 ± 0.04	33	15
Threonine	1.49 ± 0.02	42	23
Valine	2.4 ± 0.1	66	39
Lysine	2.3 ± 0.2	65	45
Iso-leucine	1.47 ± 0.09	41	30
Leucine	2.7 ± 0.1	75	59
Phenylalanine	1.3 ± 0.1	36	-
Tryptophan	0.21 ± 0.03	9	6
Cystine	1.1 ± 0.1	30	-
Phenylalanine + Tryptophan	-	110	38
Cystine + Methionine	-	47	22

Table 2.5: Amino Acid profile from the different substrates.

Reference	[149]	[149]	[149]	[149]	[150]	[135]	[135]	[135]	[135]
Substrate	A	B	C	D	E	F	G	H	I
Essential Acid Amino	g/kg DM								
Arginine	20.9	21.1	20.6	20.1	20.5	20.0	20.3	19.9	20.3
Histidine	14.2	13.9	13.9	13	31.6	12.4	13.5	13.8	13.6
Isoleucine	18.4	18.3	17.7	17.5	15.6	17.3	18.4	19.1	17.2
Leucine	28.6	28.1	28.1	27.4	27.1	28.0	29.5	30.6	28.6
Lysine	24	24.6	24.1	23.4	23.2	22.6	25.7	23.0	23.4
Methionine	8	8.1	7.9	7.5	22.4	7.6	8.7	7.1	7.6
Phenylalanine	18.1	18.5	18.3	17.2	18.6	16.3	18.7	16.4	17.0
Threonine	19.1	19.5	18.4	19.2	18.4	15.4	16.8	16.2	16.4
Valine	19.7	19.5	18.4	19.2	18.7	24.8	24.9	28.2	24.1

2.6.4. Chitin and Chitosan

BSFL also contain a valuable biopolymer called chitin, which, according to various studies, exists in amounts of less than 10% of the dry mass [123]. Natural polysaccharides, chitin and its chitosan derivatives comprise two monosaccharides: N-acetyl-D-glucosamine and D-

glucosamine, connected by β-1,4-glycoside linkages [124]. Chitin is found in crustaceans, insects, and certain fungus and yeast species, serving as a hard and protective exoskeleton for the creatures. Compared to other natural sources of chitin, there has been a lack of studies of BSFL chitin. One study found a way to obtain these chitin and chitosan by combining BSFL with a deacidified derivative to create the chitosan-melanin complex [125]. Another study investigated BSFL's chitin matrix content/index in the larvae, prepupa, puparium, and adult stage and found the former to be 3.6%, 3.1%, 14.1%, and 2.9%, respectively [126]. The adult chitin crystalline index rose by 33.1%, 35.1%, 68.4%, and 87.9%, respectively [127]. Several other researchers are also experimenting with using chitin as a food packaging and transportation alternative to plastic and for water purification [128]. Furthermore, chitin is a potential substance that may enhance plant resilience and soil fertility by acting as a soil improver [129, 130].

Chitosan, a chitin derivative, has high economic value due to its characteristics and possible uses. The degree of deacetylation, molecular weight, crystallinity, and degradation all influence the physicochemical characteristics of chitosan [131]. Chitosan has a variety of applications, including wound healing and tissue regeneration, wastewater treatment, agriculture, food safety, cosmetics, papermaking, and textiles [132-136]. Using additive printing technology, chitin was used to create a 3D copy of fungus-like adhesive materials, one method to recycle waste using BSFL [137]. The extraction, characterisation, and bioactivity of chitin and chitosan from BSFL are illustrated in **Fig. 2.14** [65]. The elemental composition of chitin isolated from BSFL pupae exuvial (BSFE) and BSF imago (BSFI) are tabulated in **Table 2.6**, and the comparative values of chitin content, deacetylation (DA), CrI, and DTGMax from BSF are presented in **Table 2.7**.

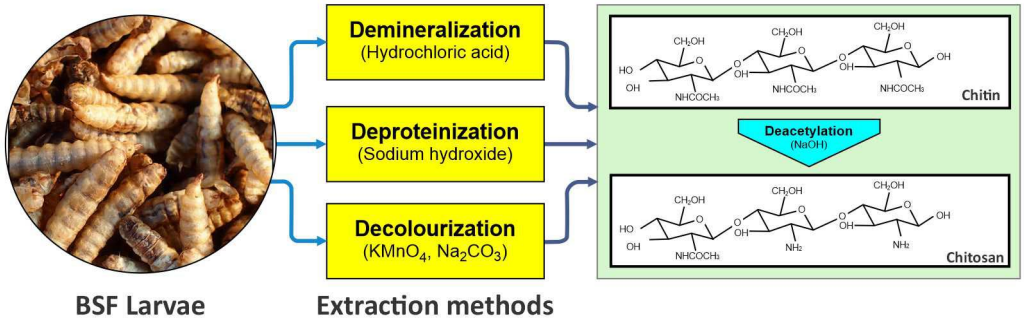

Fig. 2.14: The extraction, characterisation, and bioactivity of chitin and chitosan from BSFL.

Table 2.6: Elemental composition of chitin from BSF imago and BSF pupal exuviae [151].

BSF phases	BSFI	BSFE
Carbon (%)	39.74	43.74
Hydrogen (%)	5.46	5.82
Nitrogen (%)	6.00	6.14
C/N Ratio (%)	6.62	7.12
Degree of acetylation (%)	86.00	115.00

Table 2.7: Comparative values of chitin, DA, CrI, and DTGMax for various insects [151].

BSF phases	Larvae	Imago	Pupae exuviae
Chitin content (% dry wt)	-	23.0	9.0
Degree of acetylation (%)	86.2	71.6	115
Crystalline index (%)	35.0	49.4	25.5
Maximum degradation temperature (DGT_{max}) (°C)	389	363	371

Chitosan-based materials can be used as new eco-friendly products because of the natural ingredients in its sources, as well as its biodegradability, biocompatibility, sustainability, and renewability. Chitin and chitosan can also produce hydrogels and aerogels, which are widely used in biomedical. Hydrogels, highly water-absorbent cross-linked networks of polymers, possess remarkable water absorption capabilities. These hydrogel-forming polymers contain hydrophilic functional groups, such as amine (NH_2), hydroxyl [-OH], amide (-CONH-, -

$CONH_2$), and sulphate ($-SO_3$ H), within their polymeric structure. These hydrophilic groups play a crucial role in enabling hydrogels to absorb water and watery fluids, leading to their expansion and a significant increase in volume, a process known as swelling. Notably, the cross-linked structure of hydrogels provides a safeguard during swelling, preventing the breakdown and destruction of the hydrogel cross-links [152, 153].

Aerogels are porous, lightweight materials produced from a gel in which the liquid component is replaced by gas without causing the gel structure to collapse significantly [91]. They consist of a complex 3D network structure with a substantial number of air-filled holes and have a unique combination of characteristics, including high porosity, a large available specific surface area, low density, and variable surface chemistry [154]. As chitosan has a high degree of deacetylation, it may be used to make a chitosan-based aerogel with excellent mechanical characteristics, including high porosity and lightness. Because of their ease of preparation and appropriateness for laboratory use, chitosan-based aerogels in the form of beads are most popular. However, unlike chitosan-based hydrogels, the production of chitosan-based aerogels in the form of scaffolds is still restricted [155]. Scaffolds are materials that have been developed to promote the creation of new functioning tissues for medicinal reasons by causing desired cellular relationships [156].

Several types of aerogels are classified based on their chemical composition, such as oxide (silica, alumina, zirconia, and titania) [157-160], carbon (carbon, carbon nanostructure, graphene, and graphene oxide) [161-164], polymers (polyamide, polyurethane, polyimide) [165, 166], biomass (chitosan, cellulose, polysaccharides) [167-169], metals (gold, platinum, silver, and copper) [170, 171], non-oxide ceramic (boron nitride, silicon nitride, and carbide) [172] and semiconductors (cadmium sulphide, zinc sulphide). The properties of

instantaneous membranes, spheres, sheets, beads, powders, blankets, granules, microparticles, and coatings vary depending on the aerogel employed and the structure of the aerogel. **Table 2.8** shows the chitosan-based hydrogel/aerogel with their crosslinker for other applications.

Table 2.8: Combination of Chitosan with other crosslinkers or biopolymers using 3D printing technique and other applications.

Material	Form	3D Printing	Properties	Application	Ref
Chitosan-hydroxyapa-tite (HA)	Hydrogel	Extrusion Bioprinting	Improved cell viability, proliferation, and osteogenic differentiation.	Bone tissue engineering	[173]
Chitosan-based gelation with KOH, Na2C02 or NH3 Vapours	Hydrogel	Extrusion printing	Those different media able to retain the 3D printed structure accurately and enhance and drive cell growth	Tissue engineering	[174]
Chitosan - PEGDA	Hydrogel	Extrusion printing	The PEGDA can regulate the mechanical properties and have good fatigue resistance and can be extruded smoothly via 3D printing	Tissue engineering	[175]
PLA/CS/SA	Hydrogel	DIW	Biocompatibility is higher for the scaffold when different CS and SA added to PLA	Tissue engineering	[176]
Chitosan/ halloysite nanotubes/tea polyphenol	Hydrogel	Extrusion printing	A good antioxidant capacity	Food packaging	[177]
Chitosan-gelatinee	Hydrogel	Extrusion Bioprinting	Increase the fixation of the prosthesis-bone interface and to avoid postoperative infection	Artificial joint replacement	[178]
Chitosan-collagen	Hydrogel	Extrusion Bioprinting	Rapid thermo-induced sol-gel transition and contraction, tunable mechanical properties, proper microstructure, and biodegradability for 3D cell culture, as well as improve cytocompatibility	Tissue engineering	[179]
Chitosan/ Guar Gum	Hydrogel	Extrusion Bioprinting	Increased the printability and viscosity and shape fidelity	Tissue engineering	[180]
Chitosan-Cellulose	FLAM	Extrusion printing/FDM	Mechanical properties of the bio-composites were within the range of soft-wood, high-density polymeric foams and high porosity metal foams.	Future construction material	[181]

2.6.5. Minerals

Several studies have also shown BSFL to produce additional components such as minerals. The latter include iron, zinc, magnesium, calcium, potassium, manganese, calcium, and others. The Simplified flow chart displaying the extraction of minerals from BSFL is shown in **Fig. 2.15** [182]. BSF V instar larvae and prepupae mineral and heavy metal content are presented in **Table 2.9.**

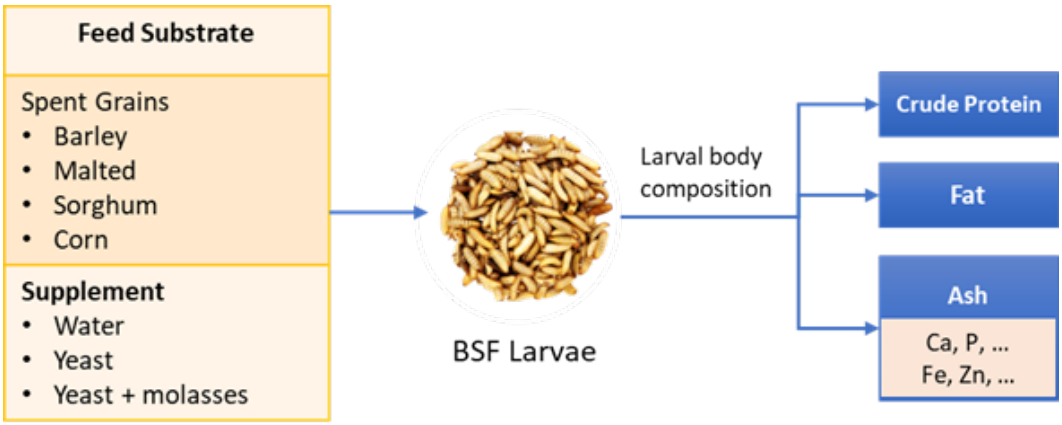

Fig. 2.15: Simplified flow chart displaying the extraction of minerals from BSFL.

Table 2.9: Mineral and heavy metal content of BSF V instar larvae and prepupae [26, 183].

Mineral	V Instar Larvae	Prepupae	EU Directive 2002/32/EC (mg/kg)
As	1.01	0.96	2.0
Ca	0.72	0.92	-
Cd	0.37	0.24	2.0
Fe	84.0	89.0	-
Hg	>0.05	>0.05	0.1
K	0.79	0.84	-
Mg	0.26	0.33	-
Mn	212	268	-
P	0.58	0.71	-
Pb	0.39	0.32	10
Zn	68.0	98.0	-

(Ca, P, K, Mg: % dry matter; Fe, Zn, Mn, As, Cd, Hg, Pb: mg kg^{-1}, dry matter)

2.6.6. Vitamins

BSFL are also good sources of vitamin E and can be professionally manufactured. BSFL produces approximately 0.62 mg/100 g of vitamin E [184]. Vitamin E seems to be the only vitamin found in BSFL that meets 50%-100% of the Norwegian National Research Council's (NRC) standards. According to one research, the majority of total vitamin E found in BSFL is of the alpha-tocopherol form, and adding seaweed to the BSFL diet may help boost levels [130]. Furthermore, with diet alterations, BSFL may also synthesise vitamin A [185].

2.7.Extraction of black soldier fly larvae (BSFL)

After rearing the BSFL with the food waste, the insects are ready to turn the low-value waste into high-value products. The BSFL can produce lipids, proteins, chitins, minerals, and vitamins, as stated above. To harvest these products from BSFL, various extraction methods are used, the most popular of which are chemical extraction [121] and enzymatic extraction [186]. Before conducting chemical or enzyme extraction on BSFL, they have to be devitalised. The chemical components of BSFL, like proteins and lipids, may be affected by various devitalisation mechanisms [132]. As a result, the choice of pre-treatment or devitalisation is critical in obtaining high-quality BSFL products. The extraction process of BSFL is shown graphically in **Fig. 2.16** [132], and the valuable compound's extraction type from BSFL is illustrated in **Fig. 2.17** [6]. While the products of chemical and enzymatic extraction of BSF are tabulated in **Table 2.10**.

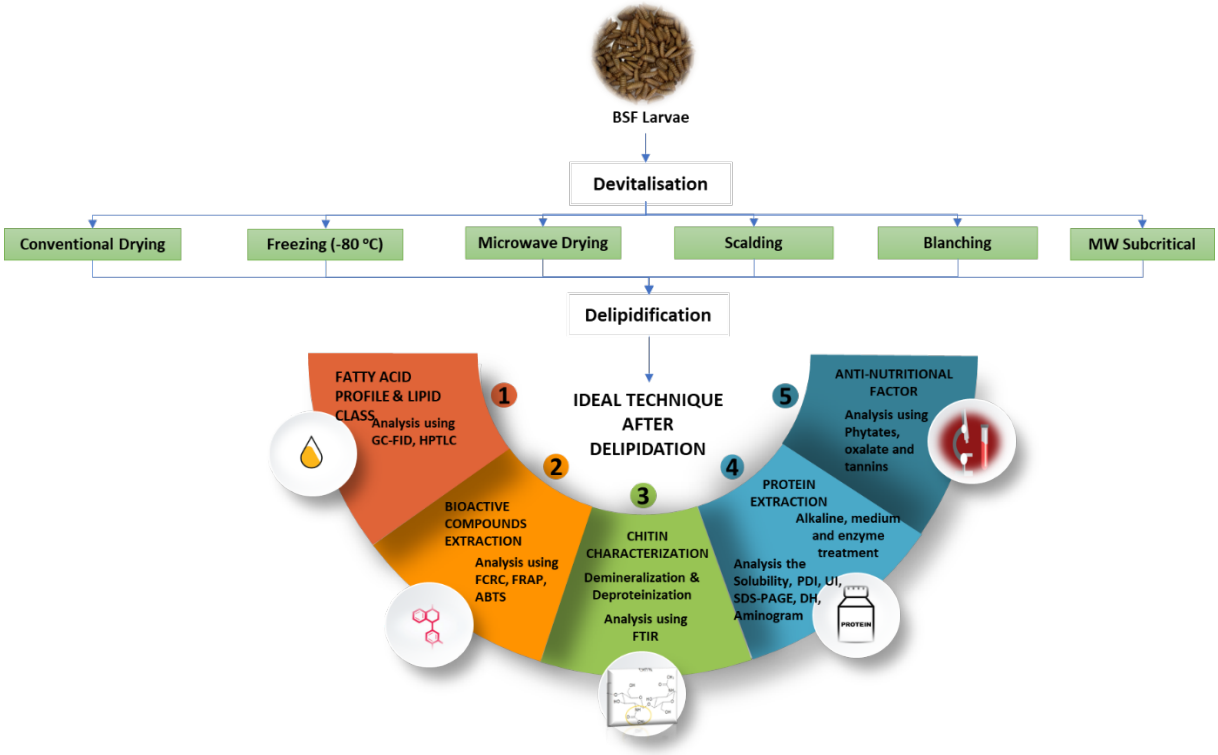

Fig. 2.16: The experimental design of topological representation for extracting BSFL.

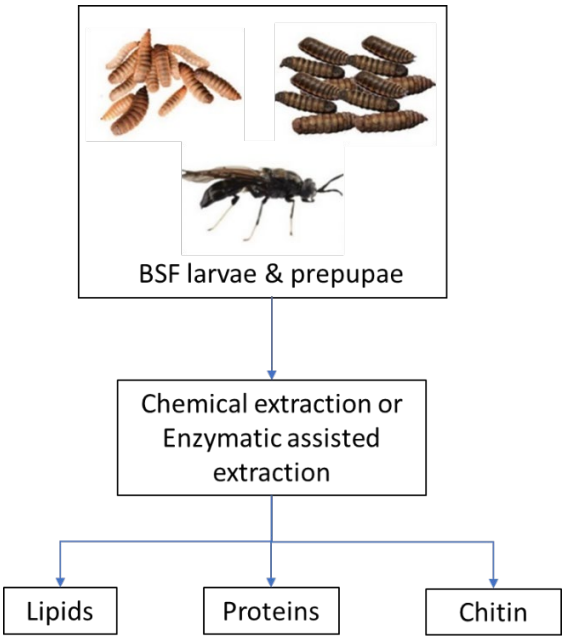

Fig. 2.17: Type of extraction of a valuable compound from black fly larvae.

Table 2.10: Type of extractions and the various products yielded of BSFL.

Refs	Feeding Substrate	Extraction	Protein*	Lipid*	Chitin*
[6]	Unknown	Chemical	32%	37%	9%
[23]	Bread, fish & mussels	Chemical	34%	37%	-
[24]	Unknown	Enzymatic	-	7%.	-
[25]	Unknown	Enzymatic	42%	21%	7%
[26]	Fruit & vegetable	Chemical	37%	33%	-
[27]	Waste coconut	Chemical	53%	19%	-
[28]	Fermented waste Coconut	Chemical	58%	15%	-
[29]	Soybean curd residue	Chemical	53%	26%	-
[6]	Unknown	Enzymatic	-	10%	3%
[30]	Unknown	Enzymatic	67%	10%	-

*Average

2.7.1. Chemical extraction

Most BSFL studies have relied on sequential chemical extraction to obtain lipids, proteins, and chitin from BSFL. The first step to extract lipids is the defatting process of BSFL, then deproteinisation of the defatted sample using an alkaline solution, followed by demineralisation treatment using an acidic solution and, finally, decolourisation of the obtained product using an alkaline solution treatment [21]. This process is also frequently used to separate chitin from BSFL and chitosan, which results from chitin deacetylation. Conversely, solvent extraction using ethyl ether, petroleum ether, hexane, or pentane is the most utilised technique of delipidation [187]. The polarity of the lipids present in contrast to the polarity of the solvent determines the efficiency of solvent extraction. Polar lipids, such as glycolipids and phospholipids, dissolve in alcohols rather than non-polar solvents like hexane. Glycerides, mainly triglycerides, make up most of the lipid content of BSFL [121], and hexane is the most suitable solvent frequently used to extract lipids from BSFL. On the other hand, the Folch Technique extraction is another popular lipid extraction method that

uses chloroform and methanol as solvents and is often used in small-scale laboratory experiments [188].

One of the more recent methods of chemical lipid extraction is supercritical carbon dioxide extraction (SC-CO2). Conventional defatting (lipid extraction) procedures typically use high quantities of organic solvents and protracted extraction durations, frequently resulting in thermal deterioration and poor product quality [39]. Furthermore, employing organic solvents raises issues about pollution, health safety, and product contamination owing to solvent residues [39, 40]. Whereas the SC-CO2 extraction method is an environmentally friendly alternative technique for extracting natural bioactive compounds, particularly lipids and oils, from natural materials. It is non-toxic, non-explosive, widely accessible at high purity, easily removed from the extracted product, and has a broad range of solvent characteristics at various pressures and temperatures [41]. The extraction process is also feasible at close to room temperature and is an excellent procedure for extracting thermally sensitive compounds since the critical temperature and pressure must remain relatively low, at 31.1 °C and 73.8 bar, respectively [189]. SC-CO2 has recently been used to extract fat from BSFL, proving to be a viable option for further processing of larvae feedstocks [44] and with SC-CO2 at 350 bar for 6 hours at 35 °C, the fat content in powdered form could be further optimised.

2.7.2. Enzymatic extraction

Enzymatic extraction is more extensively employed to extract valuable chemicals from BSFL. Enzymes are used to break down the cell wall of the raw material, this kind of extraction is typically more expensive than their chemical extraction counterparts. However, since less alkaline is required, no organic solvent is used, and less acidic solution is needed, enzymatic extraction techniques are more ecologically friendly than their counterparts [30].

The potential of employing an enzymatic-assisted protein extraction was also investigated, their results yielded maximal nitrogen solubilisation of approximately 60% in the best instance (with *Bacillus licheniformis protease*) [6]. Microorganisms such as *Lactobacillus* are used in other enzymatic extraction methods [190], *Pseudomonas aeruginosa* K-187 [191] and *Bacillus subtilis* [192] may be used to decrease chitin degradation and contaminants to a level that is acceptable for a particular application [186]. However, the ultimate result of the Life Cycle Analysis (LCA) of BSFL extraction using chemical or enzymatic methods indicates that chemical extraction is more efficient than its equivalents. One comparison study indicated that the enzymatic extraction technique could only yield 10%, 67%, and 35% lipids, proteins, and chitin purity, respectively, while the chemical extraction technique yielded 87% lipid, 84% proteins, and 92% chitin purity. Also, the mechanical extraction method yielded 87% lipid, 84% proteins, and 92% chitin purity [30]. The literature has shown that enzymatic extraction is not cost-competitive yet compared to mechanical and chemical.

2.8. Human use of BSFL products

Products from BSFL are not very widespread as of this day; however, the topic is gradually evolving more recently, especially for human foods. According to food futurists, insects will increasingly be used as alternative human food sources. Inspect species that have been researched and are the easiest to raise are not always the most sustainable, acceptable, or tasty. Conversely, the BSFL can effectively convert a broad range of organic resources, including food waste and manure, into protein [193]. Scientists are testing larvae fat as a substitute for butter in waffles, cakes, and cookies, claiming that the fat from insects is more sustainable and ecologically friendly than dairy fat and that taste testers cannot tell the difference [34]. BSFL fat contains about 70% saturated fatty acid, with lauric acid being the most prevalent (>40%)

[194]. Lauric acid has nutritional benefits since it is more easily digested than butter. At room temperature (20°C), it generally becomes solid and also inhibits the development of gram-positive bacteria, fungi, and viruses [140].

A few researchers from South Africa are trying to change food concepts by using insects as an alternative protein source. They make BSFL milk, called Entomilk™, and ice cream from it [195]. Beer is also another product from BSFL for human consumption. The beer, a combination of cricket and BSFL, was developed through a collaboration between the ANU Research School of Biology and an Australian beer company [196]. The nutritional value of insects as a food source is tabulated in **Table 2.11,** and the possible foods produced from BSFL sources are presented in **Fig. 2.18** [34, 195].

Besides food for human consumption, using additive manufacturing technology, chitin from BSFL has also been used in the circular manufacturing of bio-composites via bioconversion to develop a 3D replica of fungus-like adhesive materials (FLAM) [197]. The research on using BSFL for human food is still progressing, and it still needs ample time for the market to reach critical mass for the demand for this kind of food.

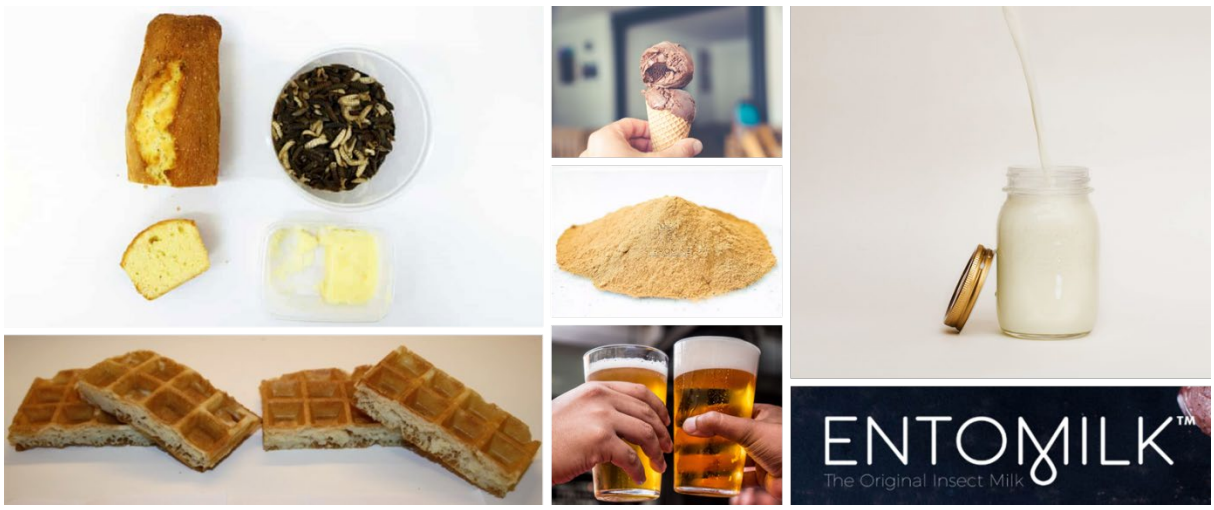

Fig. 2.18: Human nutrition from BSFL sources.

Table 2.11: The nutritional value of insects as a source of food.

Insects	BSFL	BSFL	BSFL	Cricket	Cricket	Mealworm	Cricket	BSFL + Cricket
Food Type	Pet Food	Butter	Milk	Flour	Burger	Fitness Bar	Pasta	Beer
References	[198]	[34]	[195]	[199]	[200]	[33]	[201]	[196]
Average quantity per	100gg	100 g	N/A	20gg	100 g	100 g	100 g	N/A
Energy	1790 kJ	N/A	N/A	N/A	1180 kJ	1623 kJ	1587 kJ	N/A
Protein	17.2 g	N/A	N/A	13 g	20.8 g	18g	15g	N/A
Fat, Total	14.9 g	N/A	N/A	4.5 g	19 g	13.8g	6.2 g	N/A
- Saturated	5.1 g	70g	N/A	1.5 g	2.1 g	2.9g	1.7 g	N/A
- Monounsaturated	4.5 g	N/A	N/A	0.92 g	N/A	N/A	N/A	N/A
- Poly Unsaturated	5.0 g	N/A	N/A	0.15 g	N/A	N/A	N/A	N/A
- Trans	0.3 g	N/A	N/A	0.05 g	N/A	N/A	N/A	N/A
Carbohydrates	55.6 g	N/A	N/A	1 g	4.5 g	44.8 g	64 g	N/A
- Sugar	7.3 g	N/A	N/A	0	1.4 g	39g	3.8 g	N/A
Sodium	20 mg	N/A	N/A	85 mg	1.6 g	0.26 g	0.54 g	N/A
Moisture	8.3 g	N/A	N/A	1.328g	N/A	N/A	N/A	N/A
Ash	4.0 g	N/A	N/A	1.12	N/A	N/A	N/A	N/A

2.9. Patent search and review

This section critically evaluates the patented innovation in utilising BSFL for converting food or agricultural waste into value-added products. The research used the World Intellectual Property Organisation (WIPO) database, a leading global intellectual property information and services repository. Analysis indicates a slower-than-anticipated advancement in BSFL-related patent technology compared to journal publications. The methodology for the patent search and selection process is depicted in **Fig. 2.19.** Guided by the PRISMA statement and illustrated in the figure, this systematic patent review was conducted using the latest available data as of May 2021 [202]. Initially, 350 patents were identified, with 3 excluded due to irrelevance and 29 for duplication, leaving 318 for detailed examination. After further exclusions of non-English patents and duplicates, 302 patents related to BSFL were finalised for analysis, covering patents published between January 2010 and December 2020. Exclusions included patents not in the WIPO database, those needing more titles or abstracts, and some non-English texts due to database limitations. The final set of patents was categorised into proteins, lipids, chitin, and other uses, focusing on the sequential extraction and characterisation of these components from BSFL. Findings revealed 85-98% amino acid contents, 40-47% lipid contents, and 3-4% chitin levels, as given in **Fig. 2.20** [121].

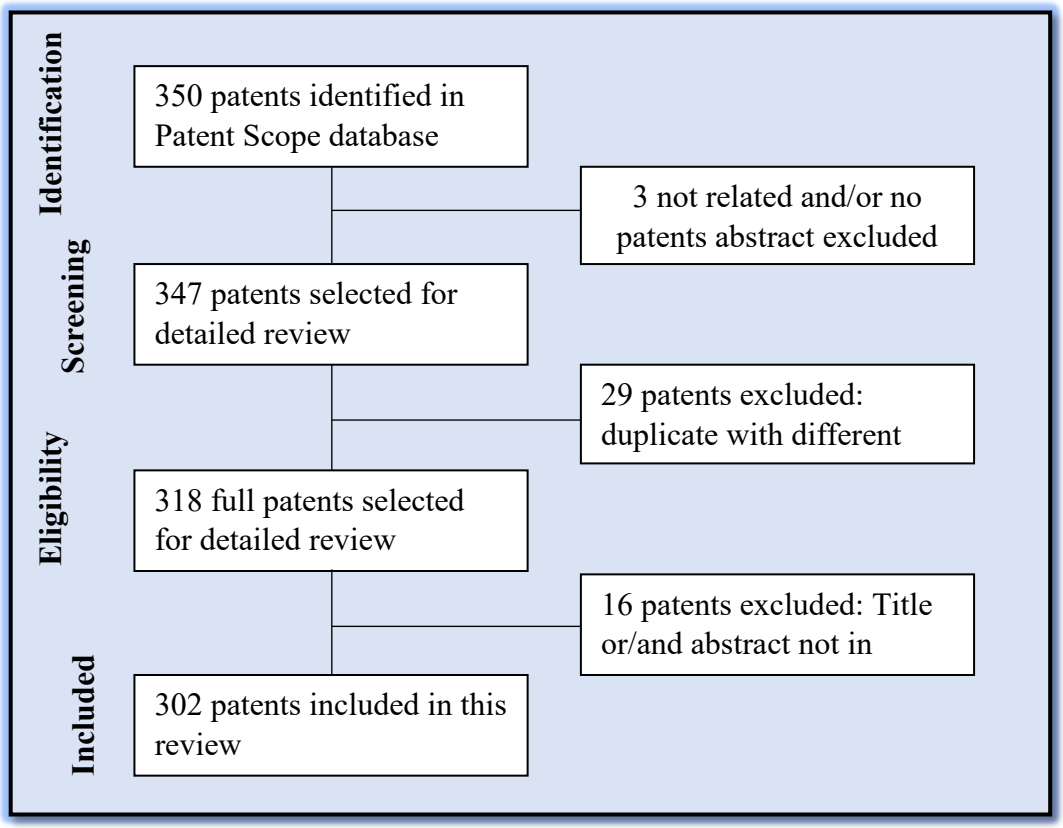

Fig. 2.19: Workflow for the selected patent search process.

2.9.1. Patent landscape

This patent analysis, focusing on the period up to 2021, includes 302 patents related to BSFL technology. Most of these patents originated from China (253), followed by South Korea, the United States, and Russia with 14, 14, and 5 patents respectively. Additionally, 11 other countries contributed to this patent pool, albeit in smaller numbers. The distribution of patents by country, the distribution of patents by country, the classification of patents published on BSFL patent innovation vs country, and the distribution of patents by Country are illustrated in **Fig. 2.21**: (**a**) (**b**) (**c**) and (**d**), respectively—a separate graph for China due to its disproportionately high contribution. The first BSFL-related patent was filed in 2010, with a peak of 106 patents in 2018. The breakdown of patents by-product derived from BSFL is as follows: proteins (160 patents), lipids (26 patents), chitin (5 patents), and other

innovations (128 patents). This upward trend in BSFL patent filings is likely to continue due to growing environmental concerns and the rise of the circular economy.

2.9.2. Technology updates

Potential commercialisation generally refers to products made using the technology available in the patent database. This typically includes current developments concerning the available commercialised product or a new product that claims something potentially to be commercialised in the patent database. The product's commercialisation potential could also include the outcome of these patent-diverse technologies as well as the existing product that is already in the market but with some innovation in production that is more efficient. Recent patent developments regarding the product outcome that can be commercialised from BSFL-patented inventions are discussed below. Detailed technology updates about BSFL products are presented in **Table 2.12**.

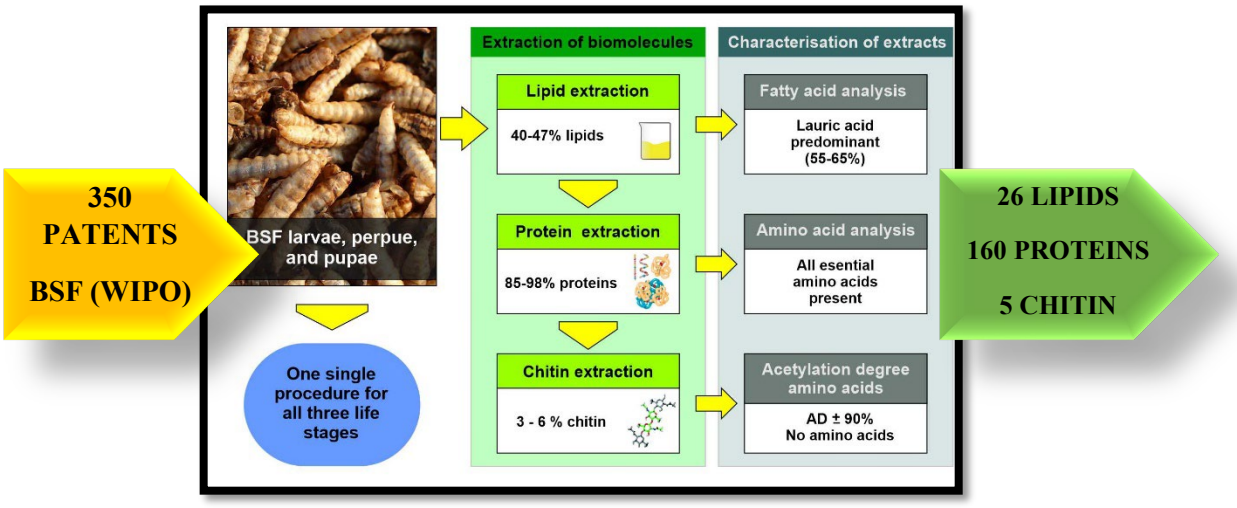

Fig. 2.20: Patents search and categories.

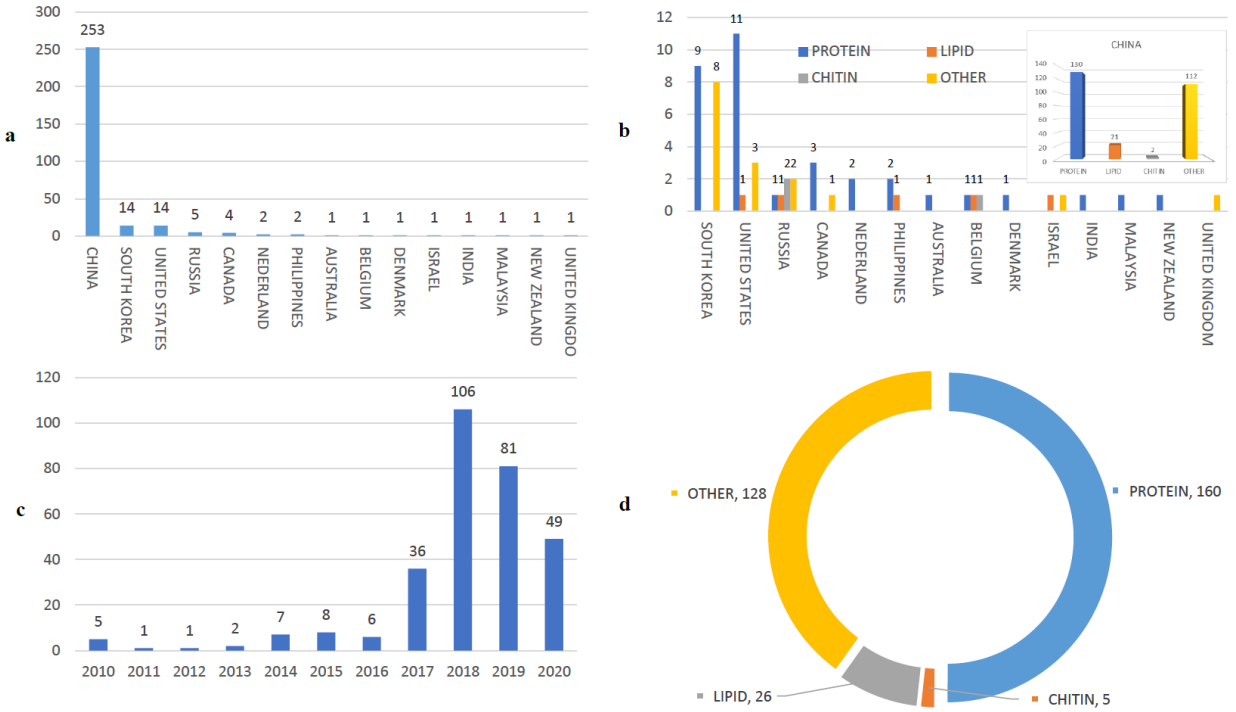

Fig. 2.21: (a) The distribution of patents by country, **(b)** Classification of patents published on BSFL patent innovation vs country, **(c)** Distribution of patents by Country, and **(d)** Categorisation of patents published on BSFL from 1990 to 2020.

Of the 350 patents identified in BSFL technology, 302 are pertinent to this study. A systematic analysis reveals that China is the predominant contributor to BSFL-related patent documentation, followed by South Korea, the United States, and Russia. Most of these patents concentrate on animal feed and protein extraction applications, with a significant number also focusing on lipids and chitin or chitosan derivatives. Despite the technology's potential to advance the biological aspect of the circular economy, there has been a noticeable decrease in patent publications since 2018. Crucially, this review indicates an absence of patents specifically related to the extraction of BSFL utilising SC-CO2, a gap this study aims to address.

Table 2.12: Technology updates concerning BSFL patent invention.

Group	Date	Patent Title	Patent ID	Finding Innovation
Protein	28.09.2018	Application of black soldier fly larvae to feed for improving meat quality of aquatic products.	CN231666276	The innovation here is that rather than using raw BSFL larvae, the inventor aimed to use BSFL larvae powder instead. The patent claims that the powder is high in nutrients and proteins essential to the aquatic product, and the inventors believe this product has good prospects in the market.
	20.10.2020	Method for breeding giant spiny frogs by using black soldier flies	CN310432875	The patent stated that by mixing the BSFL eggs, pupae, nymph and adult with vegetable leaves in feeding the frog, and claimed that by using the BSFL for feeding, the survival rate of the giant spiny frogs would be enhanced.
	14.01.2020	Pigeon feed was added with black soldier fly polypide protein and preparation method thereof	CN282390859	This patented innovation explains that 5 to 10% of BSFL polypide protein is mixed with puffed corn, rice flour, soybean, and plasma protein powder and reduces the cost of diet, increasing survival and weight gain of young pigeons faster.
Lipid	10.11.2010	Application of black soldier fly larvae as oil-crop insect	CN84075436	This oil is edible or can be used for biodiesel or other chemical industries. The BSFL oil content is about 30 – 35% and includes various unsaturated fats, which are a high-quality health oil required by the human body.
	26.04.2019	Lipid type antibacterial composition, extraction method, detection method and application	CN241955413	This patented innovation mentions using one of the lipids for anti-bacterial and claims that the product can be used for Escherichia coli and enteritis-type salmonella.
	26.11.2020	Modified black soldier fly larvae oil with modified lauric acid for treatment against	WO2020234884	This patent provides methods, formulations, and production systems by extracting BSFL larvae oil and subsequent use of

		biofilm formation and microorganism growth.		the oil for dermal, oral, topical and industrial therapeutic applications and medical use.
Chitin	25.02.2019	Method of obtaining chitin from *Hermetia illucens* black soldier fly larvae.	RU238341407	This patent explains in detail how to obtain chitin from BSFL larvae. This invention aims to simplify the process of producing chitin from BSFL.
	29.07.2020	Method of producing covalent-linked chitosan-melanin complex from black soldier fly *Hermetia illucens*	RU301723456	This patented innovation is related to producing a covalent chitosan melanin complex using BSFL. These combinations can produce this patent claiming complex chitosan-melanin biopolymers.
	02.05.2019	A method for separating larvae in a pulp and a liquid fraction	WO2019081067	This patent claims had developed a procedure for separating the BSFL into a liquid and powdery fraction. The inventors claim that using BSFL as feedstocks can create a pulp high in chitin.
Other	21.06.2019	Method of using edible insects to produce novel insect tea	CN246693909	The patent innovation has been invented using edible BSFL insects to make new tea.
	11.01.2019	Application of insect culture products in cat litter preparation	CN236590496	The innovation of the patent is about using the BSFL product for cat litter treatment.
	30.04.2019	Composite organic fertiliser, and preparation method and application thereof	CN242425028	The patent is about the production of organic fertiliser composite and its method of preparation using BSFL as raw materials.
	13.09.2018	Skincare products containing *Hermetia illucens* extract	US225645353	The patent presented the production of the skincare product using BSFL.

CHAPTER 3: MATERIALS AND METHODS

This chapter is outlining the materials and methods employed in the study, this section provides comprehensive information on SC-CO2 extraction, cell culture, as well as the materials for chitin and chitosan extraction, and the synthesis of hydrogels. The procedures encompass lipid extraction and optimisation, cell culture tests, isolation of chitin and chitosan, along with their characterisation using techniques such as FTIR and SEM. Additionally, it details the synthesis and analysis of hydrogels. Emphasising the significance of rigorous statistical analysis, the chapter underscores the need to validate the research findings thoroughly.

3.1. Materials

The material used was fresh BSFL purchased from Future Green Solution, Perth, Western Australia. This is a live insect that was used in this study. Meanwhile, the chemicals used, toluene and acetyl chloride, were purchased from Merck KGaA, Germany. The methanol anhydrous, 99.8% and FAME Mix (Supelco 37 Component) from Sigma Aldrich. Dichloromethane from Chem-Supply, Australia, Potassium Carbonate was purchased from Ajax Finechem, and methyl heptadecanoate (C17:0) for the internal standard from PolyScince Corporation, USA. The other reagents were distilled water, n-hexane, phenolphthalein, ethanol, and demineralised water. All the chemicals and reagents were of a high enough quality to be used in an analytical standard. According to new market research by Meticulous Research, the global BSFL market will develop at a 33.3% compound annual growth rate from 2019 to 2030, reaching US$2.57 billion in a decade. This species is native to the neotropical area but has spread across all continents in recent decades, becoming virtually worldwide [102]. BSF may be found in the US, Europe, and Russia's Krasnodar

Territory [7-9]. It also exists in the Afrotropical, Australasian, East Palaearctic, Nearctic, North African, Southern African, and Indo-Malayan realms [10-14]. A comprehensive explanation of BSF is provided in subsection 2.5. The life cycle and phases of BSF development, as well as the average length of each stage, are shown in **Fig. 2.9.**

3.1.1 SC-CO2 Extraction Material

Supercritical carbon dioxide (SC-CO2) extraction in the context of BSFL represents a fascinating intersection of green technology and innovative solutions for waste management and nutrient recovery. **Fig. 3.1**. illustrates the classification of sequential extraction and characterisation of proteins, lipids, and chitin from BSFL, prepupae, and pupae found to have 85 - 98% amino acid content. At the same time, the lipid contents are between 40 - 47%, whereas the chitin is only between 3 - 4% [121]. Furthermore, the fresh BSFL was purchased from Future Green Solution (Perth, Western Australia). Toluene and acetyl chloride were purchased from Merck KGaA (Germany); anhydrous methanol, 99.8% and Fatty Acids Methyl Ester (FAME) Mix (Supelco 37 Component) from Sigma Aldrich; dichloromethane from Chem-Supply (Australia); potassium carbonate from Ajax Finechem; and methyl heptadecanoate (C17:0) for the internal standard from PolyScince Corporation (USA). All the chemicals and reagents were of a high enough quality to be used in an analytical standard. SC-CO2 extraction's application in processing BSFL is a promising approach that embodies the principles of a circular economy. It offers a sustainable method for managing organic waste and extracting valuable nutrients and compounds, potentially revolutionising waste management, agriculture, and industrial processing.

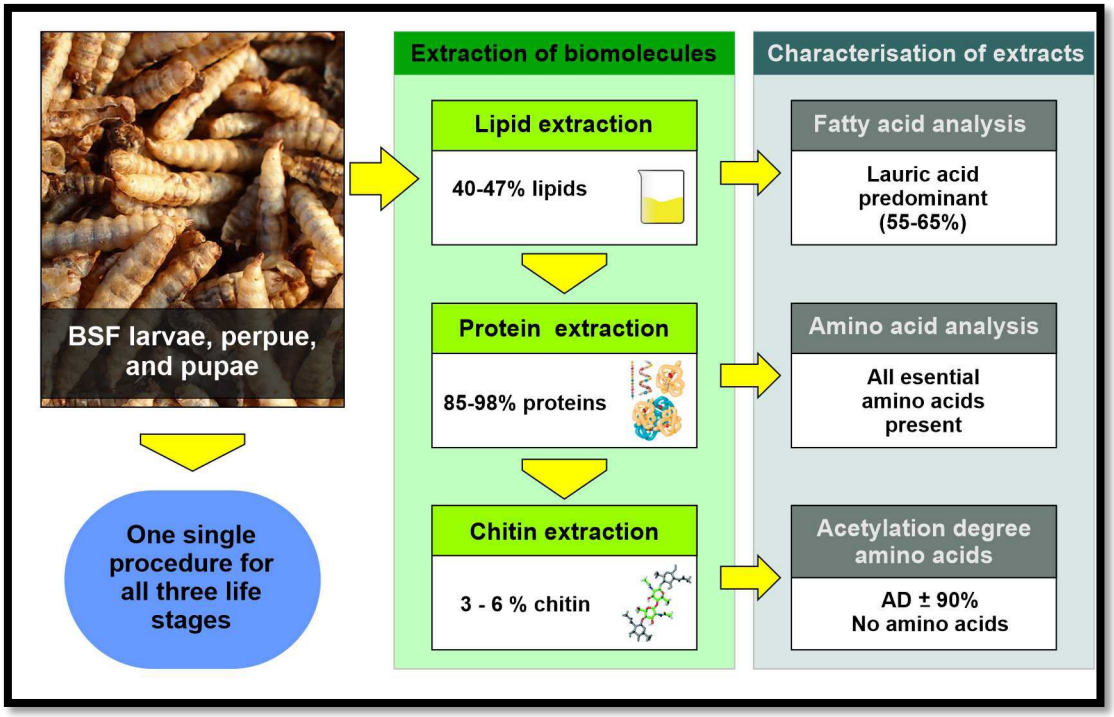

Fig. 3.1: The BSFL, prepupae, and pupae bioconversion product.

3.1.2 Cell Culture Material

The cell bank of the University of Sydney obtained fibroblast 3T3 cells. Dulbecco's modified Eagle's medium (DMEM, Thermo Fisher), DMSO, phosphate buffer saline (PBS) (Sigma), fetal bovine serum (FBS), Trypsin (Thermo Fisher),, 4% paraformaldehyde (Sigma), bovine serum albumin (BSA, Gibco Laboratories), MTS (3-(4,5-dimethylthiazol-2-yl)-2,5-diphenyltetrazolium bromide) assay (Promega), Tween-20 detergent (Sigma), Triton X-100 (Sigma), DAPI and phalloidin (Abcam). All the chemicals and reagents were of a high enough quality to be used in an analytical standard.

3.1.3 Chitin and Chitosan Extraction Material

Various specific chemicals were carefully selected in the experimental setup for their high purity and efficacy. These include sodium hydroxide (NaOH) and acid hydrochloride (HCl), which were procured from Chem Supply, known for its reliable chemical supplies.

Additionally, chitosan was utilised, a versatile biopolymer derived from prawn shells with a deacetylation level greater than or equal to 75%. This chitosan is notable for its high degree of purity and consistency in composition. Alongside this, chitin, another valuable biopolymer extracted from prawn shells, was sourced from Sigma Aldrich, a reputable provider known for its stringent quality control and superior-grade chemical products. These chemicals were selected by the need for analytical grade reagents, ensuring the highest precision and reliability in experimental results. Analytical grade chemicals are characterised by their high purity and are typically used in scientific research where accuracy and consistency are paramount. Using such high-quality reagents is crucial in obtaining valid and reproducible data, especially in experiments where chemical reactions and interactions are observed and analysed. The procurement of these chemicals from trusted suppliers like Chem Supply and Sigma Aldrich further underscores the commitment to maintaining rigorous standards in the experimental procedures.

3.1.4 Hydrogel Synthesis Material

The selection of chemicals for the experiment was purchased from reputable suppliers to ensure optimal quality and consistency. Sodium hydroxide (NaOH) and acid hydrochloride (HCl) were acquired from Chem Supply, a trusted source known for its reliable chemical products. From Sigma Aldrich, a 50 wt % Glutaraldehyde (GA), Acetic Acid at 99% purity, and lysozyme extracted from chicken eggs were procured, each meeting stringent quality standards. Furthermore, gelatine was sourced from Ajax Finechem, which is recognised for its high-grade biochemical products. Additionally, a phosphate buffer saline with a 20x concentration (PBS, pH 7.4) was obtained from Rowe Scientific Pty Ltd, another esteemed supplier in the field. All these chemicals and reagents were confirmed to be of analytical grade, ensuring high precision and reliability in the experimental outcomes. This careful

selection underscores the commitment to maintaining rigorous scientific research and experimentation standards.

3.2. Methods

This section discusses a range of intricate procedures and analyses. It encompasses lipid extraction and optimisation, starting with moisture determination, sample preparation, and assessing acid value and fatty acid percentage, followed by using supercritical CO_2 and solvent extraction techniques. This is complemented by an experimental design for optimising SC-CO2 extraction and a detailed fatty acids analysis. The section also covers in-vitro cell culture tests, including cell counting and proliferation assays, detailed cell morphology analysis with DAPI and Phalloidin staining, and wound healing migration assays. For the isolation of chitin and chitosan, the study describes the extraction process, deacetylation, and subsequent characterisation through elemental analysis, FTIR, TGA, SEM, and XRD. Additionally, the synthesis and characterisation of chitosan-based hydrogels are discussed, involving various analyses like FTIR, TGA, swelling, and biodegradation tests. The section concludes by emphasising the need for extensive statistical analysis to interpret the diverse experimental results, highlighting the comprehensive and systematic approach of the research.

All experiments were conducted at the School of Chemical and Biomolecular Engineering (CBE) and the School of Biomedical Engineering (BME) at The University of Sydney. The primary location for Chapters 4, 5, and 7 was Lab 429 in the CBE. Additional analyses were performed in various laboratories, including the School of Chemistry for fatty acid analysis using GCMS and the Solid State & Elemental Analysis Unit at the Mark Wainwright Analytical Center, University of New South Wales (UNSW), for elemental analysis. XRD analysis was conducted at the Sydney Analytical Center. Cell culture activity experiments

for Chapter 6 were conducted at the School of Biomedical Engineering at the University of Sydney.

3.2.1 Lipid Extraction and Optimisation

This subsection discussed the lipid extraction and optimisation process from BSFL. It begins with determining the moisture content of BSFL, which is crucial for efficient extraction. The larvae are then prepared through grinding and homogenising to maximise lipid yield. Key quality indicators, such as the acid value and free fatty acid percentage, are measured to assess lipid quality. Two extraction methods are compared: the environmentally friendly SC-CO2 extraction and conventional solvent extraction. An experimental design optimises SC-CO2 extraction conditions, focusing on variables like pressure, temperature, and flow rate. Lastly, the extracted lipids undergo fatty acid analysis, typically using Gas Chromatography-Mass Spectrometry (GC-MS), to profile their fatty acid composition, which is crucial for understanding their potential applications. This section emphasises a strategic approach to lipid extraction, which is pivotal for sustainable waste management and resource recovery.

3.2.1.1 Moisture Content Determination

The moisture content of the BSFL was ascertained utilising the Association of Official Analytical Chemists (AOAC) method [203]. This measurement performed a 24-hour incubation in an oven set at 105 °C, conducted in triplicate, with the resultant average value being documented. The BSFL exhibited a dry matter content of 34%, aligning closely with findings from a prior study [6]. This experiment has been meticulously replicated to ensure accuracy.

3.2.1.2 Sample Preparation

To initiate the extraction method, the experiment commenced with a fresh BSFL treatment, which underwent a preliminary heat treatment in an oven at 60 °C for 48 hours. This step was crucial to remove any existing free moisture, continuing until a consistent weight was attained. Subsequently, the sample was finely ground in a mortar and meticulously stored in airtight plastic bags within a laboratory freezer, preserving it for subsequent extraction processes.

3.2.1.3 Acid Value and Free Fatty Acid Percentage

The acid value (AV) is defined as the quantity of free fatty acid (FFA) in the oil that requires a calculated mass of potassium hydroxide (KOH) to neutralise. The acidity is an expression of the content (mg/g of KOH) of free fatty acids in fat/oil. Briefly, 1 g of BSFLO was weighed and transferred into 150 mL of the beaker. 25 mL of absolute ethanol was added to the sample and stirred until the oil dissolved. The solution was then treated with 3 to 5 drops of phenolphthalein. Titration was performed with 0.1 N KOH until the solution coloured pink (the colour remained the same for 20 seconds). Equations 3.1 and 3.2 were used to obtain the AV and FFA% of BSFLO respectively.

$$equal Acid\ Value\ (AV) = \frac{(V_s - V_b) \times N \times M}{Wt} \quad (3.1)$$

Where,

V_s = tritation volume of sample,

V_b = titration volume of blank,

Wt = weight of the BSFL oil,

N = Molecular weight of KOH and

N = Concentration of KOH

Then, the FFA % can be stated on the scale of lauric acid.

$$FFA\ \% = \frac{AV \times M\ KOH \times MMFFA}{10 \times Wt} \quad (3.2)$$

Where,

AV = Acid Value

M KOH = Molecular weight of KOH

MMFFA = Average molar of fatty acids (Lauric Acid) , 200.32 g/mol

Wt = weight of the BSFL oil

3.2.1.4 Supercritical CO_2 Extraction

The instrumental set-up of the SC-CO2 extraction process consists of a unit of the SC-CO2 extractor from the Spe-ed SFE Basic completed with the high-pressure CO_2 pump, extraction vessel, band heater, temperature indicator, collection vial, rotameter, and other accessories. The equipment ware supplied by Applied Separation, Allentown, USA. The schematic diagram of SC-CO2 unit using Spe-ed SFE Basic is presented in **Fig. 3.2**. The Spe-ed SFE Basic instrument can withstand pressures up to 690 Bar and temperatures up to 240 ºC. Within this range of pressures and temperatures, a wide range of extractions may be conducted. A liquefied carbon dioxide cylinder (G Size, Gas Code: 081 with gas composition is greater than 99.9% CO_2) and a compressed air cylinder were supplied by BOC company, Sydney. Compressed air is necessary to drive the pump. Maximum air pressure should be 125 psig (8.6 Bar); the minimum is 100 psig (6.9 Bar). The pump required recirculating coolant, or a chiller supplied by Julabo (Model F12) for CO_2 pressurisation. The recirculating coolant (80% Ethylene Glycol (GE) – 20% Water) should be maintained at a controlled temperature of 0 º C. Polypropylene (PP) wool or frit was used before loading the sample into the extraction vessel. Two grams (2 g) of ground BSFL samples were loaded and tamped, followed by some PP wool/frit. Subsequently, the Spe-ed matrix supplied from Applied Separation was loaded into the extraction vessel, followed by the PP wool/frit for

finishing. The parameter, such as the temperature and pressure of the experiment, is discussed in Section 3.2.1.6.

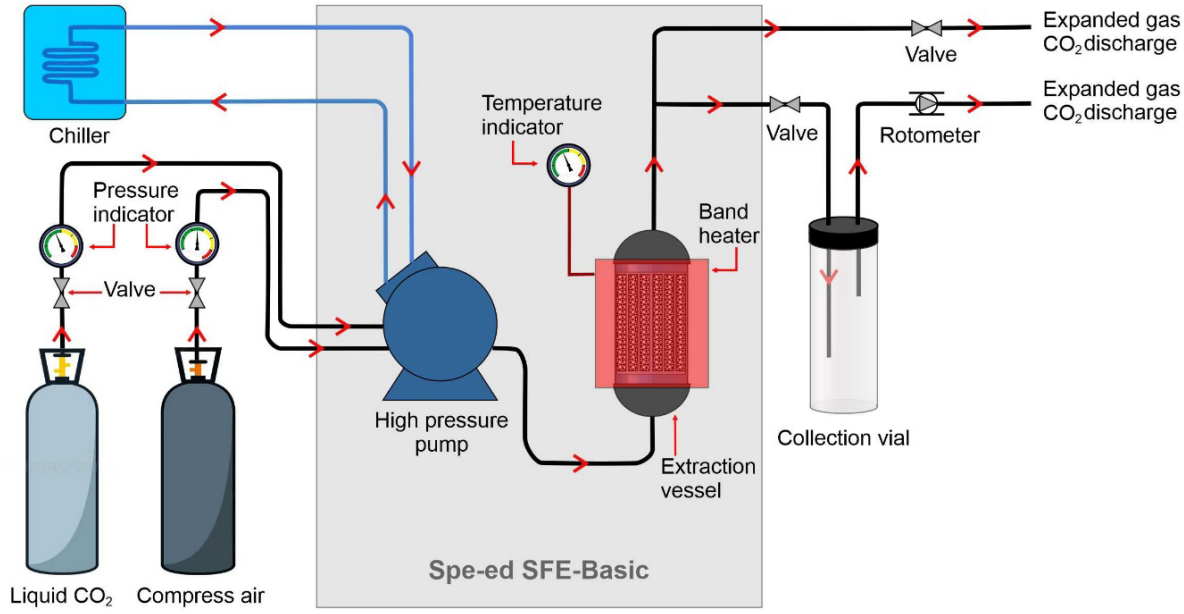

Fig. 3.2: Schematic diagram of supercritical CO_2 unit using Spe-ed SFE Basic.

To guarantee that the supercritical fluid diffuses evenly throughout the sample matrix, the sample bed was packed tightly. The extraction vessel was placed in the Spe-ed SFE Basic, and the chiller temperature was reduced to 0 ºC. The CO_2 could flow through the system then be pumped into the extraction vessel and was pre-liquefied by transient through the band heater where the pressure and temperature were kept at the desired conditions. The supercritical state of CO_2 was reached at this point. The oil extracted from the larvae was collected in a collecting container. The larvae oil was weighed as yield and stored in the refrigerator for further examination after the required extraction time was reached. The total larvae oil yields were calculated using the following equation, which was expressed as a percentage of the BSF larval sample on a dry basis:

$$\text{Oil yield (\%)} = \frac{\text{Mass of extracted larvae oil}}{\text{Mass of ground BSFL}} \times 100 \quad (3.3)$$

3.2.1.5 Solvent Extraction

The BSFL oil was extracted using the Folch Method with minor modifications [23, 188]. A sample BSFL of 75 mg was homogenised with 1:20 (v/v) of dichloromethane:methanol (2:1, v/v) in a 2 mL Eppendorf tube. The sample was vortexed for 10 seconds using the vortexes with medium speed and centrifuged sample for 1 minute with the maximum speed of 20,000rpm. The liquid phase was pipetted and rinsed with 0.2 volume of 0.9 % NaCl solution before the solid phase was set aside. The sample was then centrifuged again for 1 minute at a similar speed to induce phase separation. The bottom phase was then transferred to another Eppendorf tube. To get the maximum larvae oil yield, the solid phase was homogenised again, and repeating the process, transferring the bottom phase to the Eppendorf tube containing the larvae oil. The solvents were evaporated under the fume cupboard until the oil sample dried. Weighted the oil sample and calculated the yield by using Equation 3.3. The extraction was carried out in triplicate and resulted in 30% oil content, on a dry basis which is less than the previous study [121].

3.2.1.6 Experimental Design for SC-CO2 Optimisation

The optimisation of the SC-CO2 extraction parameters was examined using response surface methodology and optimised using the Box Behnken design (BBD) through MODDE 13.0 software (Sartorius). The model comprised three factors, which are pressure from 150 – 400 bar (X_1), temperature from 30 – 50 ^{o}C (X_2), and extraction time 1 – 3 hours (X_3) to optimise the yield (Y) of the larvae oil and the constant flowrate of CO_2 has been selected around ~1.2 lpm. All of the variables and ranges were determined based on preliminary experimental and screening findings obtained from SC-CO2 oil extraction from BSFL literature [44]. Initially,

the pressure range setting was between 200 – 400 bar, which is for screening purposes, and found that the identified pressure range was not in the envelope of the optimisation of the larvae oil. The pressure was lowered down from 200 to 150 bar, and the result obtained from the optimisation was within the envelope of the response surface created through the modelling**. Table 3.1** shows the independent parameters ranges, low, middle and high levels, coded as -1, 0 and +1, respectively. The experimental design provides 3 centre points and a total of 17 runs of experiments. The visual and physical properties of the BSFL are presented in **Fig. 3.3**.

Table 3.1: Independent variables and coded levels for SC-CO2 extraction.

Independent Variables	Symbol	Coded Levels		
		Low (-1)	Middle (0)	High (+1)
Pressure (Bar)	X_1	150	300	400
Temperature (°C)	X_2	30	40	50
Extraction Time (hours)	X_3	1	2	3

Three responses were assessed using the experimental design which were yield of larvae oil (Y_1), lauric acid (C12:0) composition (Y_2), and SFA ratio (Y_3). The second-order polynomial (Equation 3.4) was used to describe the relation of independent coded variables (X_1, X_2 and X_3) to the responses.

$$Y = \beta_o + \sum_{n=1}^{k} \beta_n X_n + \sum_{n=1}^{k} \beta_{nn} X_n^2 + \sum_{n-1}^{k} \beta_{nm} X_n X_m \qquad (3.4)$$

Where β_o is the value of the fixed response at the central point, while β_1, β_{nn} and β_{nm} are the linear, quadratic and interaction terms, respectively and k is the number of variables.

3.2.1.7 Fatty Acids Analysis

The BSFL oil was extracted using SC-CO2 and solvent extraction techniques, and the fatty acids were derivatised before gas chromatography analysis. Briefly, the resulting larvae oil extracted were weighed 3 mg into a 20 mL vial and 150 ul internal standard solution (2mg/mL methyl heptadecanoate in dry toluene) and 2.85 mL of dry toluene were added. This is to create a 1000 ppm of lipid concentration. Methanolic HCL (acetyl chloride: methanol (1:10, v/v)) was freshly prepared and 180 uL of methanolic HCL was added into the vial. The vial was tightly capped and vortexed at a slow speed for 10 seconds. The vial was then heated at 70^{o}C for 1 hour. After the methylation occurred, the vials were cooled to room temperature and 1 mL of 6% K_2CO_3 was added and vortexed at high speed for 5 seconds. The top layer was transferred to a 2 mL centrifuge tube and spun at 20,000 rpm for one minute. Whereas The upper layer, which comprised the fatty acid methyl esters, was aspirated into GC-MS vials. The subsequent FAMEs were examined with GC-MS (Perkin Elmer Clarus 680 GC, with the following setting in **Table 3.2**. Under the same circumstances, the fatty acids were characterised by assessing their retention times to the FAME standards.

Table 3.2: GC-MS setting for the fatty acid analysis.

Parameter	Setting
Column	Perkin Elmer Elite 5ms- 30m x 0.25 mm ID x 0.25um film thickness
Carrier gas	Helium at 1.3mL/min
Ratio split injector	10:1 Split, 0.5uL injection
Oven Program	90 ºC held for 2 minutes, 10ºC/min to 190 ºC, hold for 1 minute, 3ºC/min to 250ºC, hold for 3 minutes (total GC time 38 minutes)
GC/MS interface temp.	250 ºC
MS Source temp.	150 ºC
Oven Equilibrium Time	0.5 minutes
Ion Source MS	Positive ion EI, 70 eV
Scan Type MS	Solvent delay 0-2 minutes, then scan from 45-600 m/z over 200 ms and a 100 ms interscan delay

3.2.2 Cytocompatibility of BSFL Oil Test – Invitro Test

Mouse fibroblasts (3T3 cell line) were cultured in complete media containing of DMEM, 10% fetal bovine serum (FBS) (Gibco), L-Glutamine (1%) and sodium pyruvate (1%) and 100 mg/mL penicillin. Cultures were maintained at 37 ºC with a CO2 supply of 5% CO_2. The cells were used in the experiments upon attaining 70% confluence, BSFLO was diluted in complete media, and dose dependent effect of oil on cell growth and proliferation was evaluated. five (5) different concentrations (1, 2.5, 5, 7.5 and 15 µl/mL) were initially used for the cytotoxicity test. All the stock solutions of BSFLO concentrations were prepared under sterile conditions. The mitochondrial activity of the fibroblasts cultured with oil was investigated by colorimetric assay which identified the conversion of 3-(4,5-dimethylthiazol-2-yl)-2,5-diphenyltetrazolium bromide (MTS Promega, Madison, WI, USA) to formazan as detailed previously [204]. Briefly, the 3T3 cells were seeded in 24

well plates at a concentration of 1.5 x 104 cells/mL per well using complete DMEM culture media supplemented with different concentrations of BSFLO as mentioned above and untreated cells were used as control. This control serves as a negative control. The cells were allowed to grow for 1, 3 and 7 days at 37 °C in a humidified atmosphere of 95% air and 5% CO2. At the end of each time point freshly prepared MTS reaction mixture was diluted in PBS at 1:5 (MTS: PBS) volume ratio and added to the wells cultured with cells and oil and incubated at 37 ^{o}C for 4 h. Three replicates of each oil concentration were tested at each culture time point. After 4 h of incubation, the purple formazan crystals were transferred into 96 well plates for absorbance reading. The wavelength was recorded at 490 nm (sample) using SPECTROstar Nano® Absorbance Plate Reader by BMG LABTECH. The experiments were conducted in triplicates. The results were shown as means OD. The percentage proliferation of the cells was calculated by Equation 3.5:

$$Proliferation\ \% = \frac{OD\ of\ untreated\ cells - OD\ of\ treated\ cells}{OD\ of\ untreated\ cell} \times 100 \quad (3.5)$$

Where, OD = Optical density

3.2.2.1 Microscopy for Cell Morphology - DAPI staining

The morphology of the cells was using 8-well chamber slide to seed cells at a low density ranging from around 5,000 to 10,000 cells per well. Following incubation for either 24 or 48 hours, the cells underwent three rounds of washing with PBS and were then fixed in 4% paraformaldehyde in PBS for 10 minutes without light. Subsequently, DAPI was added to the cells, which were incubated in darkness at room temperature for 15 minutes. After aspirating the DAPI solution, the cells underwent three additional washed rounds with PBS. Finally, the cells were submerged in PBS and preserved at -4°C until they were ready for microscopy. The visualisation was performed with an Olympus BX41 microscope, and the

images were captured with CSV1.14 software and a CAM XC-30 (Olympus Europa, Hamburg, Germany).

3.2.2.2 Cell Migration Assay

The 3T3 cells were seeded at a density of 200 x 104 cells/well in 12-well plates and incubated for 24 hours at 37°C for the cells to attach for the migration assay. After incubation, the cell layer was scraped in a straight line using a 1 mm pipette tip. The point was carefully kept perpendicular to the bottom of the well, and another line was scratched perpendicular to the first, resulting in a cross-shaped wound in each. Following the scratching, any cell debris was gently removed with PBS. The cells were then treated with BSFLO, placed in the incubator, and observed cell migration on the phase-contrast microscope. A microscope (Nikon ECLIPSE Ts2-FL with WiFi camera) was employed to observe the image every 4-8 hours until cells migrated to meet in the middle. The image was used to do the image analysis.

3.2.3 Isolation of Chitin and Chitosan

In this section, the 'Isolation of Chitin and Chitosan', the extraction and detailed characterisation of these biopolymers from BSFL are methodically presented. The process begins with the extraction of chitin, ensuring high purity, followed by its deacetylation to produce chitosan. For characterisation, elemental analysis determines the composition of these biopolymers FTIR spectroscopy is employed to elucidate their molecular structures, particularly focusing on functional group identification. TGA assesses the thermal stability and decomposition properties, crucial for application development. SEM reveals the surface morphology, providing microstructural insights. Finally, XRD analysis determines the crystallinity, essential for understanding material properties. This section highlights the

systematic approach in extracting and analysing chitin and chitosan, underpinning their potential in various scientific and industrial fields.

3.2.3.1 Chitin Extraction

The solid phase (defatted) and undefatted sample underwent a demineralisation process using the acidic solution at a solid ratio of 1:10 (m/v) with 1M HCL at room temperature for 1h under slow stirring conditions. After that, the samples were deproteinisation using the alkaline solution at a solid ratio of 1:25 (m/v) with 1M NaOH at 80 ^{o}C for 24 hr under stirring (150 rpm) (repeated until the colour was removed, which was about 3 times and more). Once the colour was faded and cleared, the sample was filtered and washed with demineralised water until the sample reached pH 7 and dried at 50 ^{o}C for 24 hrs. Finally, the total chitin content was calculated using Equation 3.6:

$$\text{Chitin (\%)} = \frac{\text{Mass of extracted chitin}}{\text{Mass of ground BSFL}} \times 100 \quad (3.6)$$

3.2.3.2 Chitosan Extraction (Deacetylation of Chitin)

Deacetylation was performed using the concentrated alkaline solution and a heat treatment to the solution (1:20 (m/v) sample in 50% NaOH, at 110 ^{o}C for 6 hours and stirring) to the extracted chitin in pressure-resistant glass vials. After that, the samples were filtered via water until the pH was neutral and dried for 24 hours at 50 ^{o}C. Finally, the total chitin content was calculated using Equation 3.7:

$$\text{Chitosan (\%)} = \frac{\text{Mass of extracted chitosan}}{\text{Mass of ground BSFL}} \times 100 \quad (3.7)$$

3.2.3.3 Elemental Analysis

Each extracted chitin sample's carbon and nitrogen concentrations were quantified through elemental analysis, specifically carbon-to-nitrogen ratio (C/N), using a Vario micro cube (Elementar, Langenselbold, Germany). To accurately determine the C/N ratio and

subsequently infer the average degree of acetylation (DA) [205], approximately 30 mg of the dry chitin sample was weighed and subjected to high-temperature combustion at 1150 °C. This process was calculated by Equation 3.8, ensuring precise calculation of the C/N ratio, which is pivotal in assessing the chemical composition and potential applications of the chitin samples:

$$DA\ (\%) = \frac{(C/N) - 5.14}{1.72} \tag{3.8}$$

3.2.3.4 Fourier-Transform Infrared (FTIR)

The FT-IR spectra of the extracted chitin and chitosan samples were analysed by Nicolet 6700 ATR0FTIR spectroscopy from 4000 to 600 cm^{-1}. Absorbance patterns corresponding to different wavenumbers were used to investigate the chemical bonds present in the samples. Equation 3.9 was used to assess the degree of acetylation (DA%) of chitin based on the FTIR spectra [205]:

$$the\ DA\ \% = \frac{\left(\frac{Area_{\ 1500-1700}}{Area_{\ 2700-3600}}\right)}{1.33} \times 100 \tag{3.9}$$

Where Area 1500 – 1700 represents the location of amid 1 band, Area 2700 – 3600 is the hydroxyl band, and the factor 1.33 is the ratio value for fully N-acetylated.

3.2.3.5 Thermogravimetric Analysis (TGA)

The TGA of the samples was performed using a TA Q5000 Thermogravimetric Analyser. For each analysis, approximately 15 mg of the sample was used. The temperature was progressively increased to 625 °C at a rate of 10 °C per minute under a controlled nitrogen atmosphere with a flow rate of 15 mL per minute. This systematic approach ensures precise thermal decomposition profiling of the samples, which is essential for understanding their thermal stability and composition under high-temperature conditions.

3.2.3.6 Scanning Electron Microscopy (SEM)

SEM pictures were captured with a Phenom XL microscope. Before imaging, the samples were prepared by coating them with a thin layer of platinum/palladium (Pt/Pd) alloy, specifically 1.5 nm of 80/20 wt% Pt/Pd, using a Sputter Coater HP208 Cressington. This coating enhances the electrical conductivity of the samples, which is crucial for obtaining high-resolution and clear SEM images, thereby allowing for detailed analysis of the surface morphology and microstructural characteristics.

3.2.3.7 XRD

X-Ray Diffraction (XRD) patterns of chitin and chitosan samples were studied for all chitin extracted from BSFL and also for the commercial chitin extracted from prawn using a PANalytical X'Pert Powder X-ray diffractometer system running at 45 kV, 40 mA and 2θ with a scan angle between 5° and 50 °C. Before the measurement, each sample was grounded in a mortar. The crystalline index value (CrI) was determined from the intensity (counts) at 15° (I_{am}, amorphous phase) and 19.3° (I_{110}) according to the below Equation 3.10 [206] :

$$CrI = \frac{I110 - Iam}{I110} \times 100 \quad (3.10)$$

3.2.4 Synthesis of Chitosan-based Hydrogel

The synthesis of the chitosan-based hydrogel with a combination of chitosan BSFL – gelatine – GA (CH-G-GA) started by dissolving 2% of chitosan extracted from BSFL in 1% acetic acid aqueous solution at ambient temperature, left all-night on a magnetic stirrer at 150 rpm. Next, 10% of the gelatine solution was formulated in distilled water at 40 °C. To make mixed hydrogels, CH-G, aqueous solutions of gelatine (10%) and chitosan (2%) were mixed with various weight ratios in a total volume of 10 mL. Every mixture was vortexed for 10 seconds at high speed to produce a homogeneous solution, and then 1% (w/w) of

glutaraldehyde was add up as a crosslinker. The solution was vortexed for another 10 seconds and put in a petri dish plate to form hydrogel scaffolds for 3 hours. After gelation, the hydrogel was dried at 35 ºC for 4 hours. Finally, all the hydrogel scaffolds were performed in triplicate.

3.2.4.1 Characterisation using FTIR

The FT-IR spectra of the commercial chitosan, chitosan derived from BSFL, gelatine, and CH-G-GA hydrogel samples were meticulously examined using a Nicolet 6700 ATR-FTIR spectrometer, scanning across a wide range from 4000 to 600 cm^{-1}. This analysis focused on identifying distinct absorbance patterns at varying wavenumbers, which are indicative of the specific chemical bonds present within each sample. This approach provided a detailed insight into the molecular structure and bonding characteristics of these materials.

3.2.4.2 Characterisation using TGA

Thermogravimetric analysis (TGA) was performed using a TA Q5000 Thermogravimetric Analyzer. For this analysis, approximately 15 mg of the sample was used. The temperature incrementally increased to 800 °C at a rate of 10 °C per minute in a controlled nitrogen atmosphere, maintaining a flow rate of 15 mL per minute. This procedure ensures a detailed understanding of the samples' thermal stability and decomposition behaviour under elevated temperatures, providing critical insights into their thermal properties.

3.2.4.3 Swelling Test

The swelling behaviour was examined by immersing the samples in excess PBS solution (pH 7.4). Dried hydrogels were weighed (W_0) and immersed in PBS solution at 37◦C. The swollen sample was extracted at regular intervals, the surface water was removed with filter

paper, and the samples were weighed (Wt) until they reached constant values. The swelling rate was calculated using Equation 3.11.

$$Swelling\ Rate\ \% = \frac{W_t - W_0}{W_0} \times 100\% \quad (3.11)$$

3.2.4.4 Bio-degradable test using enzyme

The degradation test of chitosan-based hydrogels (1 cm^2 = 1 cm x 1 cm) was performed in 15 mL phosphate-buffered solution (PBS, pH = 7.4) at 37 °C comprising 1.5 µg/mL lysozyme. The concentration of lysozyme was preferred to correspond with that of human serum [207, 208]. During the investigation, chitosan hydrogels were incubated in a lysozyme solution at 50 rpm. The lysozyme solution was refilled on a daily basis to ensure that the enzymes remained activeSamples were taken out of the medium at regular intervals (7, 14, and 21 days), rinsed with distilled water, and then dried in an oven at 35 °C for 4 hours or until constant weight. The weight loss calculated the degree of degradation: as per Equation 3.12:

$$Weight\ Loss\ \% = \frac{W_0 - W_t}{W_0} \times 100\% \quad (3.12)$$

where W_0 is the dry weight prior to the degradation test, and W_t is the dry weight at prearranged time *t*.

3.2.5 Statistical Analysis

Statistical analysis was conducted by employing response surface methodology (RSM) using Modde 13.0 software (Sartorius). Analysis of Variance (ANOVA) was utilised to examine the data, providing a robust framework for examining the relationships and interactions within the dataset. The efficacy of the statistical model was assessed based on the R^2 value,

which quantifies the proportion of variance in the dependent variable that is predictable from the independent variables, thereby offering a measure of the model's explanatory power.

CHAPTER 4: EXTRACTION AND OPTIMISATION OF LIPID FROM BSFL USING SC-CO2 EXTRACTION

BSFL have been proven to be a good resource of nutrients, such as protein, lipids, and minerals. The content of fat in BSFL is mainly saturated fatty acid (SFA). SFAs, such as lauric acid, myristic acid, palmitic acid, and stearic acid, contain only single bonds between the carbon atoms in their fatty acid chains. Most medical, scientific and governmental organisations, including the World Health Organisation (WHO) have agreed that saturated fat consumption is a risk factor for cardiovascular disease (CVD). However, there is still a controversy concerning this. Saturated fats in the diet can elevate total cholesterol and shift the balance to more harmful low-density lipoprotein (LDL) cholesterol, resulting in heart and arterial blockages. Most nutritionists recommend reducing saturated fat to less than 10% of total calories per day [209]. For someone eating 2,000 calories a day, that equates to about 11 to 13 grams of saturated fat. Therefore, a lower concentration of SFA in the diet is beneficial to reducing CVD and subsequently improving human health.

The primary fatty acid content in the BSFL is composed of oleic acid (C18:1 n-9), palmitic acid (C16:0), lauric acid (C12:0), and linoleic acid (C18:2 n-6) [122]. Lauric acid is a saturated fat-containing medium-chain fatty acid (MCFA) or medium-chain triglyceride (MCT), found in coconut oil and palm kernel oil. It has been recently determined that the lauric acid composition in BSFL oil is around 45-47 % of the total saturated fat, similar to that found in palm kernels and coconut oils [133].

Supercritical carbon dioxide extraction (SC-CO2), deemed a ‘green’ process, is a favourable technique to the environment and can be an alternative for the effective extraction of natural bioactive compounds from natural matter such as lipids or oils. Carbon dioxide is low-cost,

non-toxic, non-explosive, readily available at high purity, easily removed from the extracted product, and provides a broad range of solvent characteristics at various pressures and temperatures [41]. The critical temperature (31.1 °C) and pressure (7.2 barg) of CO_2 are relatively low, making SC-CO2 an excellent solvent for extracting thermally sensitive compounds, since extraction is feasible at ambient temperature [41].

Response surface modelling (RSM) offers an efficient statistical approach for optimising experimental conditions and studying crucial process factors with fewer experimental trials [42]. Optimisation of extracted yields from insects using RSM has been reported recently but only for sorghum bugs, silkworm species, and *Tenebrio molitor* larvae, indicating yields of 75 – 97 % and at ideal circumstances [43]. BSFL have also been defatted using SC-CO2 to remove excess fat so that they may be utilised as fodder for aquaculture and livestock [44]; however, the use of RSM to optimise the yield of oils is limited. For the BSFL oil product, there is still no information regarding the SC-CO2 extraction parameters, composition, physicochemical characteristics, or the analysis of fatty acids compared to the oil yield and composition of insects and vice versa.

One of the aims of this study is to study the lipid extracted from the BSFL. The response surface modelling (RSM) method was employed to investigate the SC-CO2 extraction of BSFL oil to optimise the yield of the larvae oil, fatty acid composition, and saturated fat concentration ratio in the BSFL oil. The optimal conditions are investigated, and the fatty acid composition is compared between SC-CO2 extraction and conventional chemical solvent extraction.

4.1 Material and Methodology

For comprehensive details on lipid extraction and optimisation, including an in-depth exploration of the materials and methodologies utilised, please refer to Chapter 3 of this thesis. Specifically, Sections 3.1.1 and 3.2.1 provide extensive information and discussion on the various aspects and techniques for the lipid extraction method, ensuring a thorough understanding of the procedures and principles applied.

4.2 Result and Discussion

This section discusses a detailed analysis of lipid extraction methods, beginning with evaluating solvent-based techniques, focusing on lipid yield and quality. This is complemented by a discussion on using response surface methodology to understand the impact of varying extraction variables on lipid yield and quality. To maximise efficiency, the section then shifts to optimising supercritical carbon dioxide (SC-CO2) extraction conditions, fine-tuning temperature, pressure, and flow rate. A critical comparative evaluation between SC-CO2 and solvent extraction methods is presented, examining each technique's efficiency, environmental impact, and the quality of extracted lipids. The influence of SC-CO2 extraction conditions on fatty acid composition is also explored, highlighting the method's importance for specific industrial applications. Finally, the section discusses the precision required in SC-CO2 extraction to isolate specific fatty acids, showcasing the method's adaptability and effectiveness. This comprehensive analysis underscores the section's focus on innovative lipid extraction techniques and their implications in the field.

4.2.1 Solvent Extraction Analysis

The extraction process was conducted in triplicate, yielding an oil content of 30% on a dry basis. This result is slightly lower than the findings reported in a previous study [6, 121], as

indicated in **Table 4.1**. This discrepancy highlights potential variations in extraction efficiency or methodology, emphasising the need for further investigation to understand the underlying factors contributing to these differences.

4.2.2 Response Surface Analysis

Many factors influence the optimal performance of the SC-CO2 extraction process, such as temperature, pressure, time, flow rate of the solvent, matrix particle size and moisture, and additional modifiers of a co-matrix [39]. In this work, only three factors are explored: pressure, temperature, and extraction time. **Table 4.1** summarises the results from the RSM experiments showing actual vs predicted yields. The yield percentage varies from 16.60 to 33.89 % of actual and 17.78 to 32.84% of predicted value, depending on the combination of factors. The best yield was 33.89%, corresponding to 300 bar, 40 °C, and 2 hours of extraction time, higher than 3.89% from the solvent extraction method.

The RSM analysis shows that pressure is a more dominant factor in the extraction yield than the other parameters. According to the analysis, the pressure has a positive and linear effect on oil recovery which agrees with a previous study [210]. The increased pressure leads to an increase in density and solubility, which in turn would result in a higher recovery [41, 211]. **Table 4.1** also shows that the high pressure of 400 bar recovered more larvae oil (29.90%) than the low pressure of 150 bar (23.34%) at the same temperature. Meanwhile, at a higher temperature, more oil is produced and extracted than at a lower temperature. The effect of temperature on the extraction process is considerably more complicated to evaluate than the impact of pressure on the extraction process [212]. The reason for the difficulty is the double impact of the temperature on the extraction process, as it depends on which factor dominates, either solute vapour pressure or the density of the solvent. As temperature rises, the oil solubility and density of SC-CO2 decline [211, 213], leading to an increase in oil extraction

because the vapour pressure is higher. Alternatively, increased extraction time has been shown to improve larval oil recovery. The relationship between pressure, temperature and extraction time with larvae oil yield is shown in **Fig. 4.1** and **Fig. 4.2.**

The lauric acid (C12:0) composition results varied from 48.14 to 62.21 g/100g of experimental and 50.20 to 60.22 g/100g of the predicted values. These values were reliant on the various combinations of the factors. Based on the experimental modelling, the highest lauric acid content was achieved with the pressure of 150 bar, at 40 °C, and within 1-hour extraction. With a rise in pressure, the quantity of fatty acids, particularly lauric acid, dropped and increased when the temperature was increased from 30 °C to 40 °C at a constant CO_2 flow rate of approximately around 1.2 L/min. The lauric acid content gradually increased within 2 hours of extraction time and slowly decreased when it reached 3 hours.

The concentration of SFA is determined by using the ratio of SFA to unsaturated fat (USFA). The total SFA for this BSFL is contributed by lauric acid, myristic acid, palmitic acid, and stearic acid. In contrast, USFA is a combination of the rest of the fatty acids (palmitoleic acid, oleic acid, linoleic acid and α Linoleic Acid, as per **Table 4.1.** The maximum concentration of SFA with a value of ratio 7.0 was obtained with the pressure of 300 bar, at 40 °C and within 2 hours of extraction. Meanwhile, the minimum value of the concentration of SFA of 4.0 was found with the pressure of 150 bar, at 40 °C and within 3-hour extraction. **Fig. 4.1** shows the RSM showing the effects of the variables tested factors on oil recovery, and Fig. 4.2 shows the response contour plots showing the effects of the temperature and pressure on oil recovery, lauric acid composition and the SFA ratio at constant time of 2 hours.

Table 4.1: Designed experiments and results (experimental and predicted) of lipid extraction of *Hermetia illucens* larvae using Supercritical CO_2 extraction.

Experiment Number	Factors			Responses					
				Lipid Yield (%)		Lauric Acid [g/100 g]		Ratio of SFA	
	Pressure (X_1)(Bar)	Temperature (X_2) (° C)	Time (X_3) (hour)	Experimental	Predicted	Experimental	Predicted	Experimental	Predicted
N1	200	30	2	23.03	22.02	57.05	58.39	6.1	5.8
N2	400	30	2	27.56	26.13	50.66	50.00	4.8	5.1
N3	200	50	2	29.78	28.14	55.19	54.06	5.4	5.2
N4	400	50	2	29.90	31.26	51.07	49.82	4.7	4.5
N5	200	40	1	22.23	23.29	61.18	60.54	5.0	6.0
N6	400	40	1	27.5	27.37	55.62	55.60	6.1	5.4
N7	200	40	3	26.82	27.08	58.43	57.49	6.8	5.5
N8	400	40	3	30.30	30.24	48.14	49.80	4.3	4.8
N9	300	30	1	16.60	17.78	56.61	56.95	6.0	5.9
N10	300	50	1	27.60	26.56	51.70	52.94	5.2	5.4
N11	300	30	3	23.01	24.27	51.78	50.77	5.3	5.4
N12	300	50	3	27.70	26.74	50.38	50.27	4.7	4.8
N13	300	40	2	31.84	32.84	55.83	56.97	6.3	6.8
N14	300	40	2	32.34	32.84	56.66	56.97	6.4	6.8
N15	300	40	2	33.89	25.61	57.97	54.64	7.4	6.8
N16	150	50	2	23.34	22.02	53.39	58.39	4.2	4.4
N17	150	40	1	21.59	26.13	62.21	50.00	5.6	5.2
N18	150	40	3	25.03	28.14	58.53	54.06	4.0	4.7

Note: At the constant CO2 flow rate of an average of 1.2 lpm**,** the pressure is ± 5-7 bar due to the kinetic of a pneumatic pump.

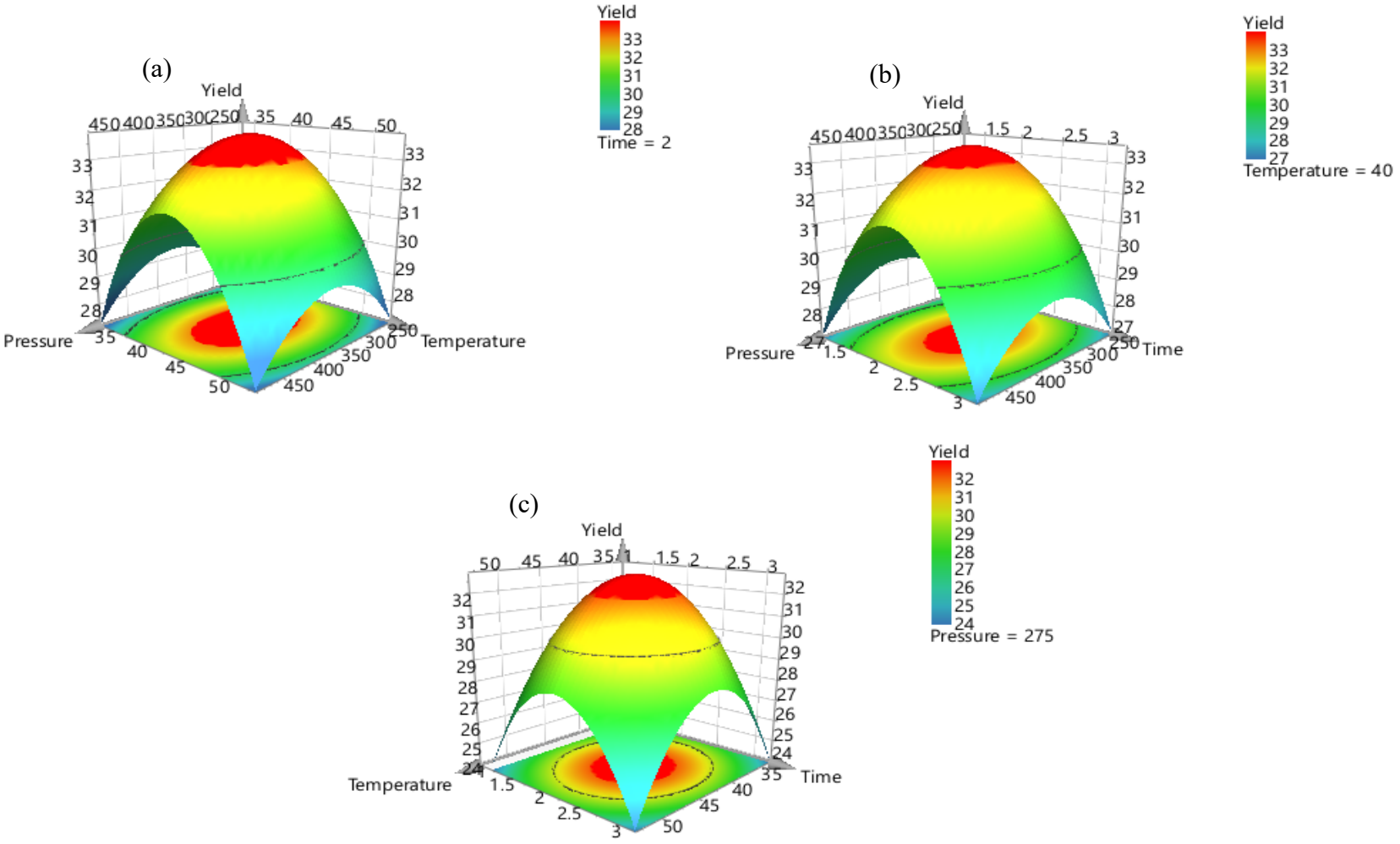

Fig. 4.1: Response Surface plots showing the effects of the variables tested factors on oil recovery: (**a**) Pressure and temperature at a constant time of 2 hours, (**b**) Pressure and time at a constant temperature of 40°C, and (**c**) Time and temperature at a constant pressure of 275 bar.

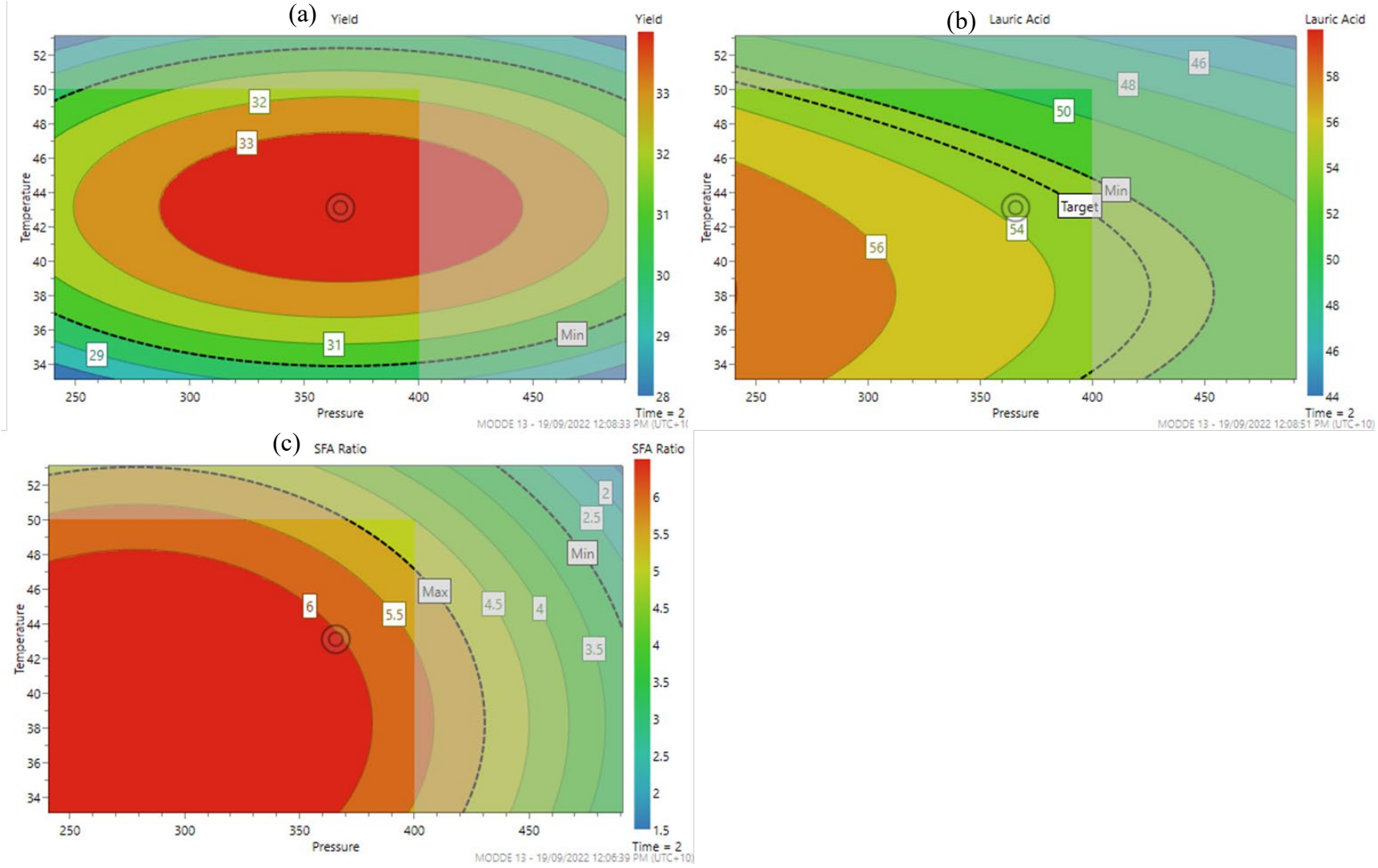

Fig. 4.2: Response contour plots showing the effects of the temperature and pressure on (**a**) oil recovery, (**b**) lauric acid composition and (c) SFA ratio at a constant time of 2 hours to achieve the objective of maximum oil recovery.

Table 4.2 shows the coefficients of the second-order polynomial equation obtained from the models while the ANOVA results are presented in **Table 4.3**. To find the best correlation between the larvae oil recovery and the lauric acid recovery with the factors, three models were compared: linear, two-factor interaction, and quadratic models. The p-value of the model regression for both larvae oil recovery and lauric acid was 0.000, and for the SFA concentration ratio, it was 0.037, which fulfils the requirement and shows that if the p-values are less than 0.05, the model terms are significant. The Lack of Fit F-value was 3.02 for the oil recovery, 2.38 for the lauric acid recovery and 3.43 for the SFA concentration ratio. This means that the lack of fit is not substantial compare to the pure error; therefore, a non-significant lack of fit indicates that the model is good.

For the larvae oil recovery, the linear terms of X_1, X_2, X_3, and the quadratic of X_2^2, X_3^2 are the important model elements, suggesting that certain model variables have a strong influence on conversion yield. However, the p-values for the quadratic term of X_1^2, interaction of X_1X_2, interaction of X_1X_3, and interaction of X_2X_3 are greater than 0.05, indicating that these model terms are not significant.

Suppose the model has a large number of model terms that are not statistically significant (apart from those needed to support the hierarchy). In that case, the model may be improved by removing these model terms, which will increase the accuracy of the predictions. After removing the less important model components, the extraction yield is expressed using a second-order polynomial equation as follows:

$$Y_{Larval\ Oil} = 32.28 + 3.09X_1 + 2.84X_2 + 1.73X_3 - 2.12X_1^2 - 4.51X_2^2 - 4.49X_3^2$$

A similar condition was applied for the lauric acid recovery, and SFA ratio, and the second-order polynomial equation for the lauric acid recovery as below:

$$Y_{Lauric\ Acid} = 56.93 - 3.53X_1 - 1.26X_2 - 2X_3 - 3.47X_2^2$$

The second-order polynomial equation for SFA is as follows:

$$Y_{SFA\ Ratio} = 6.83 + -1.25X_1^2 - 0.85X_2^2$$

The quadratic model's coefficient of determination (R^2) is 0.90, 0.87 and 0.65, indicating that the process parameters describe 90% of the larvae oil recovery, 87% of the lauric acid recovery and 65% of the concentration of SFA ratio derived from this research were influenced by the process parameters.

4.2.3 Parameter Optimisation of SC-CO2 Extraction

Objective functions were developed to determine the conditions that maximise or minimise the different responses. For this study, the optimisation objectives for the SC-CO2 extraction parameters were to maximise oil recovery, maximise lauric acid content and minimise SFA ratio. Parameter optimisation was conducted using the optimisation tool (second-order algorithms for objective functions) within the MODDE package, which resulted in the optimal values of 30% oil recovery, 52 g / 100 g lauric acid content, and 5.0 SFA ratio. These optima corresponded to optimal extraction parameters of 400 bar, 46.8 °C and 1.4 hours of extraction time. Different optimal settings for temperature, pressure, and extraction time can be obtained by modifying the objectives. The predicted and actual values of the optimised experiment were compared for verification purposes. The results show that the values predicted by the model are excellent approximations of the actual values. However, only two objective functions were verified for this study: the maximum oil recovery and lauric acid content. The optimisation results are shown in **Table 4.4**

The Machine Learning (ML) model utilised in the present invention composed of a set of model equations, factor and response variables, and a set of model parameters. The model parameters are estimated using the parameter estimation algorithm shown in **Fig. 4.3**, using data collected from historical experimental runs. Once the model is validated against

experimental data, it may be used for prediction of responses, as a data-driven model that works well within the range of the given factors. The set of parameters within the model is adaptive and continuously tuned using the optimisation algorithm in **Fig. 4.4**, thus constituting a machine-learning approach. Other factors, such as the variation in feed conditions, can be included in the model to enable the prediction of responses under changes in feed conditions.

The parameter estimation algorithm shown in **Fig. 4.4** is effectively a model regression step, where equations are used along with the set of model parameters to minimise the difference between the model predictions and the experimental observations. The result is a set of optimal model parameters and a validated model that can now be used for the prediction of responses under various combinations of factors. The optimisation algorithm shown in **Fig. 4.5** is dependent on the ML model and serves two functions:

- Optimise the process conditions that maximise a certain objective e.g. maximise the lauric acid concentration (R2) of the product, and
- Update the ML model parameters using optimal sets of data for F and R.

The algorithm is constantly learning from new data collected from future experimental runs and improving the model prediction via re-estimation (re-tuning) of the model parameters. Variations in feed conditions are captured by this ML algorithm. The effect of feed variations is measured through the conducted experiments and such knowledge translates into recalculations of the model parameters. The result is repeated control of the quality of the product in the form of maximised objective (i.e., maximum R2, for example) at every future run.

Table 4.2: Estimated coefficients of the second-order polynomial equations before and after eliminating the insignificant model terms.

Item	Before eliminating insignificant model terms						After eliminating insignificant model terms					
	Lipid Yield (%)		Lauric Acid [g/100 g]		Ratio of SFA		Lipid Yield (%)		Lauric Acid [g/100 g]		Ratio of SFA	
Term	Coefficient	*P*-value	Coefficient	*P*-value	Coefficient	*P*-value	Coefficient	*P*-value	Coefficient	*P*-value	Coefficient	*P*-value
Constant	32.30	0.0000	57.74	0.0000	6.82	0.0000	32.29	0.0000	56.94	0.0000	6.83	0.0000
X_1	3.14	0.0008	-3.70	0.0000	0.0394	0.8866	3.0891	0.0003	-3.526	0.0000	0.0692	0.7773
X_2	2.88	0.0012	-1.38	0.0248	-0.3190	0.2605	2.8392	0.0006	-1.263	0.0351	-0.2955	0.2381
X_3	1.72	0.0121	-2.04	0.0021	-0.2934	0.2571	1.7340	0.0093	-2.006	0.0015	-0.2800	0.2286
X_1^2	-2.19	0.0521	-0.61	0.4820	-1.2080	0.0234	-2.1223	0.0517	-	-	-1.2491	0.0082
X_2^2	-4.55	0.0006	-3.52	0.0012	-0.8204	0.0614	-4.5085	0.0003	-3.471	0.0005	-0.8483	0.0302
X_3^2	-4.45	0.0006	-0.72	0.3401	-0.5989	0.1484	-4.4865	0.0003	-	-	-0.5741	0.1188
X_1X_2	-0.31	0.7428	1.29	0.1398	0.2014	0.6398	-	-	-	-	-	-
X_1X_3	-0.29	0.7163	-0.86	0.2264	-0.3355	0.3582	-	-	-	-	-	-
X_2X_3	-1.58	0.0979	0.88	0.2598	0.0500	0.8985	-	-	-	-	-	-

Note: The model terms are significant if the p-values are less than 0.05.

Table 4.3: Analysis of variance (ANOVA) of the modelled responses.

Source	DF	SS	MS	F-value	*P*-value
Lipid Yield					
Model/Regression	6	301.69	19.71	16.57	0.000
Residual	11	33.37	50.28		
Lack of Fit	9	31.09	3.40	3.02	0.273
Pure Error	2	2.29	3.45		
Total	18	13138	729.90		
Lauric Acid Recovery					
Model/Regression	4	243.34	56.83	22.52	0.000
Residual	13	32.80	2.52		
Lack of Fit	11	30.47	2.77	2.38	0.333
Pure Error	2	2.328	1.16		
Total	18	54974	3054.13		
SFA Ratio					
Model/Regression	6	9.94	1.66	3.43	0.037
Residual	11	5.30	0.48		
Lack of Fit	9	4.56	0.51	1.37	0.491
Pure Error	2	0.74	0.37		
Total	18	552.07	30.67		

DF = Degree of freedom, SS = Sum of squares, MS = Mean of Square, Larvae Oil Recovery: $R^2 = 0.90$, Adj. $R^2 = 0.85$, Lauric Acid Recovery: $R^2 = 0.87$, Adj. $R^2 = 0.84$, SFA Ratio, : $R^2 = 0.65$, Adj. $R^2 = 0.46$

Table 4.4: Optimisation results of the larvae oil recovery or lauric acid recovery.

Item	Objective Function				SC-CO2 Condition			Predicted			Actual		
		Lipid Yield	Lauric acid Content	SFA Ratio	Pressure (BARG)	Temp (° C)	Extraction Time (hour)	Yield (%)	Lauric Acid (g/100g)	SFA Ratio	Yield (%)	Lauric Acid (g/100g)	SFA Ratio
1	Maximum	X	X	-	400	46.8	1.4	30.1	52.0	5.0	33.67	57.53	3.6
	Minimum	-	-	X									
2	Maximum	X	-	-	366	43.1	2.2	34.0	53.3	6.0	35.58	54.97	3.4
	Minimum	-	-	-									
3	Maximum	-	X	-	213	42.2	1.1	25.6	60.0	6.2	28.41	58.89	3.1
	Minimum	-	-	-									
4	Maximum	-	-	-	150	50	3	22.7	53.7	3.5	23.82	55.32	3.4
	Minimum	-	-	X									

.

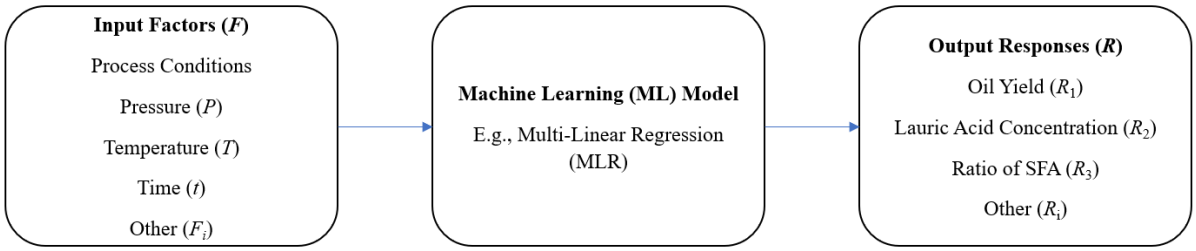

Fig. 4.3: Flowchart of the machine learning (ML) model.

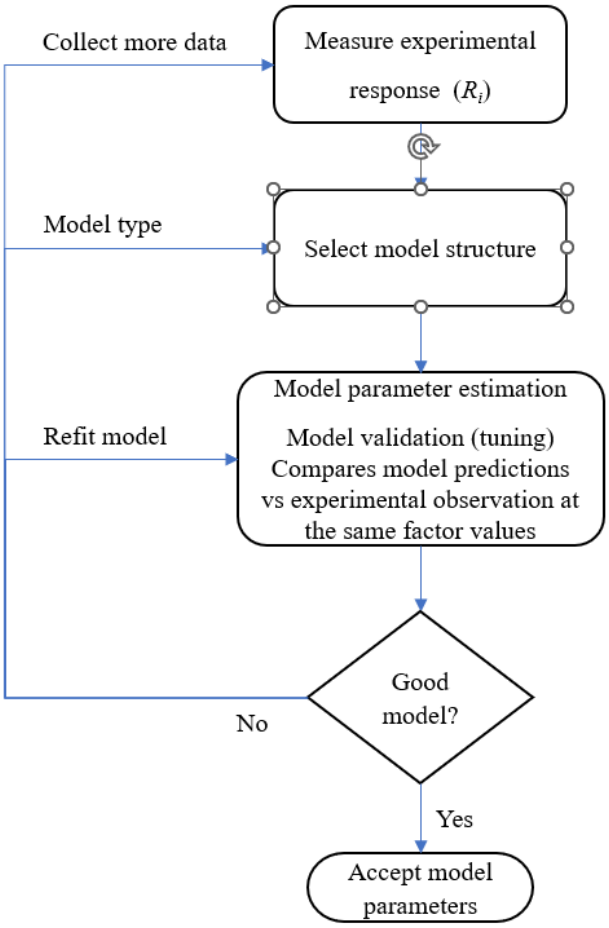

Fig. 4.4: Flowchart of the parameter estimation algorithm used in the machine learning model.

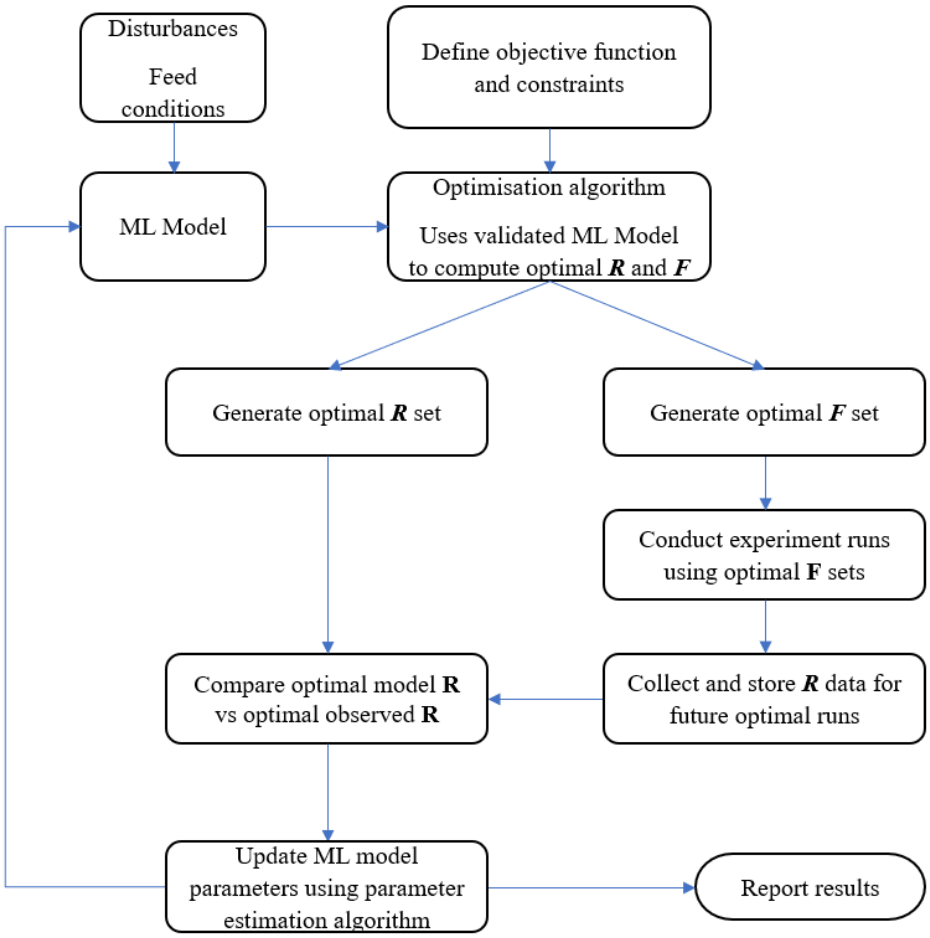

Fig. 4.5: flowchart of the optimisation algorithm used in the machine learning model.

4.2.4 Impact of SC-CO2 on the Fatty Acid Composition.

The fatty acid profile in BSFL larval oil was investigated using gas chromatography, and the results are reported in **Table 4.5**. The data revealed that lauric acid (C12:0) was the most abundant fatty acid in the larvae oil, accounting for 48-61% of the total fatty acids. The second most abundant fatty acid was palmitic acid (C16:0), accounting for 15-18% of the total fatty acids. Oleic acid (C18:1n-9) and myristic acid (C14:0) were also present in significant quantity, varying from 11-15% and 4-6%, respectively. In contrast, stearic acid (C18:0) and linoleic acid (C18:2n-6) were present in very low percentages of less than 2%

each. The total saturated fatty acid (SFA) and unsaturated fatty acid (USFA) contents varied from 72-82% and 17-24%, respectively. These findings were in line with a previous study [121]. Interestingly, the composition of each fatty acid content in the BSFL oil differed slightly, and these differences were more pronounced across samples extracted under different SC-CO2 settings. It was found that some USFA acids, such as Palmitoleic Acid (C16:1n-9) and Linoleic Acid (C18:2n-6), were not detected when a lower pressure of 150 bar was applied during the SC-CO2 extraction. Therefore, it can be concluded that some fatty acids were not detected under specific SC-CO2 extraction conditions. Nevertheless, the major fatty acids, particularly lauric acid (C12:0), were detected despite using various SC-CO2 extraction conditions.

4.2.5 Adjusting the SC-CO2 conditions to get a specific fatty acid.

The study's findings show that SC-CO2 can be used to extract specified fatty acid fractions from BSFL oil **Table 4.6** presents the highlighted percentages of particular fatty acids, with lauric acid showing the highest percentage of 62.21% under the conditions of 150 bar, 40°C, and 1 hour of extraction time. Conversely, (C18:3) α Linoleic Acid had the smallest percentage, with a high of 2.11% detected under the SC-CO2 conditions of 400 bar, 50°C, and 2 hours of extraction time. Adjusting the SC-CO2 extraction conditions could allow for the attainment of a specific fraction of each fatty acid in the extraction product. Optimising the SC-CO2 conditions enable to extract the highest percentage of various fatty acids, including those with potential medical applications and nutritional benefits. Therefore, the fine-tuning of SC-CO2 conditions could enable the extraction of specific fractions of fatty acids.

Table 4.5: Percentage (%) of concentration of each Fatty Acid out of the sum of all Fatty acids as in each experiment of SC-CO2.

Pressure		200	400	200	400	200	400	200	400	300	300	300	300	300	300	300	150	150	150
Temperature		30	30	50	50	40	40	40	40	30	50	30	50	40	40	40	50	40	40
Time		2	2	2	2	1	1	3	3	1	1	3	3	2	2	2	2	1	3
Experiment		N1	N2	N3	N4	N5	N6	N7	N8	N9	N10	N11	N12	N13	N14	N15	N16	N17	N18
Fatty Acid																			
Lauric Acid	C12:0	57.05	50.66	53.86	51.07	52.47	55.62	58.43	48.14	56.61	51.70	51.78	50.38	55.83	56.66	57.97	53.39	**62.21**	58.53
Myristic Acid	C14:0	5.26	5.40	5.33	5.80	5.57	4.82	5.37	5.84	4.99	6.01	5.05	5.97	4.84	4.77	5.04	**9.27**	3.77	7.86
Palmitoleic Acid	C16:1n-7	0.70	0.40	0.55	1.09	0.82	0.46	0.48	0.65	0.36	0.67	**1.51**	0.65	-	0.33	0.39	-	-	-
Palmitic Acid	C16:0	15.55	17.40	16.48	17.16	16.82	17.06	15.84	17.46	16.13	17.61	**17.94**	16.83	16.72	16.81	16.65	11.95	11.96	5.89
Stearic Acid	C18:0	0.85	1.15	1.00	1.38	1.19	1.23	0.96	1.19	0.79	1.15	1.57	1.06	1.40	1.26	1.19	**3.07**	-	-
Oleic Acid	C18:1n-9	11.06	13.58	12.32	12.94	12.63	11.11	10.12	14.58	11.65	12.81	13.03	13.82	10.96	10.73	9.59	**18.50**	13.99	18.02
Linoleic Acid	C18:2n-6	7.63	6.77	7.20	6.04	6.62	6.89	6.87	**9.57**	7.73	8.05	7.26	9.00	7.06	6.89	6.99	-	4.10	2.78
α Linoleic Acid	C18:3	1.11	1.41	1.26	**2.11**	1.69	1.27	1.31	1.83	1.11	1.27	-	1.47	1.64	1.40	0.95	-	-	-
Saturated FA		78.71	74.62	76.67	75.41	76.04	78.74	80.60	72.64	78.51	76.46	76.34	74.24	78.78	79.50	80.84	77.67	77.94	72.27
Unsaturated FA		12.88	15.40	14.14	16.15	15.14	12.84	11.92	17.06	13.11	14.75	14.54	15.94	12.60	12.46	10.93	18.50	13.99	18.02
Ratio of SFA		6.1	4.8	5.4	4.7	5.0	6.1	6.8	4.3	6.0	5.2	5.3	4.7	6.3	6.4	7.4	4.2	5.6	**4.0**

Note: At the constant CO2 flow rate of an average of 1.2 lpm, the pressure is ± 5-7 bar due to the kinetic of the pneumatic pump. A duplicate experiment has been conducted, and the average value was given. The highlight and bold are the maximum value of each fatty acid and concentration of the SFA.

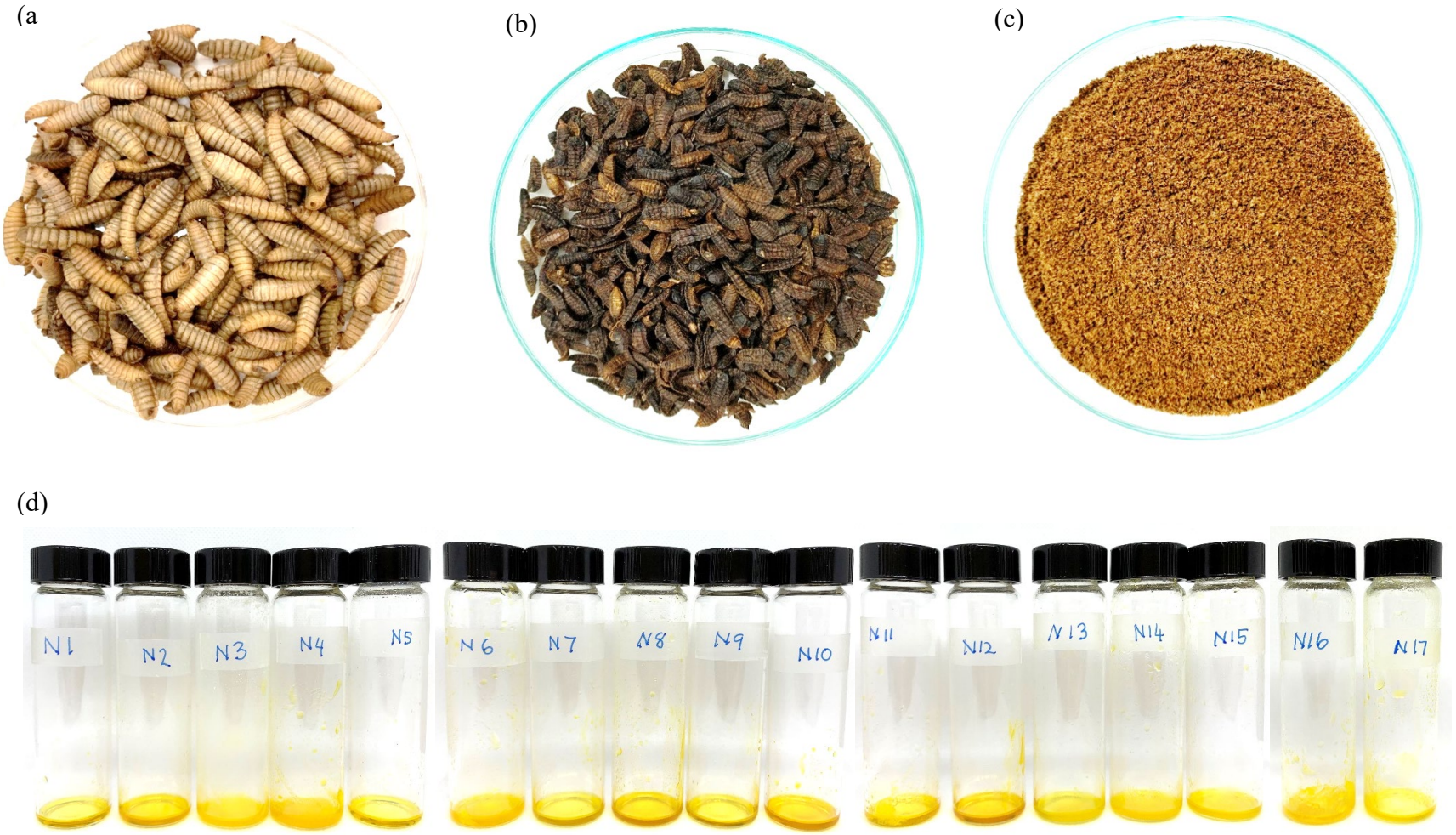

Fig. 4.6: Visual and physical properties of the BSFL; (**a**) Fresh BSFL which is approximately at ages of 14 days, (b) Dried BSFL which was dried at 60 ºC for 48 hours, (**c**) BSFL has been ground finely and ready for the SC-CO2 extraction, (**d**) Larvae Oil extracted with SC-CO2 with various conditions of pressure, temperature and extraction time. CO_2 flow rate was constant with an average of 1.2 lpm.

4.2.6 Comparison between SC-CO2 and Solvent Extraction

The comparison of fatty acid composition between the optimum SC-CO2 extraction conditions and solvent extraction is illustrated in **Table 4.6**. The results show that extraction via SC-CO2 (35.58%) obtained higher larval oil recovery than solvent extraction (30.00%). The total SFA via SC-CO2 (76.63%) is almost the same as for solvent extraction (81.10 %). The concentration ratio of SFA to the unsaturated fatty acids between both methods shows that the SC-CO2 extraction (ratio of 3.4) improved over solvent extraction (ratio of 4.5). Furthermore, lauric acid (C12:0) (54.97 %) was the highest contribution to the saturated fatty acid together with the palmitic acid (C16:0) (15%) SC-CO2 and 62.66% and 12.68 respectively for solvent extraction. This composition agrees with a previous study's [122]. Thus, BSFL fat is a potential alternative source for those two fats (lauric acid and palmitic acid) with applications in food preparation or as cooking oil, butter, and margarine for human consumption. Aside from that, BSFL contains lauric acid, which is more digestible than butter and has more nutritional benefits.

Lauric acid also possesses antibacterial, antimicrobial, and antimycotic properties, which can eliminate various harmLess viruses, bacteria, or even fungi in the body, allowing it to affect health positively [214]. Furthermore, because of its potential to enhance HDL, lower the total HDL cholesterol ratio, and lower blood pressure and heart rate, high lauric acid has been interrelated with positive cardiovascular effects [215-218]. However, a high concentration of SFA has disadvantages in heart disease to humans due to its ability to increase LDL cholesterol and very-low-density lipoproteins (VDL) cholesterol [219]. Therefore, utilising SC-CO2 extraction can be an attractive way to extract target fatty acids from the BSFL and also to obtain a lower ratio of saturated fats by manipulating the parameters of the SC-CO2 extraction.

Table 4.6: Fatty acid composition between SC-CO2 and Solvent extraction.

Fatty Acid		Percentage (%) of concentration of each Fatty Acid	
		SC-CO2 Optimum Condition (366 bar, 43 °C, 2.2 Hours)	Solvent
Oil Recovery/Yield		35.58%	30.00%
Lauric acid	C12:0	54.97	62.66
Myristic acid	C14:0	5.49	4.85
Palmitic acid	C16:0	15.00	12.68
Palmitoleic acid	C16:1n-7	0.72	0.06
Stearic acid	C18:0	1.17	0.91
Oleic acid	C18:1n-9	11.70	7.47
Linoleic acid	C18:2n-6	8.14	10.35
α-Linolenic acid	C18:3	1.17	0.06
Total SFA		76.63	81.10
Total USFA		22.34	17.94
Ratio of SFA to USFA		3.4	4.5

Note: At the constant CO_2 flow rate of an average of 1.2 lpm**,** the pressure is ± 5-7 bar due to the kinetic of the pneumatic pump and duplicated experiment. An average value was given for the solvent extraction.

4.2.7 Impact on drying time to SC-CO2 extraction

The conditions of BSFL, specifically drying time and hydration levels, significantly influence the CO2 extraction efficiency. High moisture content in the BSFL can impede the process, as supercritical CO2 is more effective at extracting lipophilic compounds when moisture levels are low. Inadequate drying can lead to microbial growth or sample degradation, negatively affecting the quality of the extracted products. Conversely, overly dried samples may degrade sensitive compounds, thus reducing product quality. Optimal drying balances moisture reduction while maintaining sample integrity, thereby enhancing extraction efficiency. These conditions also dictate the choice of processing parameters, such as temperature and pressure, during CO2 extraction. Therefore, controlling drying time and

hydration levels is essential to maximise both the efficiency and quality of CO2 extraction from BSFL.

4.3 Summary

In this study, supercritical carbon dioxide (SC-CO2) is tested for the extraction of oil from BSFL and compared against a chemical solvent extraction method. A response surface modelling (RSM) approach is used to optimise the SC-CO2 extraction conditions by investigating the effects of 3 factors, viz. temperature (30 – 50 ^{o} C), pressure (150 – 400 bar), and extraction time (1 – 3 hours), on 3 response variables, viz. larval oil recovery (lipid yield %), fatty acid (mainly lauric acid) composition (g/100g), and the ratio of saturated fatty acid (SFA). The factors ranked in descending order of influence on the performance of the SC-CO2 process are pressure, extraction time, followed by temperature. Maximum larval oil recovery of 35.58%, 5.58% higher than the solvent extraction, is achieved using the SC-CO2 extraction with 366 bar, 43 ^{o}C and 2.2 hours extraction time. Overall, the SC-CO2 process shows better performance than solvent extraction across all the three responses measured. The concentration ratio of SFA is also improved significantly by using SC-CO2 instead of solvent extraction. Adjustment of SC-CO2 extraction condition allows attainment of specific fraction of each fatty acid in the extraction product. A multi-objective optimisation is formulated, leading to maximum larval oil recovery (30.1 %), maximum lauric acid content (52.0 g/100g) and a minimum SFA ratio (5.0), found at a SC-CO2 condition of 400 bar, 46.8 ^{o} C and 1.4 hours of extraction time. The results confirm that ‘green’ SC-CO2 extraction can be a potential alternative to conventional solvent extraction to obtain oils from BSFL without using organic solvents and also be a practical way to extract target fatty acids from the BSFL, subsequently improving the SFA ratio. Furthermore, this method can be scaled up to be

utilised in industry, enhancing the circular economy performance of organic waste sources and creating new business and markets for products and by-products of BSFL.

CHAPTER 5: CYTOTOXICITY AND BIOCOMPATIBILITY ASSESSMENT OF BSFL OIL: INVITRO RESPONSE TO FIBROBLAST

The high amount of lipids or fat in BSFL, particularly in the form of saturated fatty acids (SFA), have been reported previously [23]. The main fatty acids were lauric acid (C12:0), oleic acid (C18:1 n-9), palmitic acid (C16:0) and linoleic acid (C18:2 n-6) [122]. BSFL Oil (BSFLO)'s primary lipid class component is triglycerides [131-133]. Lauric acid is a saturated fat-containing medium-chain fatty acid (MCFA) or medium-chain triglyceride (MCT) contain in coconut oil and palm kernel oil. It has been recently determined that the lauric acid composition in the larvae oil of BSF is the same to those two oils, around 45-47 % of the total saturated fat [133]. The structure of chemical is comprised of 12 carbon (C), 24 hydrogens (H), and 2 oxygen (O) atoms with the molecular formula of $C_{12}H_{24}O_2$. Lauric acid is a white solid with a melting point of 43–44 ºC and a molecular weight of 200.32 g mol–1 [137].

In most studies conducted by other researchers, the fatty acid profile is recognised to be associated to their diet. Various experiments have attempted to manipulate the profile of fatty acid using an enriched feed formulation [127-130]. A recent study indicated that dietary BSFLO improves the feed conversion ratio and boosts the incorporation of medium-chain fatty acids into the abdominal fat pad as well as serum antioxidant capacity in broiler chickens [138]. However, there are few studies or no studies regarding the metabolic reactions utilising the BSFLO that enrich with lauric acid till today.

In the human body, the lipase enzyme digests lauric acid into monolaurin, a monoester composed of glycerol and lauric acid. Detailed investigations have demonstrated that the majority of ingested lauric acid is carried directly to the liver and metabolised to energy and

other metabolites rather than being stored as fat [140]. The primary role of lauric acid, and other fatty acids, is to serve as structural components of cell membranes and to contribute to various physiological processes in the body. Lauric acid and monolaurin have antibacterial and anti-inflammatory properties that can effectively combat skin issues. Furthermore, they can accelerate the process of epithelialisation, which involves the upward migration of epithelial cells to repair damaged areas. This is due to their capacity to enhance the proliferation and migration of cells. In the wound healing process, the cells at the wound's edges multiply and move, leading to the re-epithelialisation of the wound surface [137, 141].

Fibroblasts or 3T3 cells are versatile cells found in connective tissue. They produce collagen, which helps shape organs and heal wounds [220]. They play diverse roles in health and disease, including fibrosis, arthritis, and cancer. Different subtypes of fibroblasts exist within tissues, and recent research suggests that universal fibroblasts can transform into specialised fibroblasts, adding to their functional diversity [221]. Fibroblasts have a significant role in the process of wound healing. This method involves three phases: inflammation, proliferation, and regeneration. During these phases, fibroblasts become activated and transform into myofibroblasts [222]

This study aimed to expand the application of BSFLO extracted using SC-CO2, analysing the lipid compositions, and conducting an initial evaluation of its cytotoxicity on 3T3 cells. SC-CO2 extraction was chosen for this study due to practicality, environmental friendliness, and reduced contamination for the extraction of BSFLO. Considering its high lauric acid content, the study was designed to explore the potential application of BSFLO in wound healing. Emphasising the importance of resource efficiency, this research aimed to promote sustainable production of skin formulations by effectively utilising natural resources such as insect oil.

5.1 Material and Methods

For in-depth information on cell culture methodologies utilised in *in-vitro* tests, including a comprehensive discussion of the materials and methods employed, please refer to Chapter 3 of this thesis, specifically Sections 3.1.2 and 3.2.2. These sections provide extensive details, ensuring a thorough understanding of the procedures and techniques applied in the cell culture experiments.

5.2 Result and Discussion

The study investigates on the characterisation of Black Soldier Fly Larvae Oil (BSFLO) extracted through Supercritical Carbon Dioxide (SC-CO2) and solvent methods. The acid value and free fatty acid content of BSFLO were determined and FT-IR analysis. The SC-CO2-extracted BSFLO was chosen for an in-vitro study due to its practicality, environmental friendliness, and reduced chemical contamination. Besides, the impact on 3T3 cell viability at different concentrations of BSFLO also conducted to demonstrate that BSFLO stimulated cell proliferation without inducing cytotoxic effects. Furthermore, a scratch test showing cell migration towards the wound center within 24 hours. Microscopic observations supported BSFLO's positive impact on cell proliferation and spreading. The study highlighted the significance of lauric acid in promoting cell growth and repair.

5.2.1 Acid Value and FFA Percentage

The acid value and free fatty acid content are crucial factors in determining the quality and characteristics of edible oils and fats. According to the study, the acid value for BSFLO is approximately 11.26 ± 0.18 mg KOH/g oil, while the free fatty acid content is around 4.01 ± 0.06%. These results are comparable to those obtained in a previous study [223]. The primary constituents of the BSFLO's free fatty acids are lauric acid and 2-monoglycerides, particularly 2-monolaurin, as reported by another researcher [141].

5.2.2 FT-IR Analysis of the Extracted BSFLO

Fig. 5.1 shows the FTIR spectra of the extracted under optimal SC-CO2 and solvent extraction conditions. The SC-CO2 and solvent extractions reveal no significant difference, as demonstrated in both IR. The strong absorbance in the range of 2920.09 cm^{-1} and 2851.53 cm^{-1} (SC-CO2 extraction) and between 2920.66 $cm^{-1}$and 2851.83 cm^{-1} (solvent extraction), correlated to the C-H stretching vibration, revealing a significant quantity of methyl and methylene groups of the fatty acid chains of the triglycerides [224]. On the other hand, the absorption of 1707.37 $cm^{-1}$and 1708.62 cm^{-1} are represented by the C=O group stretching absorption of the fatty acid-glycerol ester linkage is detected, and the absorption of the ester group (C-O stretch) was identified at 1111.78 $cm^{-1}$and 1111.30 cm^{-1}. The absorbance peaks in the range of 1411.29 cm^{-1} and 1464.69 cm^{-1} (SC-CO2) and between 1413.60 $cm^{-1}$and 1465.12 cm^{-1} (solvent extraction) showed the X-H stretching vibration (X=C, N) that confirmed the existence of a triglyceride functional group. Furthermore, the absorbance peak near 1192.93 cm^{-1} and 1165.00 cm^{-1} showed the presence of aromatic amine (C-N stretch), similar to other studies [37]. Thus, the FTIR spectra suggest that the extracted oil primarily comprises fatty acids, particularly lauric acid.

Hence, based on the characterisation of the BSFLO extracted from the BSFL, the larval oil that has been extracted using SC-CO2 has been chosen for the following in-vitro study. It is more practical, environmentally and less contaminated with other chemicals.

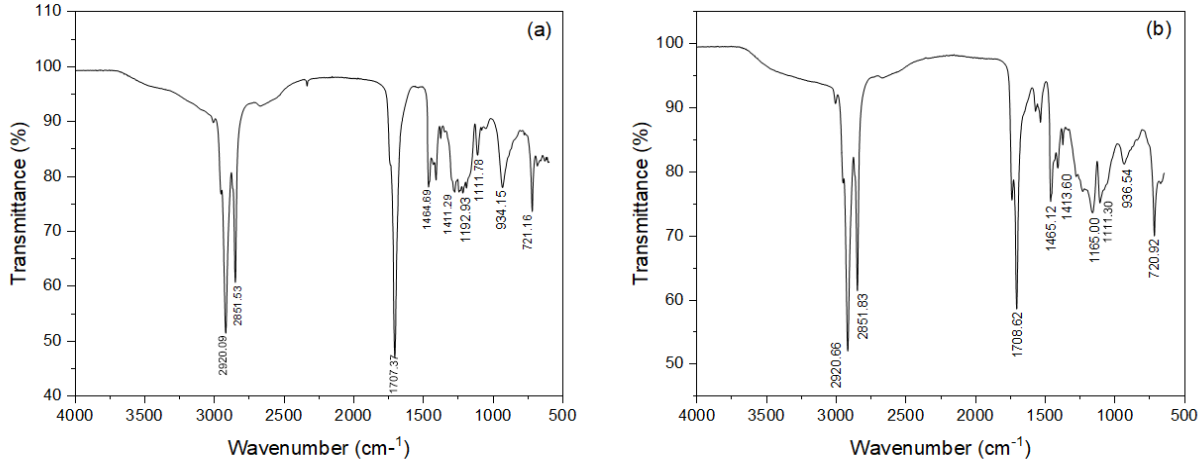

Fig. 5.1: FTIR spectra of extracted BSFLO (**a**) under the optimal SC-CO2 conditions, (**b**) using solvent extraction.

5.2.3 Identification and optimisation of the oil concentration that is viable for cell activity

An initial investigation was carried out to determine the influence of various amounts of BSFL oil on the pH of the culture media. The concentrations were chosen based on the maximum oil concentration identified in a previous study [217], and a dilution strategy was employed to ensure equal dilution until the maximum concentration was reached. After subjecting the BSFL oil to varying concentrations from 1, 2, 2.5, 5, 7.5 and 15 µl/mL, a noticeable shift towards increased acidity was observed when the concentration was raised. This change occurred after storing the oil in the incubator with media for three days, in conditions similar to those for cellular activity for this study. This observation provides evidence that pH conditions have a significant impact on cytocompatibility with respect to oil concentration, where 15 µl/mL and beyond is not recommended for cellular activity. As a result, only four concentrations, namely 1, 2.5, 5, and 7.5 µl/mL, were used for cell viability and proliferation tests. A concentration lower than 1 was also considered for optimisation to assess its possible effect on cellular activity. **Fig. 5.2** show the colour change in response to various oil concentrations.

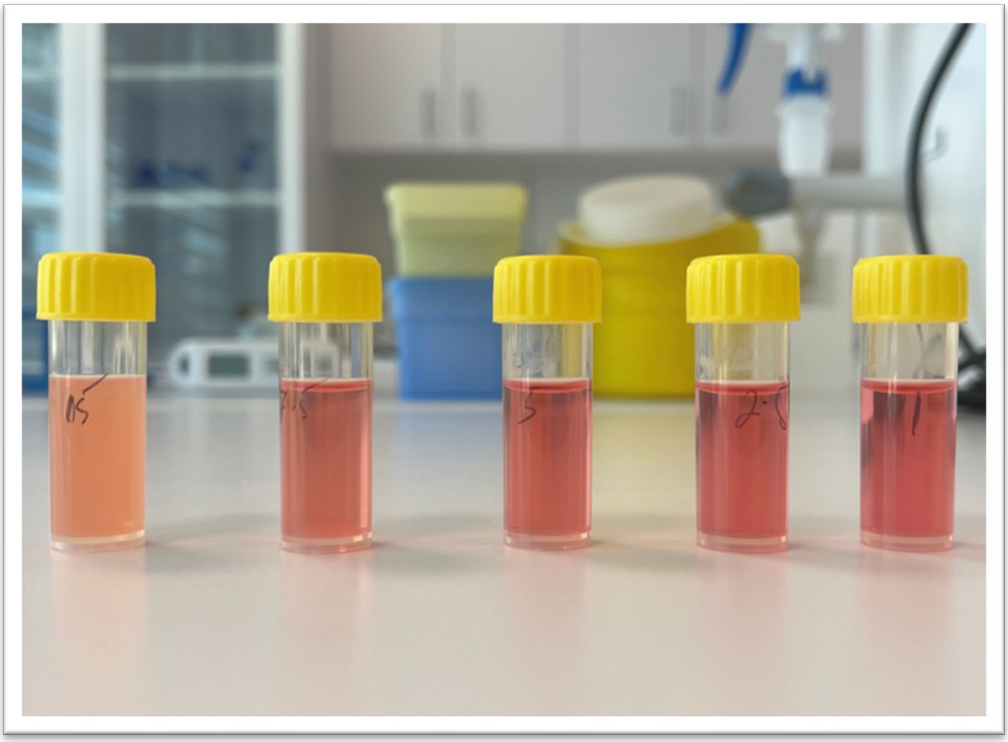

Fig. 5.2: The pH undergoes a shift in response to varying concentrations of BSFL, progressing from left to right (1, 2.5, 5, 7.5, and 15 mL). The colour transitioned from red to a subtle orange, indicating an alteration in pH.

5.2.4 Assessment of the viability of 3T3 cells in response to the oil concentration

The section examined the impact of BSFLO on the proliferation and viability of 3T3 cells over seven days with changing media twice: on Day 0 and Day 3. Four (4) different concentrations were used (1. 2.5, 5 and 7.5 µl/mL) for this experiment. The results showed that BSFLO stimulated the proliferation of 3T3 cells and did not induce cell death throughout the experiment. While there was an overall improvement in cell growth from Day 1 to Day 7 for all samples, no significant changes were observed each day. However, the instability of the samples on Day 3 suggests that the cells were adapting to the BSFLO treatment. This indicates that BSFLO did not display any cytotoxic effects, hinder cell growth, or provide additional nutrition to the cells. In other words, the treated cells behaved almost similarly or improved slightly to those untreated. This result was similar to the other study conducted

by other researcher [225] which was 3T3 cells treated with lauric acid and coconut oil. The cells remained unaltered by the therapy, and 3T3 cells showed an increase in cell proliferation.

The importance of essential fatty acids in the human epidermis is widely recognised. Research has demonstrated that lauric acid possesses antimicrobial properties and can undergo conversion into monolaurin, a substance renowned for its antiviral and antibacterial effects. [226]. Palmitic acid is renowned for its emollient properties, effectively softening and moisturising the skin by reducing water loss through the skin's barrier [227]. Myristic acid exhibits the ability to repair epidermal barrier properties and serves as a penetration lifter [228] which is also similar to oleic acid. As previously stated, fatty acids play a significant part in the skin's lipid barrier, and their use as formulation ingredients has grown due to their functional qualities and natural biocompatibility. The effect of the BSFLO is shown in **Fig. 5.3** and **Fig. 5.4**. The OD data for the experiment on Day 1, Day 3 and Day 7 is given in **Table 5.1**.

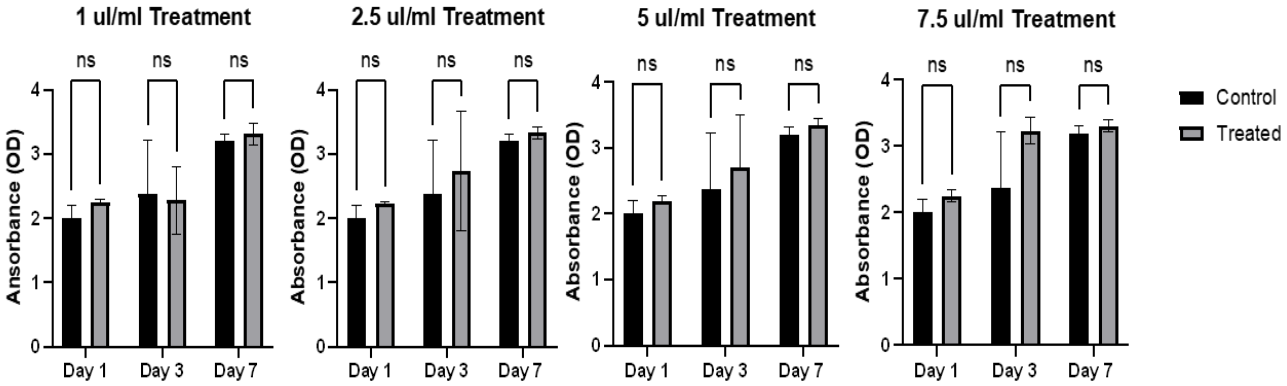

Fig. 5.3: Cell viability of 3T3 cells treated with various BSFLO concentrations (**a**) 1 µl/mL, (**b**) 2.5 µl/mL, (**c**) 5 µl/mL and (**d**) 7.5 µl/mL individual graph.

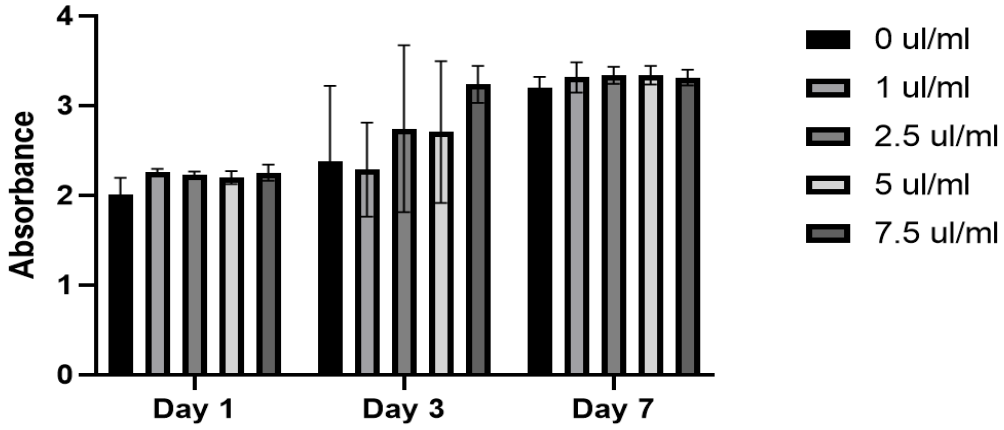

Fig. 5.4: Cell viability of 3T3 cells were treated by BSFLO with different concentrations for Day 1, Day 3 and Day 7 and measured using means OD.

Table 5.1: OD data for the experiment on Day 1, Day 3 and Day 7 of 3T3 cells using different concentrations of BSFLO.

	DAY 1					DAY 3					DAY 7				
Samples µl/mL	**0**	**1**	**2.5**	**5**	**7.5**	**0**	**1**	**2.5**	**5**	**7.5**	**0**	**1**	**2.5**	**5**	**7.5**
A	2.2	2.218	2.239	2.191	2.228	1.558	1.692	3.337	2.879	3.475	3.274	3.139	3.39	3.456	3.377
B	1.997	2.301	2.18	2.126	2.178	2.361	2.486	3.215	1.844	3.106	3.264	3.475	3.226	3.263	3.343
C	1.825	2.241	2.258	2.269	2.353	3.227	2.678	1.669	3.394	3.127	3.066	3.328	3.391	3.296	3.212
Average OD	2.007	2.253	2.226	2.195	2.253	2.382	2.285	2.740	2.706	3.236	3.201	3.314	3.335	3.338	3.311
Viability %	100.00	112.26	110.88	109.37	112.24	100.00	95.94	115.04	113.59	135.85	100.00	103.52	104.20	104.28	103.42
% Proliferation (Control)	**0**	**12.25**	**10.87**	**9.36**	**12.23**	**0**	**13.84**	**36.51**	**34.78**	**61.20**	**0**	**65.09**	**66.17**	**66.30**	**64.92**
% Proliferation vs Control on Day 1	**0**	**12.25**	**10.87**	**9.36**	**12.23**	**N/A**	**-4.06**	**15.04**	**13.59**	**35.855**	**N/A**	**3.52**	**4.2**	**4.28**	**3.42**

All samples are in triplicate (A, B and C). OD = Optical density, N/A = Not available

5.2.5 Relationship between cell growth and media consumption: daily and interval feeding.

This section examines the effects of BSFLO on 3T3 cells with two experimental conditions that were compared: feeding the cells with BSFLO every day and feeding them only on Day 0 with a small concentration of 0.25 µl/mL, 2.5 µl/mL and 7.5 µl/mL and decided to use another different concentration which is 10 times lower concentration to see the effect of the treatment. This is a different experiment setting from the previous one. The aim was to assess whether significant differences existed between the control and treated groups when treated daily and only once at the beginning of the week. The results indicated that the control and group treated with 0.25 µl/mL of BSFLO did not exhibit substantial differences. Both groups of cells showed growth and did not display cytotoxicity or inhibition. This suggests the low 0.25 µl/mL concentration of BSFLO did not adversely affect cell growth or viability. Similarly, the oil was treated with 2.5 µl/mL of BSFLO. Despite an increase of 10 times in the concentration, the cells grew similarly to the control group and showed no inhibition.

However, when the treatment was performed with 7.5 µl/mL of BSFLO and daily feeding resulted in significant differences compared to the control group. The cells did not grow as well as the control group, indicating that the higher concentration inhibited cell growth. Despite this inhibition, the cells still displayed a dynamic growth trend, suggesting they could overcome some of the stress imposed by the higher concentration. A lipid layer was observed above the media layer throughout the experiment, despite being vortexed and filtered twice. This observation raises the possibility that the hindered cell growth could be attributed to this lipid layer, which may impede oxygen transfer into the cells. Consequently, the insufficient penetration of oxygen could induce stress within the cells.

Interestingly, when the higher concentration of 7.5 µl/mL of BSFLO was administered only on Day 0 and not continued daily, the cells showed growth similar to the control group. This suggests that the initial exposure to the higher concentration did not impede cell growth when not sustained over time.

These findings demonstrate that the concentration of BSFLO used in the experiment significantly impacted cell growth. The lower concentration of 0.25 µl/mL did not inhibit cell growth, similar to 2.5 µl/mL oil concentration, while the higher concentration of 7.5 µl/mL, particularly when administered daily, hindered cell growth. This suggests that the higher concentration of BSFLO imposed stress on the cells, impeding their ability to grow effectively. However, when the higher concentration was applied only on Day 0 and not continued, the cells could grow in a manner similar to the control group. Comparison of once-off treatment versus daily treatment of BSFLO on the 3T3 cells is illustrated in **Fig. 5.5**.

5.2.6 The effect of a thin layer of BSFLO on the culture media

Throughout the experimental period, a persistent lipid layer was evident atop the media layer, even after repeated vertexing and dual-stage filtration. This observation suggests that the observed inhibition of cell growth could be ascribed to the presence of this lipid layer, potentially obstructing the diffusion of oxygen into the cellular environment. As a result, the impaired oxygen transfer might lead to cellular hypoxia, thereby inducing a state of physiological stress in the cells. This hypothesis emphasises the need for further investigation into the interplay between lipid layer formation and cellular respiration dynamics.

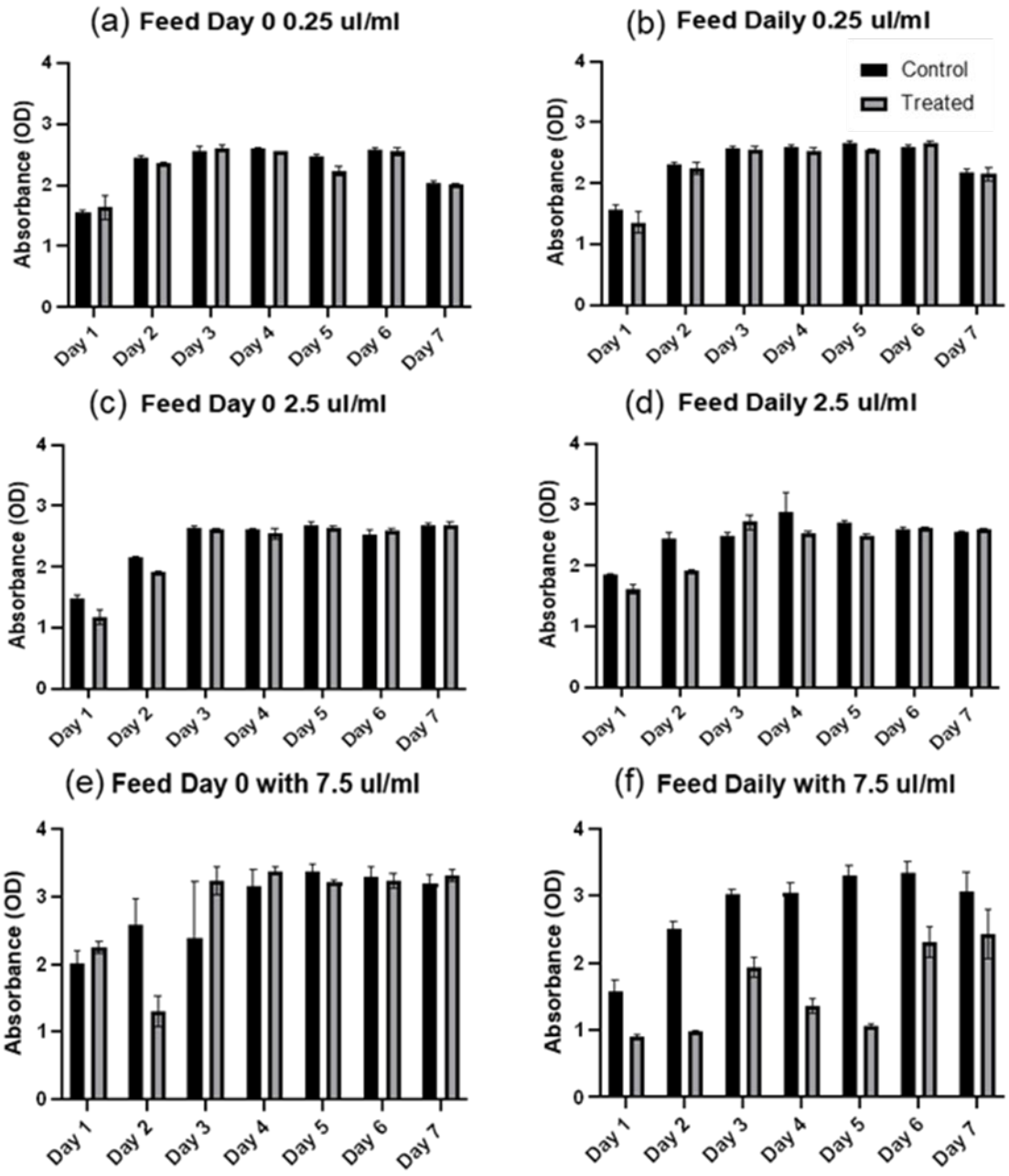

Fig. 5.5: Comparison of once-off treatment versus daily treatment of BSFLO on the 3T3 cells (**a**) feed day 0 with 0.25 µl/mL, (**b**) feed daily with 0.25 µl/mL, (**c**) feed day 0 with 2.5 µl/mL, (**d**) feed daily with 2.5 µl/mL, (**e**)feed day 0 with 7.5 µl/mL and (**f**) feed daily with 7.5 µl/mL. Triplicate experiment conducted and standard deviation has been used for analysis.

5.2.7 Microscopy visualisation to show the effect of optimisation oil concentration on the cell proliferation.

The experiment was conducted by seeding a 24-well plate with 15,000 3T3 cells per mL and monitoring their proliferation using a phase contrast microscope at 10x magnification. The results indicate that on Day 1, the cells treated with 0.25 µl/mL showed a higher proliferation rate than the control group. However, on the same day, the cells treated with 2.5 µl/mL showed lower proliferation than those treated with 0.25 µl/mL. This trend continued on Day 2 and Day 3, with the cells treated with 0.25 µl/mL proliferating faster than those treated with 2.5 µl/mL. Although the cells treated with 2.5 µl/mL showed proliferation from Day 0 to Day 2 and Day 3, their proliferation rate was lower than those treated with 0.25 µl/mL and the control group. Furthermore, the results suggest that the treatment with 0.25 µl/mL positively influenced the proliferation of the 3T3 cells on all three observation days. Conversely, the treatment with 2.5 µl/mL resulted in a slower proliferation rate than the control group and the cells treated with 0.25 µl/mL. The cells treated with the oil spread more than the control cells, although it was difficult to determine whether there was a substantial increase in cell quantity between the control and oil-treated cells. **Fig. 5.6** illustrates the phase contrast image for cell spreading from Day 1, Day 2 and Day 3 with different concentrations.

Then, upon examining the microscopic visualisation, for the DAPI staining, it is evident that there is a substantial discrepancy between the cells spreading for Day 1 and Day 3 for both the control and treated cells with 2.5 µl/mL. The cells appeared to be spreading and proliferating on Day 1 and Day 3. While the cells on Day 3 appeared to be more crowded and had reached confluence, it was still observed that there was continued proliferation happening. This indicates that the treated cells with 2.5 µl/mL treatment can proliferate

despite the crowded conditions. 3T3 cells are commonly described as fibroblast-like cells and typically exhibit a flattened, elongated morphology when they adhere and spread on a surface. They undergo morphological changes during proliferation and can transition from a round shape to a spread-out, elongated shape. These morphological changes are often associated with cellular processes such as cell adhesion, migration, and proliferation. However, based on the result, the cell morphology did not change from Day 1 to Day 3 observation. Although the treatment was conducted on the 3T3 cells with the BSFLO, the morphology of the 3T3 cells remained round after the observation with the microscope. **Fig. 5.7** shows 3T3 cell spreading after 1 and 3 days on BSFLO treatment with DAPI stain under different BSFLO treatments with a scale bar of 10µm.

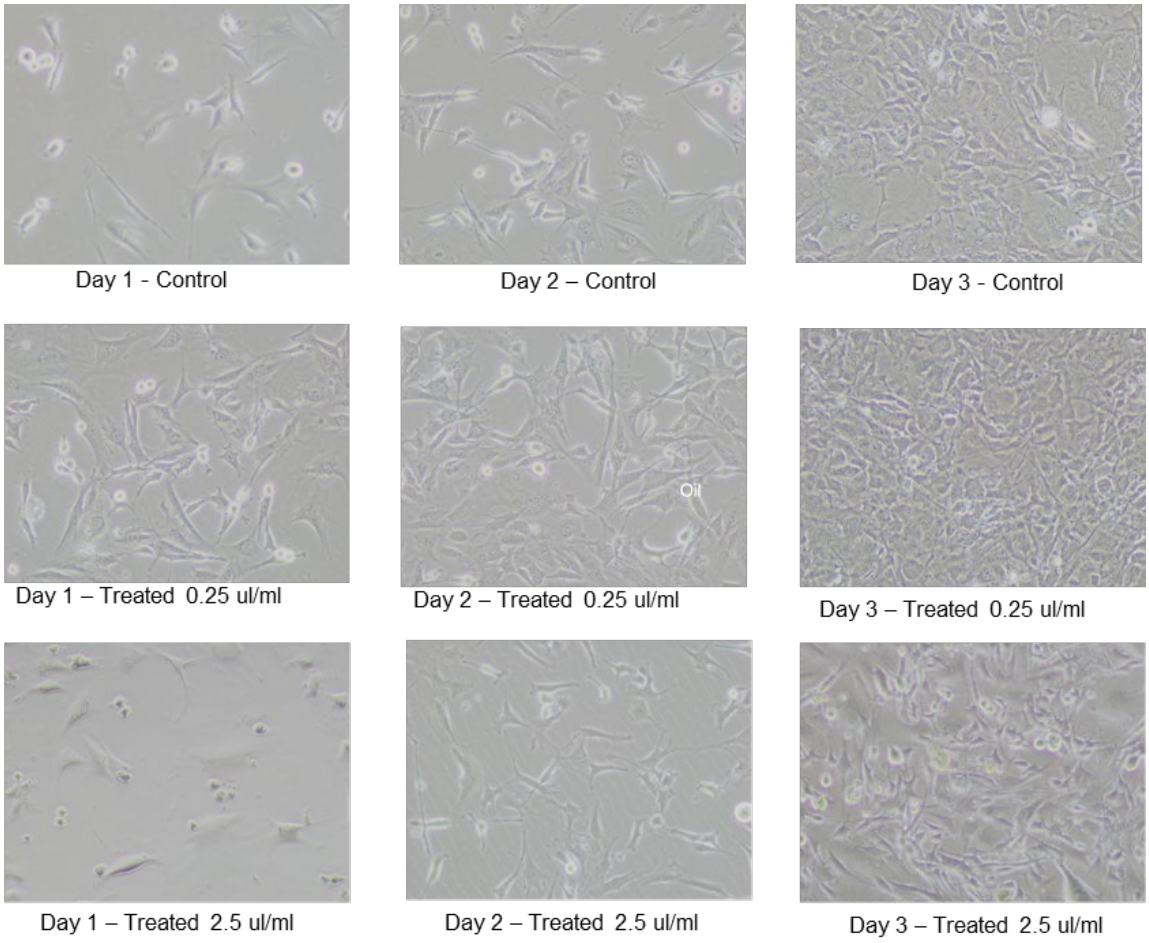

Fig. 5.6: The phase contrast images for cells treated with 0.25 µl/mL and 2.5 µl/mL with the control group.

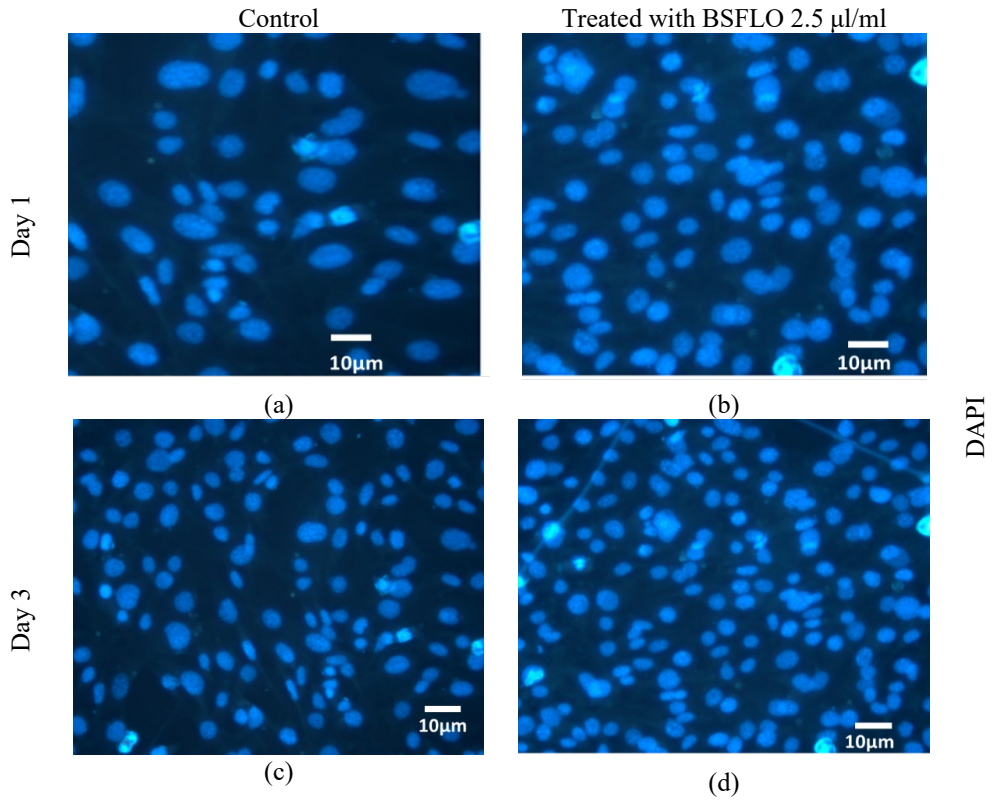

Fig. 5.7: 3T3 Cell spreading after 1 and 3 days on BSFLO treatment (2.5 µl/mL) with DAPI stain under lasers excitation (**a**), (**b**), (**c**) and (**d**) with scale bar 10µm.

5.2.8 Effect of cell migration in response to the oil concentration

A scratch test was conducted to observe the migration of 3T3 cells over several time intervals (0 hrs, 4 hrs, 8 hrs, and 24 hrs) under various treatments using BSFLO. The treatments consisted of a control group and three sets of concentrations (0.25 µl/mL, 2.5 µl/mL, and 7.5 µl/mL) of BSFLO. The scratch was made using a 1 mm tip, and the resulting image was observed under a phase contrast microscope at 4x magnification. The findings revealed that after 4 and 8 hours, both the control and treated groups exhibited cell migration towards the centre. The control group displayed slightly faster cell migration compared to the treated groups, with the 0.25 µl/mL group showing slightly slower migration than the control group, followed by the 2.5 µl/mL and 7.5 µl/mL groups. However, after 24 hours, both the control and treated groups successfully reached the centre and closed the wound/scratch. This indicates that BSFLO effectively promoted wound closure within 24 hours without any toxic

effects on the cells, regardless of concentration. The scratch test demonstrated that BSFLO treatment facilitated cell migration towards the centre of the scratch over time. Although the control group exhibited faster migration, all groups, including the treated groups with different concentrations of BSFLO, ultimately closed the wound within 24 hours. This suggests that BSFLO and its fatty acids have the potential as a wound treatment agent. The importance of essential fatty acids in the human epidermis is well recognised. Palmitic acid and its derivatives contribute to moisturising properties, while linoleic acid enhances the impermeability of the stratum corneum, also known as the outermost layer of the epidermis. Myristic acid aids in repairing the epidermal barrier and acts as a penetration enhancer. Oleic acid modulates epidermal lipid metabolism, affecting the stratum corneum's barrier function and moisture content [229].

Fatty acids derived from BSFL can also possess antimicrobial properties, which is particularly valuable given the issue of antibiotic resistance and consumer concerns regarding preservatives in cosmetic products [230]. However, antimicrobial properties have not been investigated in this study. Lauric acid, in particular, has antimicrobial properties and can be transformed into monolaurin, which is both antiviral and antibacterial. As previously stated, fatty acids are essential components of the skin's lipid barrier, and their use in formulations has expanded due to their functional benefits and natural compatibility with the body. Consequently, BSFLO, containing a combination of fatty acids, could be utilised in cosmetic applications. Lauric acid and other fatty acids exhibited in BSFLO can be used individually or as part of lipid complexes, serving as moisturisers, structural components for encapsulating active substances or fulfilling other functions within formulations. **Fig. 5.8** illustrates the morphology of the normal 3T3 cells, and **Fig. 5.9** shows

the wound-healing migration image for the 3T3 cells treated with different concentrations of BSFLO, respectively.

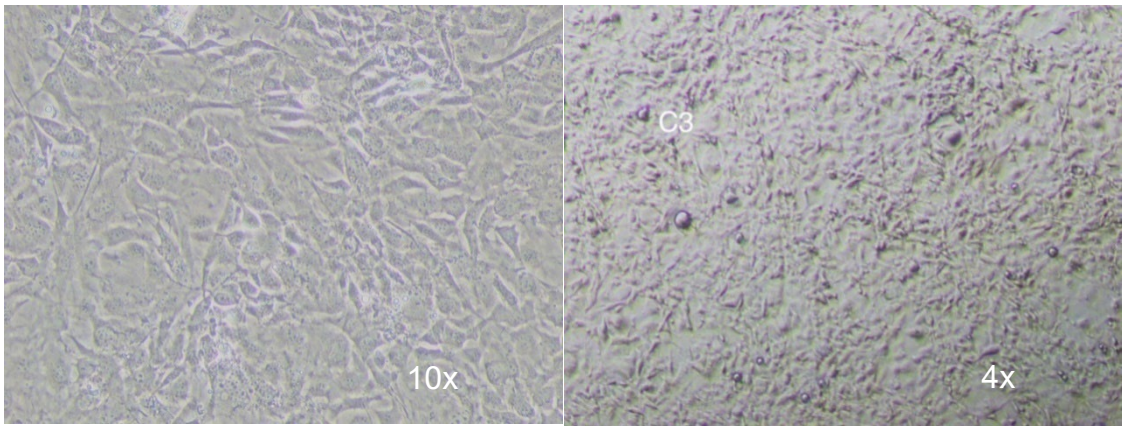

Fig. 5.8: Morphology of 3T3 cells with 10x and 4x magnification and 50 um with almost 100% confluences.

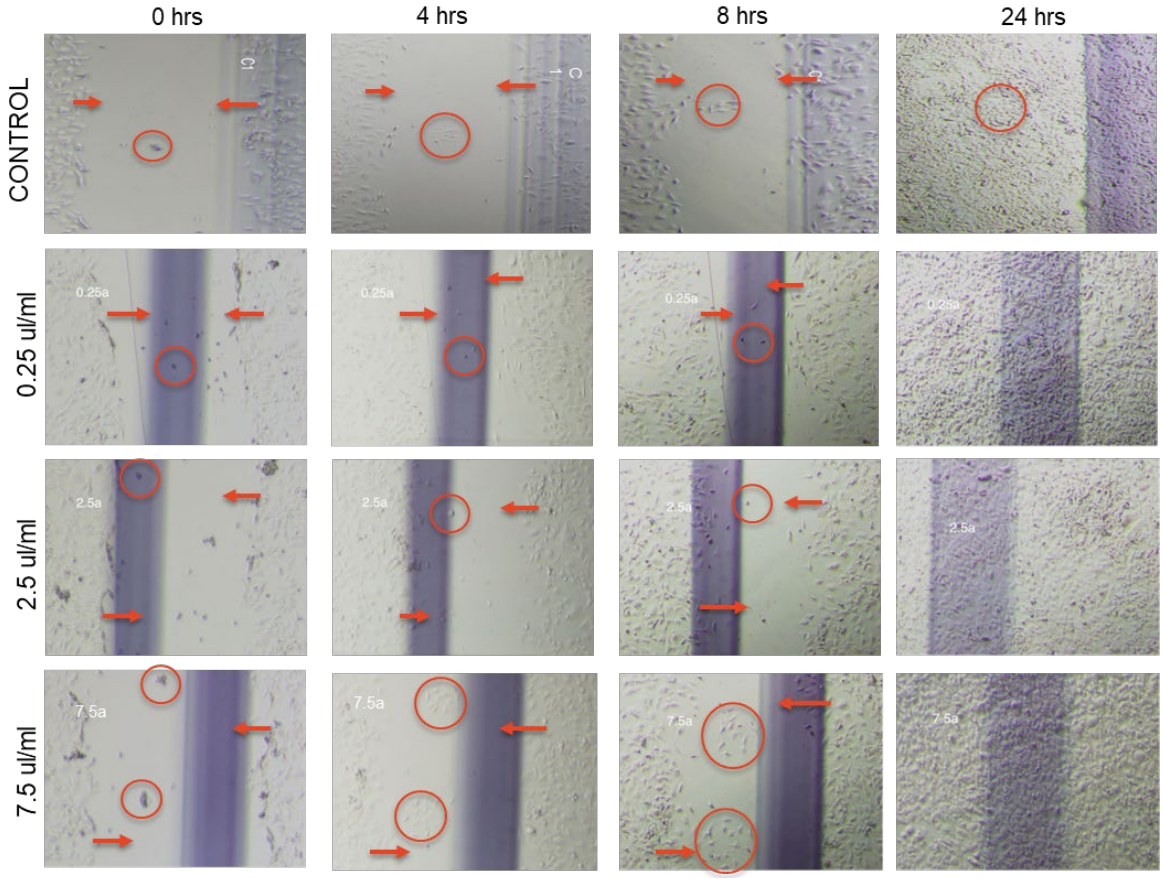

Fig. 5.9: 3T3 Cell migrations for the wound healing assay treated with difference BSFLO concentration (**a**) control group, (**b**) 0.25 µl/mL, (**c**) 2.5 µl/mL and (**d**) 7.5 µl/mL for 0 hours, 4 hours, 8 hours and 24 hours.

5.3 Summary

SC-CO2 extraction was chosen for this study due to practicality, environmental friendliness, and reduced contamination for the extraction of BSFLO. SC-CO2 extraction also yielded a higher SFA to USFA ratio than solvent extraction. BSFLO contained a significant amount of lauric acid (54.97%), known for promoting the proliferation of 3T3 cells. These findings suggest that BSFLO effectively stimulates cell proliferation without harming the cells, as lauric acid can be metabolised by cells for energy production. Different concentrations of BSFLO used in the experiment notably impacted cell growth. Lower concentrations (0.25 µl/mL and 2.5 µl/mL) did not inhibit cell growth, while the higher concentration of 7.5 µl/mL, mainly when administered daily, hindered cell growth. This indicates that the higher concentration of BSFLO imposed stress on the cells, impeding their effective growth. Curiously, when the higher concentration was applied only on Day 0 and not continued, the cells showed growth similar to the control group. Microscopic observations confirmed that the oil from BSFL promoted cell proliferation, as observed through cell spreading from Day 1 to Day 3. The migration assay suggested that the BSFLO suits the wound healing agent. In summary, this study demonstrated the positive impact of BSFLO on cell proliferation and highlighted the potential of lauric acid as a crucial nutrient for facilitating cell growth and repair.

CHAPTER 6: ISOLATION AND CHARACTERISATION OF CHITIN AND CHITOSAN FROM BSFL

BSFL are rich in fat and protein and contain the precious biopolymer chitin, which accounts for less than 10% of its dry matter [231]. Compared to other sources, there is a relative lack of research on BSFL as a natural source of chitin. However, several studies indicate that the chitin matrix can change physicochemical during the BSFL developmental phases; for example, during the larvae, prepupa, puparium, and adult phases of BSF, the chitin concentration has been determined to be around 3.6%, 3.1%, 14.1%, and 2.9%, respectively [232].

Chitin and chitosan are natural polysaccharides containing 2 monosaccharides, N-acetyl-D-glucosamine and D-glucosamine, linked by β-1,4-glycoside bonds [233]. Chitin is frequently found in crustaceans, insects, as well as some types of fungi and yeasts, and it gives organisms a tough and protective exoskeleton. Chitosan, a derivative of chitin, has a remarkable value in the economy due to its properties and various potential applications, such as in biomedicine, wastewater treatment, textiles, foods, and many more. However, most of the chitosan produced lacks purity, which is necessary in the pharmaceutical and biomedical industries but not crucial in others, such as the textiles sector, which uses low-quality chitosan [234].

Traditionally, chitin has been removed from crustacean shells via the chemical procedures of demineralisation and deproteinisation. Dilute hydrochloric acid is used to treat the raw material in order to eliminate mineral salts, primarily calcium carbonate and solid bases [235]. However, due to the high fat content in BSF, the treatment to obtain chitin needs to start by removing the fat from the larvae, followed by demineralisation and deproteinisation. Some researchers have found that chitosan isolated from different insects, such as cicada

slough, silkworm chrysalises, mealworms, and grasshopper species, has a higher potential water-holding capacity (594-795%) and fat-binding capacity (275-645%) than prawn shell chitosan. Additionally, a number of variables, including the degree of deacetylation (DA), molecular weight (MW), crystallinity, and degradation, have an effect on the physicochemical properties of chitosan [236]. The higher DA of chitin and chitosan can be obtained by fat extraction of the BSFL before proceeding to demineralisation and deproteinisation using acidic and alkali solutions. Hence, removing the fat and lipids could positively impact the purity and mechanical strength of the chitin and chitosan.

This section aims to identify the potential differences between the chitin and chitosan that experience a fat extraction process from BSFL using SC-CO2 extraction, compared to those obtained from solvent extraction, followed by acidic hydrolysis for demineralisation and alkali hydrolysis for deproteinisation of the samples. Deacetylation using a concentrated alkali solution is also utilised to obtain the final product, i.e., chitosan from BSF. This product's structure, characteristics, and behaviour morphology are compared to commercially available prawn-derived polymers.

6.1 Material and Methodology

Detailed material and methodology are in Chapter 3, Section 3.13 and 3.2.3 for isolation of chitin and chitosan from BSFL, including a thorough discussion of the materials and methodology employed in the process.

6.2 Result and Discussion

This section presents a thorough investigation of chitin and chitosan derived from biological sources. The characterisation begins with an overview of the extraction process, followed by FTIR spectroscopy to detail the molecular structure and functional groups. Elemental

analysis is conducted to determine the composition of these biopolymers. The degree of acetylation (DA) is assessed, crucial for evaluating chitosan's quality. TGA provides insights into thermal stability and decomposition, while SEM reveals the surface morphology. Lastly, XRD analysis is used to examine the crystallinity structure, offering insights into the molecular arrangement. This section emphasises the detailed exploration of chitin and chitosan, highlighting their potential utilisation.

6.2.1 Extracted Chitin and Chitosan

Extracted chitin and chitosan from the BSFL were calculated using Equation (3.6) and Equation (3.7), and the weight percentage is shown in **Table 6.1**. The results showed that the chitin extracted is around 3 – 5% less than the study conducted by Wasko et al. [147]. This result might be due to the lengthy and repeated steps during deproteinisation, where the samples need to be filtered, transferred, and washed. Therefore, some samples were lost during that process, with almost ± 3% of the original sample.

Table 6.1: Comparison between Chitin and chitosan obtained from BSFL with different extraction methods.

Sample	Weight Percentage (%)	
	Chitin	Chitosan
SC-CO2 Extraction	5	4
Solvent Extraction	3	2
No fat extraction Method	5	4

Note: Triplicate experiment with the average value. Due to lengthy and repeated steps, some samples were lost during filtering and transferring the sample was almost plus-minus (3%).

6.2.2 Fourier transform infrared (FTIR)

Prawns are a well-known source of α-chitin. The chitin from prawns and BSFL display the two anticipated absorbance bands in the 1,660 – 1,615 cm^{-1} region [151, 206]. The chitin samples from BSFL display two distinct bands at 1,654 and 1,652 cm^{-1} and 1,619 and 1,618

cm^{-1}, respectively, which is the amide I band, and thus were identified as α-chitin. Comparatively, samples with β-chitin would exhibit only one distinct band in the region. This can be explained by the bonding of partial carbonyl groups with the amino group within the same chain. For both chitin samples from BSFL, the presence of absorption peaks at 1,652 and 1,654 cm^{-1} are attributed to this. The remaining carbonyl groups would form a bonding with the hydroxymethyl group from the side chain, represented by the decline in the amide I band at 1,619 and 1,618 cm^{-1} for both samples. These interchain bonds are known to contribute to the high chemical stability in α-chitin structures [237]. However, only one absorbance band was found for the sample that was not treated with any fat extraction method at 1,620 cm^{-1}. This result may be due to a high level of fat that hindered the chitin extraction and affected the purity of the chitin. It also shows two sharp bands at 2,919 cm^{-1} and 2,850 cm^{-1} for all chitin samples extracted from BSFL but not the prawn chitin. There are no significant differences in absorbance bands based on solvent and SC-CO2 extraction. Therefore, the spectra's similarity suggests the same chitin quality for fat extraction samples except for a sample without fat extraction. This study therefore shows that it is crucial to remove the fat of the BSFL before chitin extraction to ensure the purity of the polymer. **Fig. 6.1** and **Table 6.2** show the spectrum display of the chitin-specific absorbance bands.

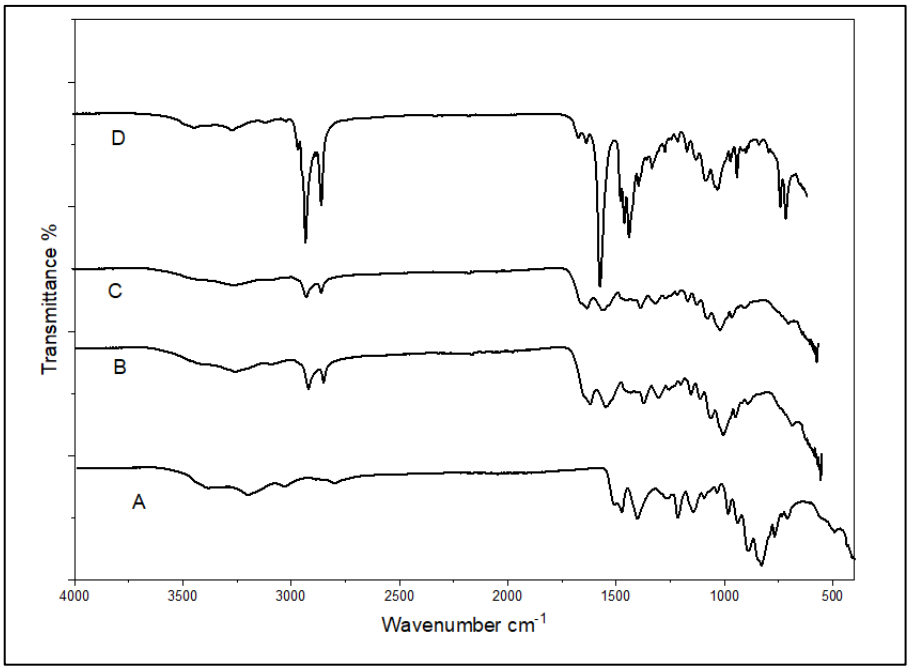

Fig. 6.1: Comparison of FT-IR spectra for chitin samples obtained from (**A**) prawn, (**B**) BSFL with SC-CO2 extraction, (**C**) BSFL with solvent extraction, and (**D**) BSFL without extraction.

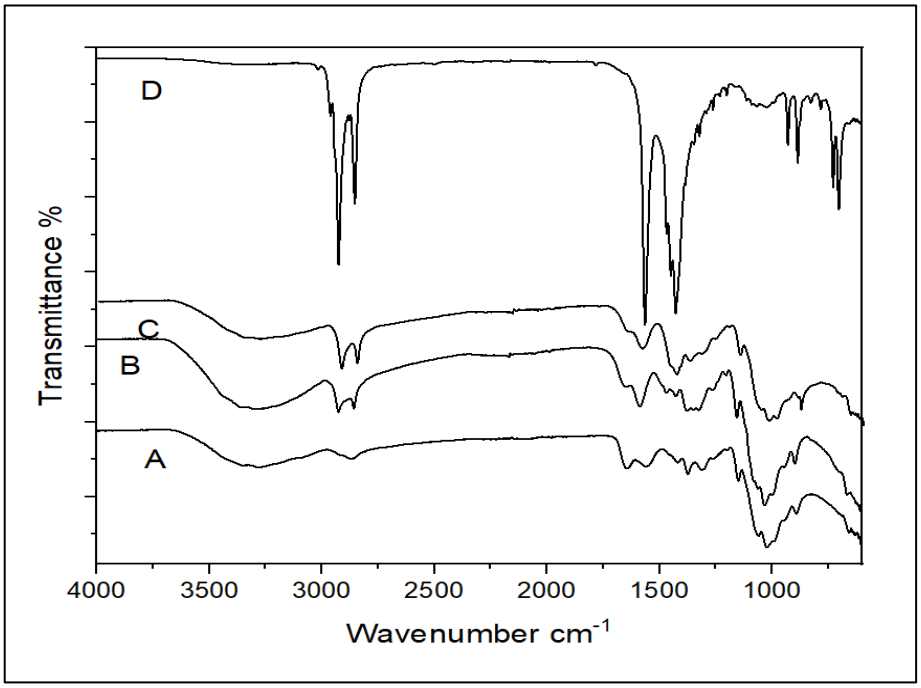

Fig. 6.2: Comparison of FT-IR spectra for chitosan sample obtained from (**A**) prawn, (**B**) BSFL with SC-CO2 extraction, (**C**) BSFL with solvent extraction, and (**D**) BSFL without extraction.

Figs. 6.2 (**B**) and (**C**) show that the peaks at 3,284 and 3,280 cm-1 in line to the stretching of N-H groups. Absorption peaks of 2,918 and 2,920 cm-1 are due to the alkane group's C-H stretching vibrations, and amide I's stretching vibration is shown by the 1,641 cm-1 peak. Furthermore, absorption peaks at 1,580 and 1,584 cm-1 are due to the presence of amide II, while the peaks at 1,419 and 1,431 cm-1 are attributed to CH2 bending and CH3 deformation, respectively. In addition, the presence of amide II are shown by peaks 1,580 and 1,584 cm-1. Amide III is represented by absorption peaks at 1,318 and 1,319 cm-1 [238]. The presence of C-O in the primary OH group is found at 1,025 and 1,021 cm-1, while the pyranose ring is represented by an 891 cm-1 absorption peak. In comparison, chitosan obtained from prawns is illustrated in **Fig. 6.2 (A)**. This spectrum results for the chitosan extracted from BSFL are compatible with the results reported by other researchers [239, 240]. **Table 6.3** shows the functional groups represented by the FTIR absorption peaks for chitosan obtained from prawn, BSFL with supercritical CO_2 extraction, BSFL with solvent extraction, and BSFL without fat extraction. It is found that the appearance of absorption peaks is similar for the chitosan obtained from either prawn or BSFL, with extraction using either CO_2 or solvents.

However, one clear difference in the spectrum shown in **Fig. 6.2 (D)** is the appearance of absorption peaks representing the presence of fats in the sample without fat extraction. This is demonstrated by absorption peaks between 2,800 – 3,000 cm^{-1} which correspond to a C-H bond, and 1,600 – 1,800 cm^{-1} which represents the C=O bond (Rohman & Man, 2011). Here, the C-H bond is represented by the 2,871 and 2,955 cm^{-1} absorption peaks. The presence of these peaks in the fat-extracted BSFL samples suggests that there is still some residual fat in these samples, even after the fat extraction process. Importantly, these peaks are not observed in the prawn sample. While the 1,774 cm-1 peak affirms the presence of

the C=O bond associated with fats, its subtle intensity suggests a potentially lower concentration of fats or a more effective fat extraction process in the other samples. This underscores the importance of fat extraction in achieving a high-purity product.

Moreover, the peaks at 1,558 cm-1 and 1,421 cm-1 are more pronounced in the sample that underwent no fat extraction, suggesting the possibility of other compounds or impurities present. A simpler spectrum with fewer pronounced peaks is typically considered a standard for purity, and the samples that underwent fat extraction exhibit less noticeable peaks at 1,558 cm-1 and 1,421 cm-1, making them potentially purer in comparison to the sample without fat extraction. This highlights the importance of effective fat removal procedures for purified chitin and chitosan products.

Table 6.2: Comparison of the FTIR bands to the respective vibration of chitin from Prawn and BSFL with different fat extraction methods.

Functional Group	Absorbance Peak (cm^{-1})			
	Prawn	BSFL with SC-CO2 extraction	BSFL with solvent extraction	BSFL without extraction
OH Stretching	3426	3425	3434	n/a
N-H stretching of an amide group	3256	3257	3257	3260
C-H asymmetric stretching	2871	2919	2920	2920
C=O Secondary amide stretch (Amide I)	1653	1653	1656	n/a
C=O Secondary amide stretch (Amide I)	1619	1618	1619	1620
N-H bending of N-acetyl group (Amide II)	1551	1550	1556	1547
C-H bending, CH_3 symmetric deformation	1374	1374	1377	1372
C-N vibration from amides (Amide III)	1307	1307	1315	1304
C-O-C asymmetric stretching	1153	1154	1153	1153
C-O-C symmetric stretching	1112 1068 1008	1112 1059 1007	1112. 1068 1011	1111 1061 1004

Table 6.3: Absorption peaks for chitosan obtained from prawn and BSFL.

Functional Group	Absorbance Peak (cm^{-1})			
	Prawn	BSFL with SC-CO2 extraction	BSFL with solvent extraction	BSFL without extraction
N-H stretch	3284	3284	3280	3301
C-H stretch	2866	2918	2920	2919
C=O in the amide I band	1641	1641	1641	n/a
N-H bending in amide II band	1556	1580	1584	1558
CH_2 bending and CH_3 deformation	1418	1419	1431	1421
C-N vibration from amides (Amide III)	1311	1318	1319	1317
C-O stretch	1023	1025	1021	1062
C-H bond	892	891	891	n/a

6.2.3 Elemental Analysis

Table 6.4 shows the elemental analysis results for chitin samples collected from the BSFL. The nitrogen percentage was found to be 6.19 % from the chitin extracted from BSFL that had been subjected to fat extraction using SC-CO2, and 6.60% from the chitin extracted from BSFL where the fat content was extracted using a solvent. These two data reveal that the percentage of nitrogen is somewhat lower than the expected theoretical value of pure chitin (~6.89%) [151], where the nitrogen levels of ~ 6.89% imply protein leftovers in the chitin sample and indicate the purity of the chitin. Therefore, very little to no protein was leftover on the chitin sample, indicating the extraction and purification process was tolerable based on the lower nitrogen content. In addition, the chitin extracted from the BSFL that have not undergone fat extraction shows a significantly lower nitrogen content of 2.12%. This lower nitrogen content indicates that the purification of chitin depends on the degree of fat removal from the BSFL.

6.2.4 Degree of Acetylation (DA)

The FTIR peaks were used to calculate the degrees of acetylation (DA) in the BSFL chitin samples, Equation 3.8, and the carbon and nitrogen ratio as per Equation 3.9. These equations resulted in differing values for the DA of the chitin, as the FTIR peaks/area were not accurate. Therefore, the best method is deemed to be using the carbon to nitrogen ratio.

The DA results for the various experimental circumstances are shown in **Table 6.4**. A high DA of 123% was achieved when the BSFL were innitially defatted by SC-CO2 extraction before the acidic and alkaline hydrolysis. Then, the DA value of 83% for the sample chitin extracted from BSFL was defatted using a solvent, and 1169% for the chitin sample that did not undergo any fat extraction method. The DA value of the chitin sample defatted by SC-CO2 is slightly greater than the theoretical value of 100%. This is possible due to water or mineral residues in the extracted chitin [241, 242]. However, the chitin sample that was not treated with any fat extraction procedure had a higher DA value, which is over 1000%; this is because the lipid hindered the deproteinisation process where the lipid holds the protein bond in the sample.

Consequently, no chitin extraction occurred for the sample with no fat extraction. This can be justified by the larvae's high fat content, which prevents phosphoric acid from interacting with the cell walls because of the hydrophobic repulsion [243]. Protein extraction is influenced by the kind of lipid extraction used, and effective fat extraction and protein precipitation are crucial for producing high yields and purifying extracted insect chitin [44].

Table 6.4: Nitrogen, carbon, hydrogen, and DA of the chitin samples under different conditions.

Item	Sample	N(%)	C (%)	H(%)	C/N Ratio	DA %
Chitin	SC-CO2 extraction	6.19	44.94	6.88	7.26	**123**
	Solvent extraction	6.60	43.75	6.80	6.63	**87**
	No extraction	2.12	53.40	8.75	25.25	1169
	Commercial Chitin (prawn)	6.71	44.07	6.85	6.57	83
Chitosan	SC-CO2 extraction	6.1	38.38	6.69	6.29	67
	Solvent extraction	6.57	38.14	6.75	5.81	39
	No extraction	1.41	35.67	5.74	25.29	1172
	Commercial Chitosan (prawn)	7.55	42.23	7.31	5.59	26

6.2.5 Thermogravimetric through TGA

TGA/DTG curves for BSFL chitin without the fat extraction process are shown in **Fig. 6.3** (a) According to a thermogravimetric examination of the sample's thermal characteristics, the degradation temperature of fat extraction samples is lower than the sample that has not experienced any fat extraction process. In the first stage, about 35% mass loss is attributed to the loss in water, which occurs between 50 and 110 °C. Next, the sample is stable until about 300 °C. Then, the decomposition of fat and chitin starts at about 425 °C, with Tmax at 418.01 °C, at which about 17.43% of the mass is lost within this temperature range. **Fig. 6.3 (b)** shows the spectrum for commercial chitin from prawn. The first stage of mass loss is caused by water vaporisation, which occurs between 50 – 100 °C. After that, no further mass loss occurs until 250 – 390 °C, where the decomposition of chitin occurs gradually, and T_{max} is recorded at 370 °C.

TGA/DTG curves for chitin obtained from BSFL with SC-CO2 and solvent extractions are illustrated in **Fig. 6.3 (c)** and **Fig. 6.3 (d)**, respectively. Three stages of thermal decomposition can be seen. For both cases, the first decomposition stage occurs in the range of 50 – 100 °C, where as much as 14.8% and 10% weight loss is observed. This is due to the vaporisation of water from the samples. Beyond this temperature range, there was no mass loss until about 210 – 390 °C for chitin with CO_2 extraction, with T_{max} recorded at 289.52 °C for chitin degradation. However, as much as 66.9 % of weight loss occurs within this region. For chitin with solvent extraction, T_{max} is observed at 338.94 °C, with 56.16% weight loss. The third decomposition stage occurs from 400 °C onwards, with the maximum temperature recorded at 450 °C**.** Hence, it is seen that chitin with solvent extraction is more thermally stable compared to that obtained using CO_2 extraction. However, it has been

discovered that chitin derived from BSFL has lesser thermal stability than chitin obtained from prawns.

Fig. 6.4(a) shows the TGA/DTG curves for commercial chitosan from prawns. The mass loss within the 50 – 100 °C region corresponds to the vaporisation of water molecules from the sample. The second stage of degradation, which happens in the range of 250 – 410 °C, is due to the decomposition of chitosan, with T_{max} recorded at 295 °C.

For BSFL chitosan without fat extraction, **Fig. 6.4(b**), the first stage of mass loss because of water vaporisation occurs from 50 – 100 °C. Whereas the second stage of mass loss (11.67%) happens between 200 to 350 °C, while the third stage occurs from 350 to 500 °C (42.77%), with T_{max} recorded at 487.2 °C. The curves for BFSL chitosan with solvent and CO_2 extraction are presented in **Figs. 6.4(c)** and **6.4(d),** respectively. In **Figs. 6.4(c)** and **6.4(d)**, the first decomposition stage occurs in the 50 – 100 °C range, where approximately 6.11% and 10.47% weight loss is observed, respectively. This is due to the vaporisation of water molecules. Beyond this temperature range, there was no mass loss until about 150 – 310 °C for chitosan with solvent extraction, with T_{max} recorded at 257.38 °C. A weight loss of 50.72 % occurs within this region. Contrary, for chitosan with CO_2 extraction, T_{max} is observed at 275.4 °C, with 58.19 % weight loss. The third decomposition stage occurs from about 350 °C onwards, with the maximum temperature recorded at 452.4 °C and 438.25 °C for solvent and CO_2 extractions, respectively. Generally, the thermal stability for chitosan obtained from BSFL is lower than that of prawns.

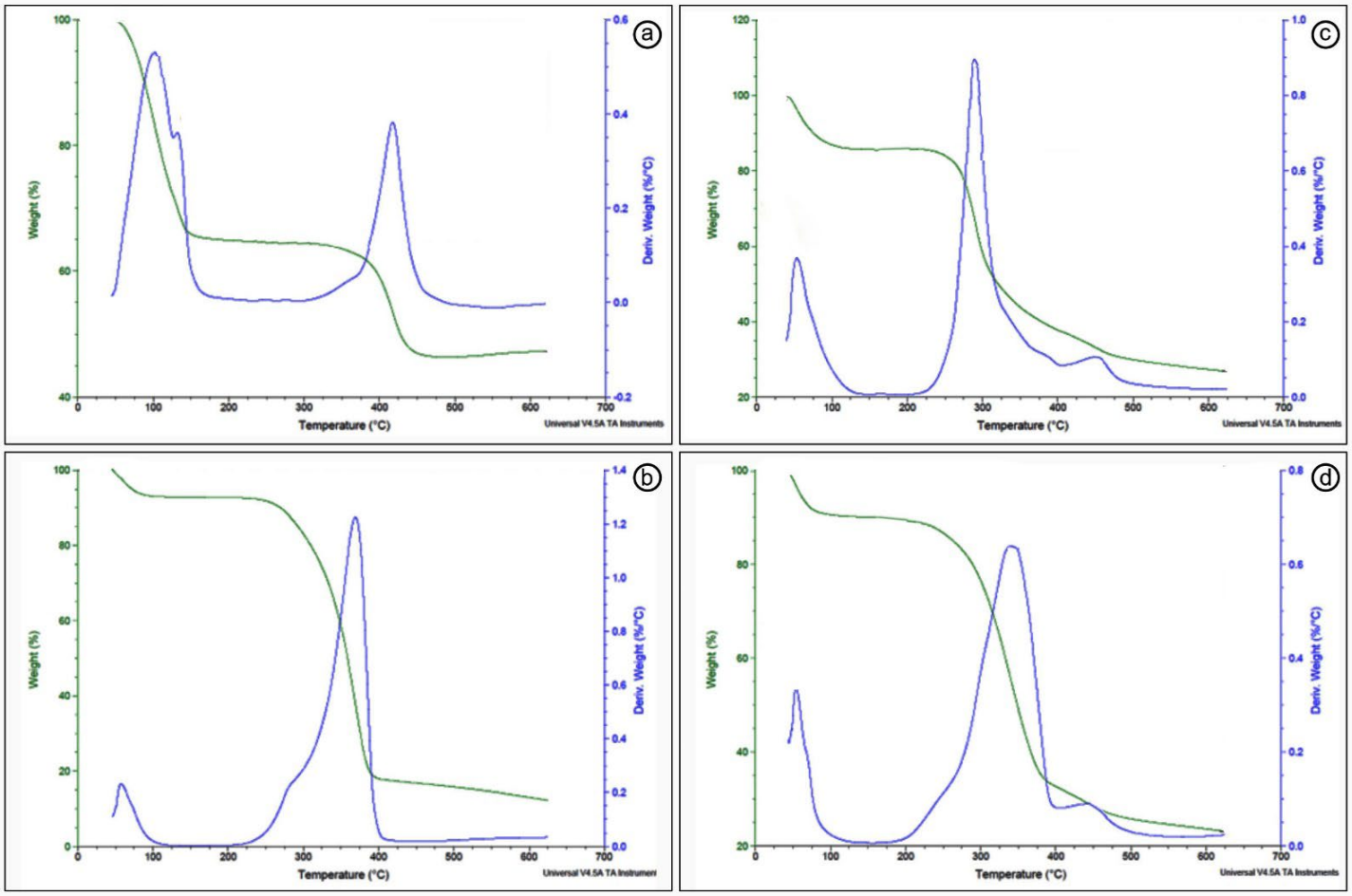

Fig. 6.3: Comparison of the TGA/DTG curve of the chitin from different samples (**a**) TGA/DTG curves for chitin BSFL without the fat extraction process. (**b**): TGA/DTG curves for commercial chitin from prawn (**c**): TGA/DTG curves for chitin BSFL obtained using SC-O2 extraction (**d**): TGA/DTG curves for chitin BSFL obtained using solvent extraction.

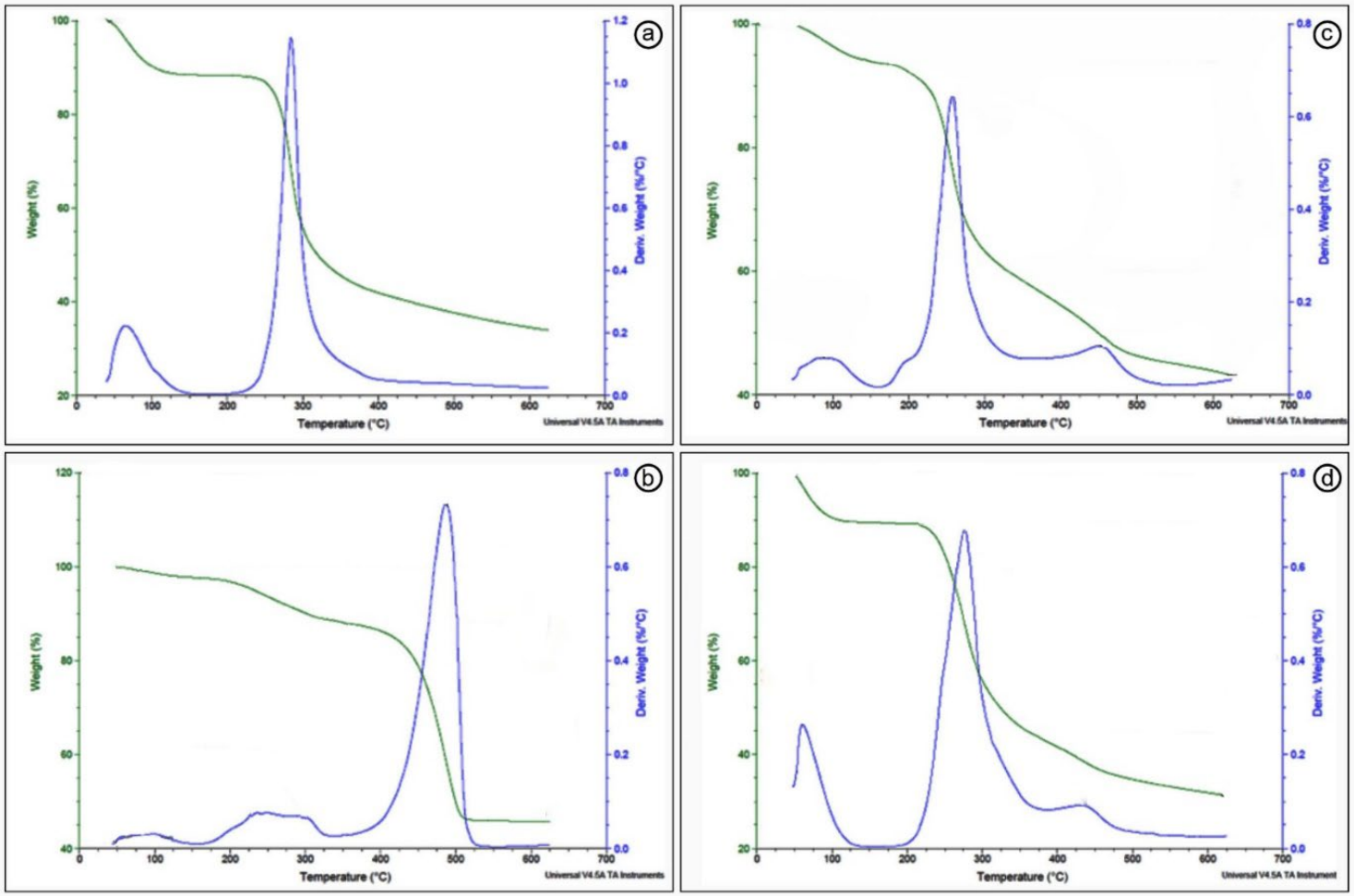

Fig. 6.4: Comparison of the TGA/DTG curve of the chitosan from different samples (**a**): TGA/DTG curves of commercial chitosan from prawn (**b**): TGA/DTG curves of BSFL chitosan without fat extraction (**c**): TGA/DTG curves of BSFL chitosan with solvent extraction (**d**): TGA/DTG curves of BSFL chitosan with CO_2 extraction.

6.2.6 Morphology through SEM

Fig. 6.5 shows SEM analysis for each treatment, evidencing the difference between the chitin and chitosan surface morphologies from BSFL that undergo SC-CO2 extraction, solvent extraction, no fat extraction process, and commercial chitin chitosan extracted from prawn. Using 1,500 x magnification with 10kv and SED, a honeycomb-like structure was seen for all of the chitin from BSFL but was not seen in the chitin samples from the commercially available prawn chitin. This finding is in line with that of other researchers [206, 231]. However, the honeycomb-like structure was hardly found in the chitin sample from BSFL, which did not undergo any fat extraction method. The honeycomb-like structure was more complex, convex and more extensive than the solvent extraction method, and no impurities were observed while using the supercritical CO_2 extraction. Chitin that has surface pores improves its capacity to take in metal ions. Chitin with a fibrous surface can be used to make textiles, and its porous structure makes it a useful tool for tissue engineering [232].

6.2.7 Crystallinity structure through XRD

The crystallinity structure of the chitin and chitosan recovered from BSFL, and commercial chitin and chitosan was characterised using X-ray diffraction (XRD) analysis, which enables the examination of the atomic and molecular structure of the crystal. **Table 6.5 s**hows the crystalline index (CrI) of all the samples, and **Fig. 6.6** visualises the XRD pattern of all the chitin and chitosan. The chitin samples showed intense peaks around 9.3°, 12.6°, 19.3°, 20.8°, 23.2° and 30°, which is consistent with prior investigations, with the exception of the sample that did not undergo the fat extraction method. The α-chitin of the samples showed intense peaks at 9.3° and 19.3°, and small peaks at 23.2° and 30° [151, 206, 231, 241], similar to the prawn chitin used for industrial purposes. For this study, the chitosan samples presented two crystalline peaks approximately at 10° and 20°, similar to another study [244].

However, unlike the chitosan that did not undergo any defatting, the XRD pattern showed many intense peaks at 7.3°, 9.8°, 19°, 22°, 30° and more until 47°. This result showed that the fat extraction process is essential to eliminate contamination and improve the purity of the chitin and chitosan. Amazingly, the crystallinity index (CrI) for all chitin extracted from BSFL using the SC-CO2 gave a slightly higher index than the solvent extraction, which is 74% and 71%, respectively. This result is higher than those of other studies performed by Purkayastha et al. and Wasko et al. [151, 231]. However, unlike the chitin that did not undergo any fat extraction, it showed a significantly lower 10% index. The results showed that insects that underwent the fat extraction gave stronger and harder chitin, subsequently more crystalline and less amorphous than insects that did not de-fat. The results also have a similar pattern to the chitosan samples.

Table 6.5: Crystallinity index (CrI) for all samples of chitin and chitosan from BSFL and commercial prawns.

Item	Sample	I_{110}	I_{am}	CrI (%)
Chitin	SC-CO2 extraction	9615	2485	74
	Solvent extraction	7795	2234	71
	No extraction	3388	3063	10
	Commercial Chitin (prawn)	11150	2234	80
Chitosan	SC-CO2 extraction	7956	4707	40
	Solvent extraction	4898	2472	49
	No extraction	4789	3155	34
	Commercial Chitosan (prawn)	9053	3567	60

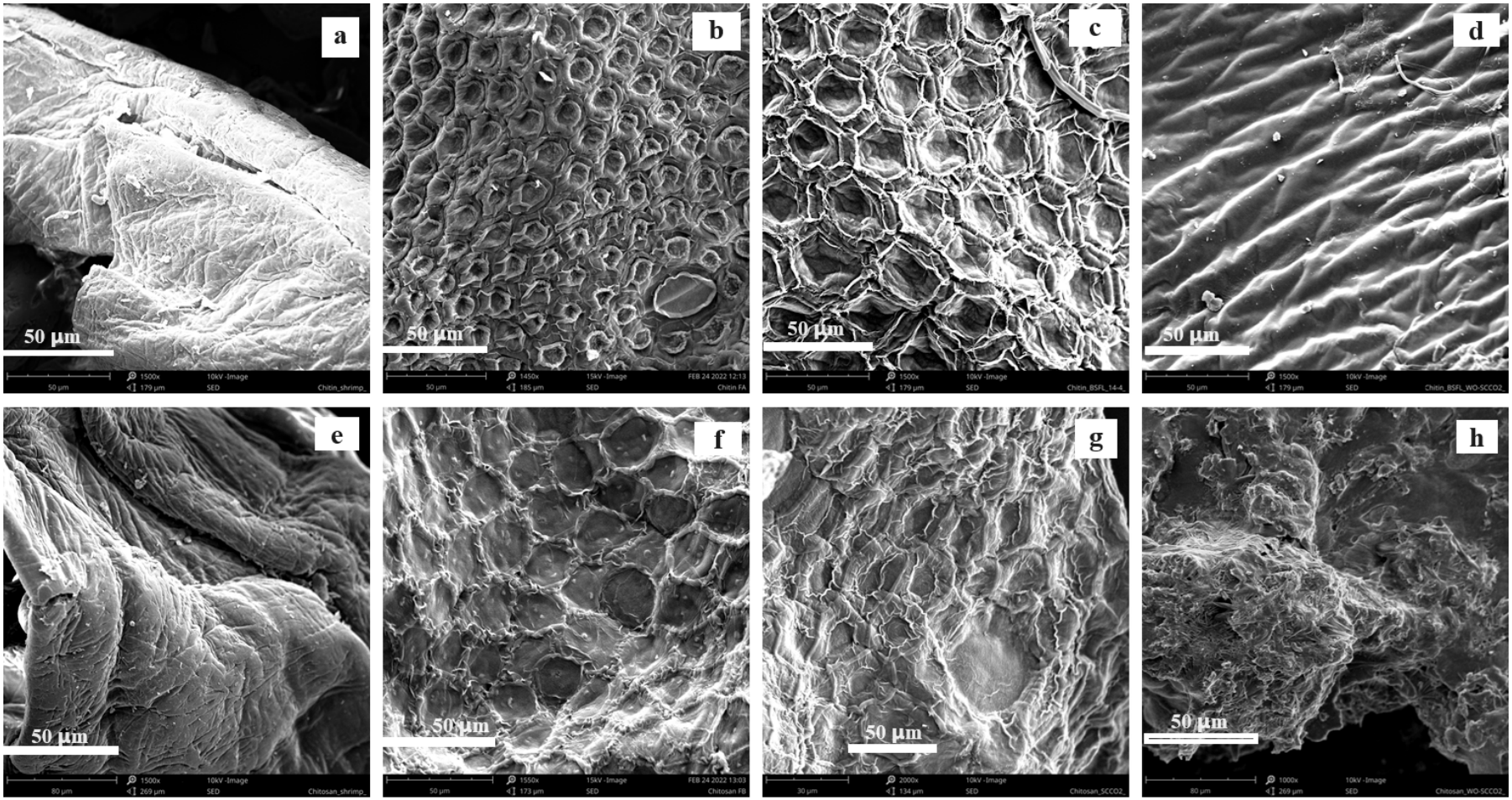

Fig. 6.5: SEM image for chitin and chitosan from different method of fat extraction method (**a**) commercial chitin (**b**) chitin extracted using SC-CO2 (**c**) chitin BSFL extracted using solvent (**d**) chitin BSFL that do not undergo lipid extraction (**e**) commercial chitosan (**f**) chitosan BSFL extracted using SC-CO2 extraction (**g**) chitosan BSFL extracted using solvent extraction and (**h**) chitosan BSFL without any lipid extraction.

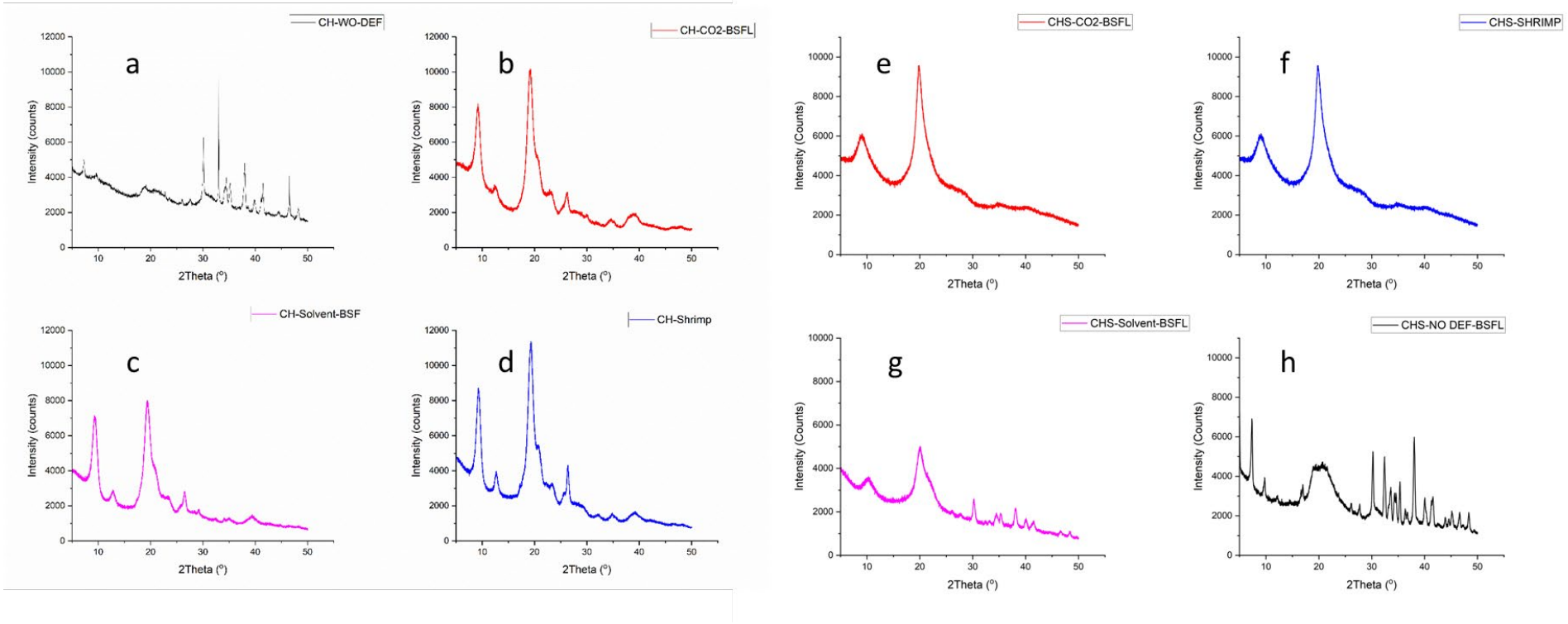

Fig. 6.6: XRD pattern of chitin and chitosan extracted from the BSFL and commercial chitin and chitosan (prawn); (**a**) chitin with no deffating, (**b**) chitin extracted using SC-CO2, (**c**) chitin BSFL extracted using solvent, (**d**) commercial chitin, (**e**) chitosan BSFL extracted using SC-CO2 extraction, (**f**) commercial chitosan, (**g**) chitosan BSFL extracted using solvent extraction, and (**h**) chitosan BSFL without any lipid extraction. Chitin and chitosan showed two crystalline peaks approximately at 10° and 20°.

6.3. Summary

The chapter thoroughly analyses chitin and chitosan extracted from BSFL using various methods. The extraction techniques, including SC-CO2, solvent, and no-fat-extraction, resulted in varying percentages of chitin and chitosan. Losses during deproteinisation affected the yield, with the no-fat-extraction method showing lower percentages, potentially due to sample loss during processing. FTIR spectroscopy revealed that chitin from BSFL displayed α-chitin characteristics, with distinct absorbance bands indicating a well-defined molecular structure. Effective fat extraction methods were crucial for ensuring the purity of chitin and chitosan, as evidenced by the absence of specific absorption peaks related to fats in well-extracted samples. Elemental analysis indicated lower nitrogen content in chitin samples from well-extracted BSFL, suggesting effective removal of proteins and higher purity. The DA varied based on the fat extraction method, with SC-CO2 extraction providing a higher DA than solvent extraction and no-fat-extraction methods. This chapter also emphasises the importance of fat extraction for achieving high-purity chitin and chitosan. TGA revealed differences in thermal stability among chitin samples obtained through different extraction methods. Effective fat extraction improved the thermal stability of chitin, with variations observed between SC-CO2 and solvent extraction methods. Surface morphology analysis through SEM indicated a honeycomb-like structure in well-extracted chitin, with differences observed based on fat extraction methods. Effective fat extraction resulted in a more complex and well-defined structure, essential for applications such as metal ion absorption and tissue engineering. XRD analysis highlighted differences in crystallinity structure among chitin and chitosan samples. Well-extracted samples exhibited higher crystallinity indices, emphasising the importance of fat extraction for obtaining stronger and more crystalline chitin and chitosan.

CHAPTER 7: NOVEL CHITOSAN-BASED HYDROGEL FOR BIOMEDICAL APPLICATIONS

Chitosan is a naturally occurring derivative polymer with a linear cationic polysaccharide of D-glucosamine and is commonly used for biomedical applications [245]. Chitosan is formed via deacetylation of chitin, the primary component of crustacean and insect exoskeletons and the second most prevalent polysaccharide after cellulose. Chitosan is a nontoxic, biodegradable, biocompatible, antimicrobial agent with a hydrophilic surface that stimulates cell adhesion and proliferation, making it an ideal candidate for usage as a biomaterial [246], specifically in wound dressing and bone tissue engineering. Thus, chitosan is one of the favoured candidates for hydrogel-based type material for biomedical applications. However, chitosan alone possesses poor structures, and in addition, swelling mechanisms in the aqueous environment can greatly reduce the stability of the resultant structures [247]. As a result, crosslinking chitosan and/or combining it with other polymers can significantly improve its water behaviour and physical chemistry properties.

Hydrogels are three-dimensional, cross-linked network structures that absorb significant water and form soft elastic materials without dissolving [248, 249]. Hydrogels possess desirable physiochemical properties that make them appropriate for a variety of biomedical treatments, including drug delivery, tissue regeneration, and wound healing. [250]. Understandably, Hydrogels are proven to be particularly useful as scaffolds in tissue engineering because they can replicate the three-dimensional environment of cells in soft tissues. Furthermore, hydrogels' adjustable properties make them adaptable and ideal for certain applications.

Thus, hydrogels produced from gelatine and chitosan blends have better mechanical and physiochemical qualities than those made from a single component. [251]. In addition, hydrogels can be crosslinked with glutaraldehyde, genipin, citric acid, and glycerol to enhance their properties further [252]. Glutaraldehyde (GA) is often used as a crosslinker for chitosan and gelatine because of its ability to bond to their amine groups, enhance their mechanical strength [239], and form a three-dimensional scaffold.

This chapter aims to fabricate a hydrogel using chitosan extracted from BSFL, combined with commercial gelatine, and both incorporated with GA to improve the physiochemical properties of the formed hydrogel suitable for biomedical applications. The chitosan is extracted from BSFL to mimic commercial chitosan (Prawn). These hydrogels' physicochemical structure, characteristics, and behaviour are subsequently investigated. Similar isolation for the chitosan has been discussed in Chapter 6.

7.1 Material and Methods

A detailed description of the materials and methods used to synthesise chitosan-based hydrogel can be found in Chapter 3, specifically in Sections 3.14 and 3.2.4. These sections provide an in-depth overview of the process, including comprehensive discussions of the materials and techniques utilised in the hydrogel synthesis for the following section.

7.2 Result and Discussion

This section discusses a comprehensive evaluation of chitosan-based hydrogel is presented. It begins with characterising the hydrogel's physical and chemical properties, followed by an FTIR analysis to determine its molecular structure. The study then assesses the hydrogel's thermal properties and its water absorption capacity through a swelling test. Finally, a biodegradation test evaluates the hydrogel's rate of degradation and compatibility with

biological systems. This analysis highlights the hydrogel's potential for applications in areas like drug delivery and wound care.

7.2.1 Characterisation of chitosan-based hydrogel

A series of chitosan-based hydrogel from chitosan-gelatine-GA (CH-G-GA) were synthesised by four various concentrations of chitosan and gelatine but with a constant concentration of 1% of GA, as per **Table 7.1**. Gelation did not occur when no gelatine was added to sample E. The synthesis was photographed and revealed that all were transparent yellow, similar to a study conducted by a researcher using commercial chitosan [253]. **Fig. 7.1** shows the photographed chitosan-based hydrogel of the mixture CH-G-GA.

Table 7.1: Design of experiment of chitosan-based hydrogel from BSFL - Gelatine – GA (CHGA) in 10 mL.

Sample	Chitosan (CH) 2% (mL)	Gelatine (G) 10% (mL)	Glutaraldehyde (GA) 25%	Result
A	2	8	1%	Gelation occurred
B	4	6	1%	Gelation occurred
C	6	4	1%	Gelation occurred
D	8	2	1%	Gelation occurred
E	10	-	1%	Gelation did not occur.

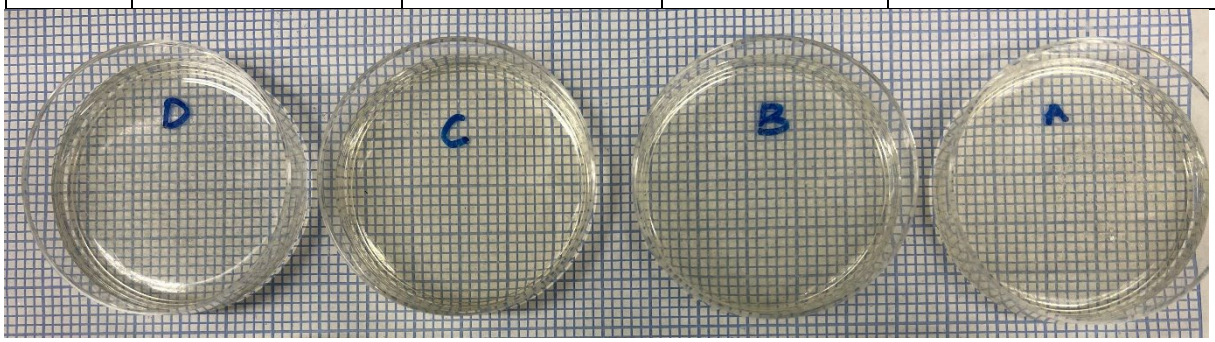

Fig. 7.1: Chitosan-based hydrogel extracted from BSFL with different concentrations of CH-G-GA: (**A**) 2/8/1%, (**B**) 4/6/1%, (**C**) 6/4/1% and (**D**) 2/8/0.5.

7.2.2 FTIR Analysis of the formed hydrogel

FTIR spectrum for chitosan obtained from BSFL is shown in **Fig. 7.2.** The vibration band at 3,264 cm^{-1} corresponds to the O-H and N-H stretching vibrations. These are the functional groups that are included in the intermolecular bonding of hydrogen and chitosan molecules [254]. Absorption peaks around 2,918 and 2,850 cm^{-1} are due to the C-H stretch. Moreover, the bands at 1,641 and 1,580 cm^{-1} correspond to C=O stretch and N-H bending vibration, respectively [246]. **Fig 7.2** also illustrates the FTIR spectrum for gelatine used in the study. The absorption peak at 3,273 cm^{-1} is because of the O-H stretching vibrations, while the absorption peak shows the stretching vibration of amide at 3,067 cm^{-1}. Concurrently, the absorbance at 2,969 cm^{-1} and 1161 cm^{-1} are due to the C-H stretching vibrations and C-O stretching of carboxylic acid, respectively. Furthermore, the absorption band at 1,525 cm^{-1} is attributed to N-H bending vibration and C-N stretching vibration.

ATR-FTIR spectroscopy also characterised the hydrogels; the spectra are presented in **Fig. 7.2** (**A**, **B**, **C**, **D**). Absorption bands in range between 1,000-1,100 cm^{-1} correspond to the C-O vibration of both GA and carbohydrates. The crosslinked reaction between chitosan and GA is shown by the absorption band 1,538 – 1,549 cm^{-1}. Furthermore, the absorption band in this region is caused by both the N-H bending and the C-N stretching vibration. The shift of this absorption band compared to pure gelatine (1,525 cm^{-1}) also indicates that the amide II gelatine band may be involved in the crosslinked reaction [255]. The absence of a band at 1,700 cm-1 indicates the complete reaction between chitosan and GA, indicating that no free aldehyde group remained in the hydrogel. With intramolecular hydrogen bonds, stretching vibrations of O-H and N-H are observable in the region around 3,276 and 3,281 cm^{-1} of the FTIR spectra [256]. The absorption band at 2,931 and 3,079 cm^{-1} is due to C-H alkyl and C-H alkenyl stretching, respectively. In addition, absorption bands around 1,627-1,633 cm^{-1}

correspond to the stretching of the C=C bond. Furthermore, band intensities shown in the FTIR spectra depend on gelatine and chitosan weight ratios in the prepared hydrogels. With increasing chitosan concentration, the vibration band 3,067 cm^{-1} that corresponds to gelatine becomes less visible. The intensity of 1,030-1,070 cm^{-1} is also seen to increase with higher CH concentration.

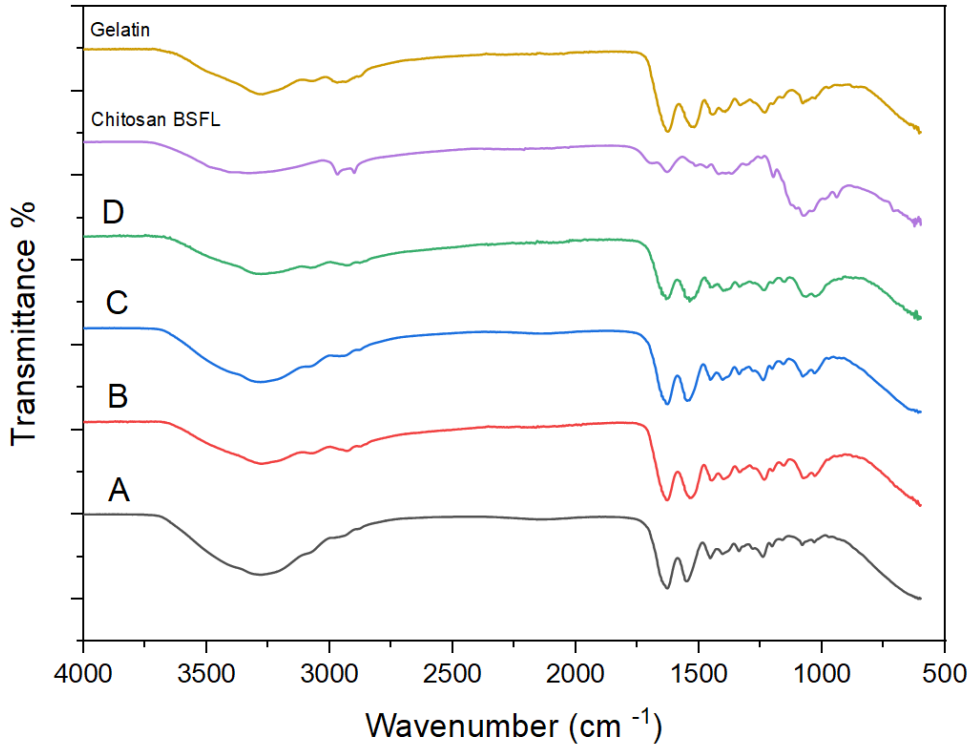

Fig. 7.2: Comparison of FTIR spectra of pure gelatine, chitosan extracted from BSFL, chitosan-based hydrogel extracted from the BSFL containing different concentrations of CH-gelatine together with 1 % of GA, (**A**) CH-2 mL, G-8 mL and 1% GA, (**B**) CH-4 mL, G-6 mL and 1% GA, (**C**) CH-6 mL, G-4 mL and 1% GA and (**D**) CH-8 mL, G-2 mL and 1% GA.

7.2.3 Thermal properties

The TGA/DTG curves for pure gelatine and chitosan obtained from BSFL are shown in **Fig. 7.3.** Gelatine degradation starts at around 300 °C and reaches the maximum at 364 °C, where about 64.81% of the mass has been degraded. For the case of chitosan, the degradation starts at about 200 °C, while rising to the maximum temperature of 360 °C. Within the temperature

range, as much as 68.66% of the initial mass has been degraded. These findings are significant for biomedical applications, where chitosan's thermal stability makes it an excellent choice for drug delivery systems, wound dressings, and tissue engineering. Furthermore, chitosan's biodegradability makes it a suitable option for agricultural and environmental applications, such as biodegradable mulch films and soil amendments for controlled nutrient release. **Figs. 7.4** and **7.5** illustrate the TGA/DTG analysis of chitosan-based hydrogel extracted from BSFL with various gelatine and chitosan concentrations with constant GA. Two significant steps indicate the weight loss process for the chitosan-based hydrogel extracted from the BSFL.

The first step is in the temperature between 40 – 180 °C with a 14 – 49% weight reduction, representing the water loss in the samples. Water loss within the sample can be further broken down into three stages. The first stage of water loss occurs in the temperature range between 40-60 °C, which is due to free water. Water loss in the 80-120 °C range refers to the water linked through hydrogen bonds, while at a higher temperature, water loss is associated with polar interactions with the carboxylate group [257].

The second step is in a temperature between 200 to 500 °C with 36 – 58% weight loss, depending on the thermal and oxidative decomposition of chitosan-gelatine mixtures with the existence of crosslinkers. The most weight loss within this temperature range is sample D (57%), followed by C (50%), B (43%), and A (36%). Hence, it is observed that more weight loss is obtained with higher chitosan concentration in crosslinked hydrogels. In other words, the samples are more thermally stable with the increase in gelatine concentration. Other researchers have reported similar trends, indicating better thermal stability in crosslinked hydrogels is achieved with higher gelatine concentrations [258]. With further temperature increase from 500-800 °C, additional weight loss occurs in the 2 – 6% range.

Decomposition within this temperature range is considered small compared to the earlier temperature ranges.

Another crucial observation from the study is that weight loss occurs during the process as water is removed. This is related to the removal of free water, which is associated with hydrogen bonding. The initial phase, ranging from 40 to 180°C, results in a weight loss of 14% to 49%. This is attributed to the removal of free water, water associated with hydrogen bonds, and water linked with polar interactions with the carboxylate group. This information is vital for wound healing and drug delivery systems, where water content plays a critical role.

The increase in thermal stability with higher hydrogel chitosan concentrations observed in thermal analysis (TGA/DTG) is due to several interrelated factors. Higher concentrations of chitosan lead to a denser polymer network, which requires more energy to break down, enhancing thermal stability. Additionally, more chitosan results in increased crosslinking points within the hydrogel, strengthening the overall structure. Chitosan's ability to form extensive hydrogen bonds due to its amino and hydroxyl groups further stabilises the hydrogel at elevated temperatures. Higher chitosan concentrations also promote increased crystallinity, as more polymer chains align and pack closely together, with crystalline regions being more thermally stable than amorphous ones. Finally, higher chitosan content reduces the overall water content in the hydrogel, as water acts as a plasticiser and lowers thermal stability. Collectively, these factors contribute to the enhanced thermal stability of hydrogels with higher chitosan concentrations.

The TGA data indicates that the hydrogels could be utilised in areas where controlled water release, thermal stability, and tunable degradation characteristics are essential. Depending

on the specific needs of each application, the hydrogels could be employed in drug delivery systems, wound healing, or tissue engineering. In conclusion, the TGA data provides valuable insights into the thermal properties of the BSFL-chitosan based hydrogels, enabling customisation of these hydrogels for specific applications based on their thermal stability, water content, and degradation characteristics.

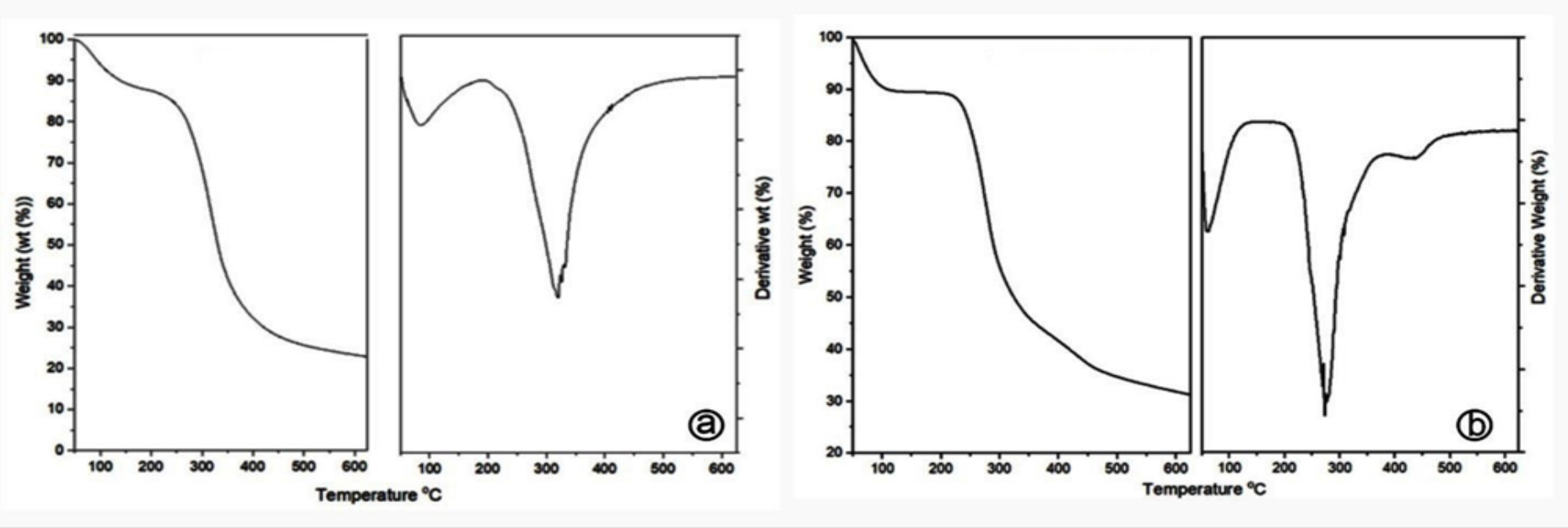

Fig. 7.3: Comparison of the TGA/DTG curves for different samples; (**a**) commercial gelatine (**b**) chitosan extracted from BSFL.

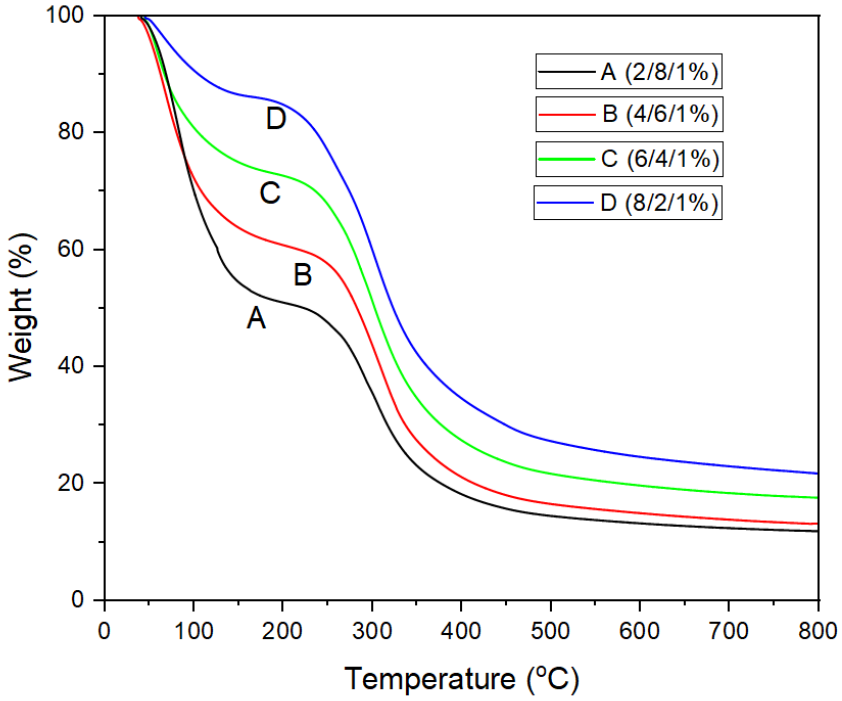

Fig. 7.4: Comparison of TGA analysis of chitosan-based hydrogel extracted from BSFL with different concentrations of the chitosan and gelatine with constant GA.

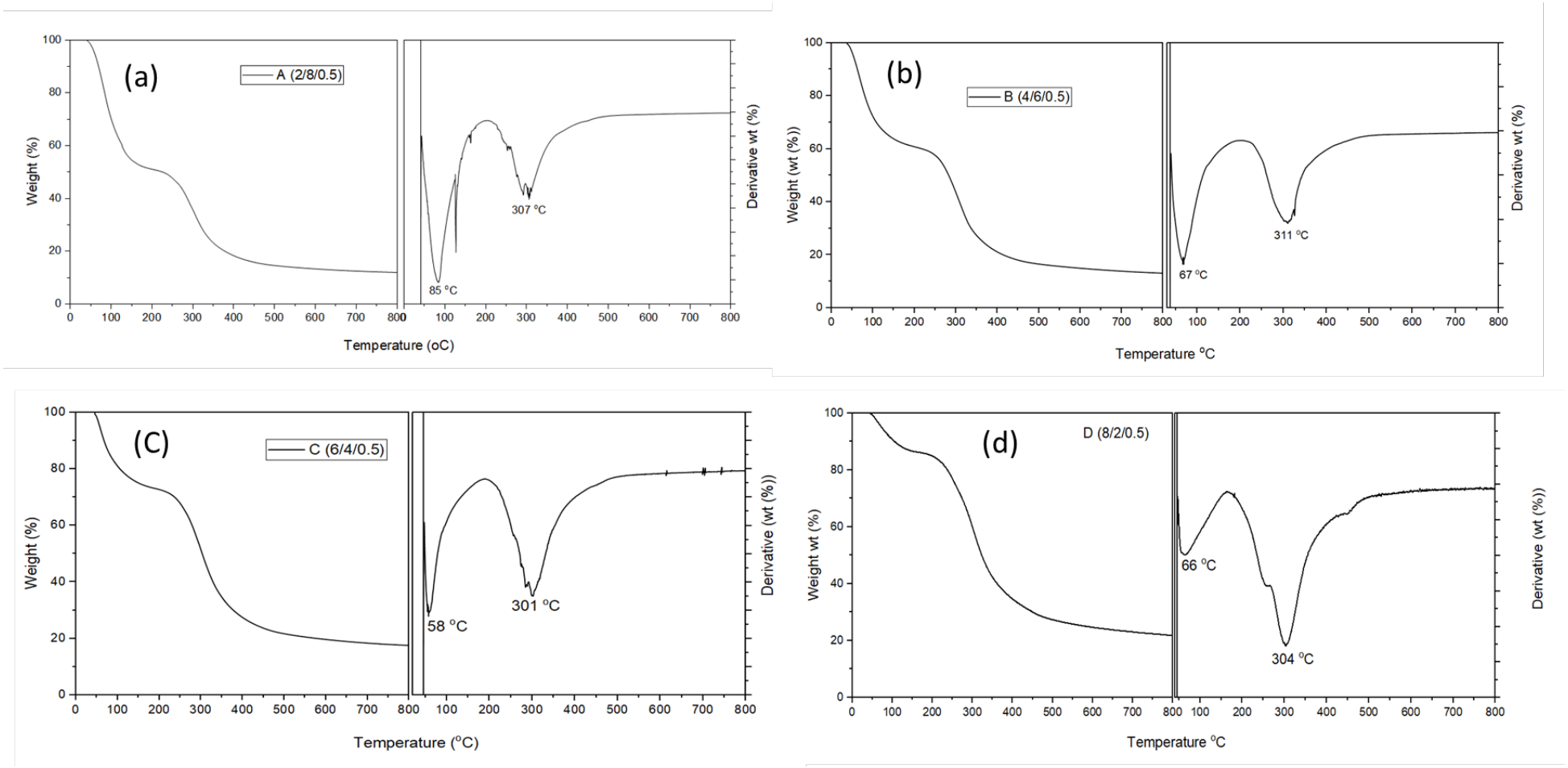

Fig. 7.5: Plot of the TGA and derivative analyses of the hydrogels with different concentrations of CH-G-A. (**a**) CH-2 mL, G-8 mL and 1% GA, (**b**) CH-4 mL, G-6 mL and 1% GA, (**c**) CH-6 mL, G-4 mL and 1% GA and (**d**) CH-8 mL, G-2 mL and 1% GA.

7.2.4 Swelling Test

In this investigation, samples were immersed in PBS and swelling tests were performed to determine the swelling rate. The amount of water that the hydrogel absorbed determined the degree of swelling. The results of the swelling experiments of the chitosan-based hydrogel (CH-G-GA) are shown in **Fig. 7.6.** The results of the swelling tests on the chitosan-based hydrogel (CH-G-GA) provide significant insights into its behaviour. Firstly, hydrogels with higher concentrations of gelatine and lower concentrations of chitosan exhibited the most pronounced swelling, indicating a clear correlation between hydrogel composition and swelling degree. Conversely, hydrogels with lower concentrations of chitosan demonstrated superior swelling capacities compared to those with higher concentrations of this component.

Secondly, the study confirms that crosslinking in hydrogels reduces hydrophilicity, as hydrophilic groups such as OH, NH2, and COOH are consumed during the crosslinking process. Thirdly, the kinetics of swelling reveal a rapid initial water absorption phase in the first 5 to 10 minutes, which is shown for samples C and D, followed by a slower increase until equilibrium is reached around 2 to 2.5 hours. Variations in swelling after 10 minutes suggest potential issues such as insufficient drying of samples or the presence of excess water. Lastly, the maximum swelling ratios, ranging from 136.78% to 287.90%, highlight the diverse swelling capacities of different samples. The data indicates a plateau in swelling after 2 hours, signifying the saturation point where the hydrogel can no longer absorb additional water, as shown in **Fig. 7.7**. The maximum swelling ratio is 287.90 % for sample **A**, and the lowest is 136.78% for sample **D**. Sample D's inconsistent swelling behaviour, marked by fluctuations over time, could be due to several factors. These include variability in composition, uneven diffusion rates, material heterogeneity, and sensitivity to

environmental conditions like temperature and pH. Mechanical stress during swelling and potential phase transitions might also contribute to the observed inconsistency.

These findings comprehensively understand the hydrogel's swelling behaviour and offer valuable insights for various applications. The correlation between hydrogel composition and swelling degree indicates possible biomedical uses, such as in dressings for wounds or drug delivery systems, where controlled swelling is crucial. The reduced hydrophilicity due to crosslinking makes it suitable for hydrophilic coatings in medical devices or implants, where enhanced biocompatibility is essential. Furthermore, the hydrogel's controlled swelling properties could address challenges in agriculture by improving water retention in soil, particularly in arid or drought-prone regions. It could also be useful in environmental remediation projects, where controlled release of water or nutrients is necessary. The hydrogel's behaviour could be harnessed for the development of devices that detect changes in moisture levels, making it valuable in environmental monitoring or industrial settings. Lastly, the hydrogel's characteristics may be advantageous in the design of contact lenses, contributing to enhanced comfort and extended wear time for contact lens users. These diverse applications highlight the potential of chitosan-based hydrogel to address multifaceted challenges across different industries, with opportunities for further research and development to tailor its properties for specific needs.

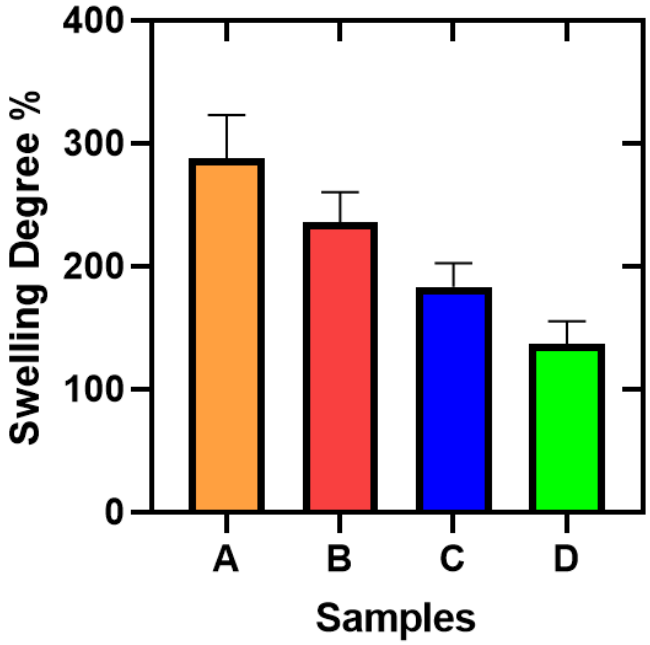

Fig. 7.6: Swelling behaviour of the chitosan-based hydrogel extracted from BSFL (CH-G-GA), which is (**A**) CH-2 mL, G-8 mL and 1% GA, (**B**) CH-4 mL, G-6 mL and 1% GA, (**C**) CH-6 mL, G-4 mL and 1% GA and (**D**) CH-8 mL, G-2 mL and 1% GA. CH-G-GA is a combination of Chitosan (CH), gelatin (G) and glutaraldehyde (GA).

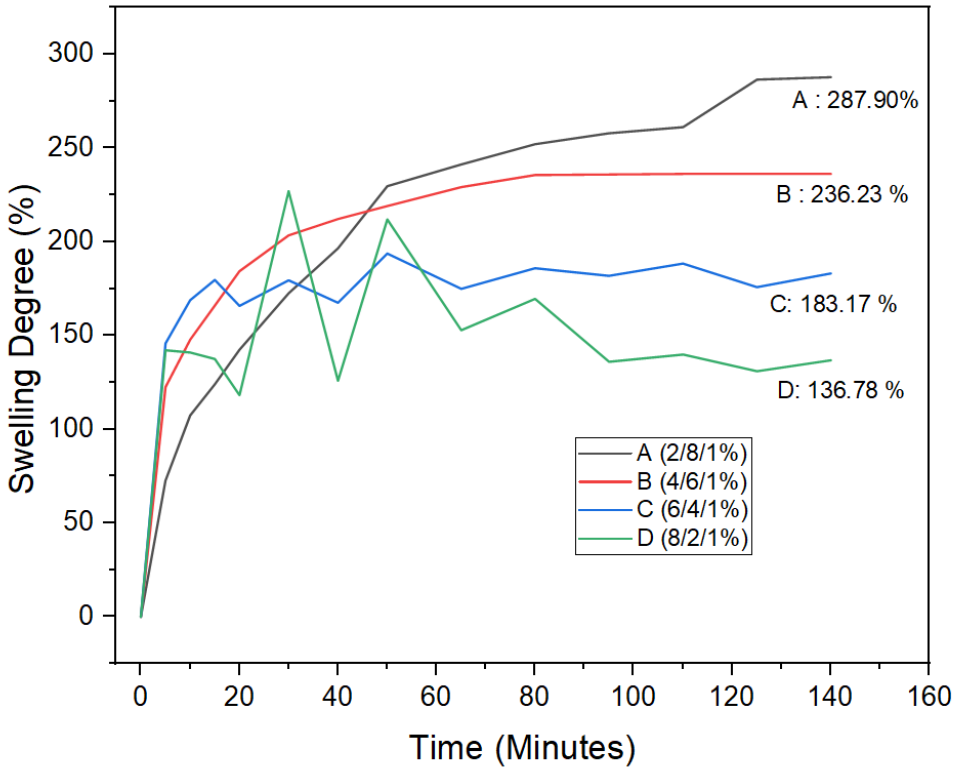

Fig. 7.7: Swelling degree of the samples with times.

7.2.5 Biodegradation Test

The enzyme biodegradability test was conducted for 21 days, for which the samples were weighed every 7 days. Lysozyme enzyme, an enzyme similar to those found in body fluids, has been used from previous study to degrade the chitosan-based hydrogel, degrading the β-(1-4)-glycosidic bonds [246]. Lysozyme finds extensive use in influencing the material properties of chitosan scaffolds or films. This is because, in vivo, lysozyme primarily degrades chitosan by targeting its acetylated part, leading to the non-toxic glucosamine as the final degradation product [259].

Samples with higher gelatine ingredients were the first to be degraded after 7 days, with almost 60% degradation for sample A. As a result, the weight loss also increases tremendously for each sample when the gelatine increases. However, the degradation rate is

slower when the chitosan concentration increases. This behaviour is likewise similar to the swelling rate, with rapid degradation detected in all samples from 0 to 7 days and slowed after approaching equilibrium, except for the sample with higher chitosan content.

Hydrogels that contain more gelatine tend to break down quickly because of their hydrophilic nature, which allows them to be hydrolysed more easily than chitosan. This is because chitosan and gelatine develop stronger covalent bonds in the presence of a crosslinker, making it more difficult to break them apart when compared to hydrogels without glutaraldehyde. Thus, adding chitosan to the mixture can increase crosslinking efficiency and reduce degradability. This increased crosslinking efficiency leads to the formation of a more stable and robust network structure, which reinforces the connections between the individual chains and makes the overall structure stronger and more resistant to degradation. As a result, the degradation of the material can be slowed down, making it desirable for various applications, such as medical implants or durable coatings.

Moreover, chitosan also improves the stability of the network, and the degradation can be managed by adjusting the ratio of the mixture (CH-G-GA) or the proportions of chitosan, gelatine, and glutaraldehyde. In summary, these findings highlight the positive impact of chitosan in the mixture by influencing crosslinking efficiency, reducing degradability, improving network stability, and providing a means for controlled degradation through careful adjustment of component ratios. These implications can be far-reaching, including in fields such as biomedicine, materials science, and environmental applications. **Fig. 7.8** presents the rate of biodegradation of the chitosan-based hydrogel extracted from the BSFL.

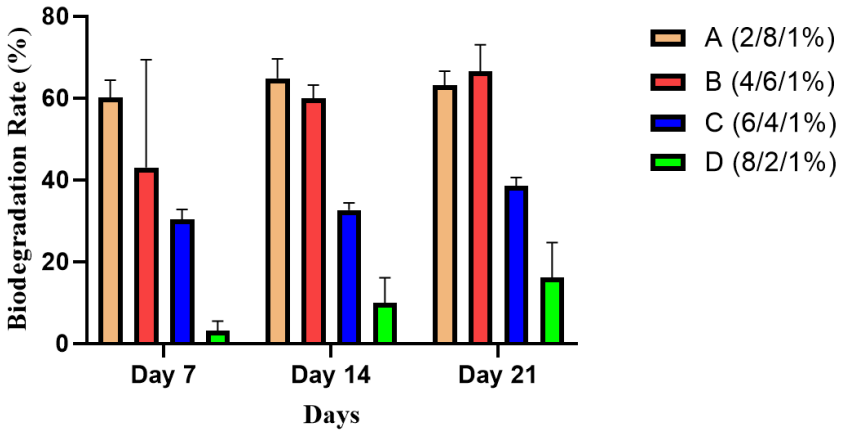

Fig. 7.8: Biodegradation behavior of the CH-G-A hydrogel incubated with lysozyme.

7.3 Summary

The insect BSF and its larvae contribute significantly to the circular economy by converting organic waste into valuable substances such as chitin and chitosan. The extraction of chitin and chitosan from BSFL with supercritical CO2 (SC-CO2) extraction offers a 'green' organic waste treatment method. Chitin and chitosan derived from BSFL have physicochemical properties as good as the commercial chitin produced from prawns, with α-chitin and a high crystal index. Therefore, chitosan extracted from the BSFL is suitable for hydrogel preparation and, combined with gelatine, is biodegradable and may be used for biomedical applications. This chapter discusses the preparation of chitosan and gelatine three-dimensional scaffolds crosslinked with glutaraldehyde (GA). The prepared scaffolds were characterised by the attenuated total reflectance Fourier transform infrared (ATR-FTIR) spectroscopy and thermal gravimetric analysis (TGA). Furthermore, their steadiness and stability were investigated by swelling rate and bio-degradation tests. As a result, the scaffolds present properties of high degree swelling and biodegradability, making the scaffolds suitable for biomedical applications, and connecting the circular economy paradigm directly to human health solutions.

CHAPTER 8: CONCLUSIONS AND RECOMMENDATIONS

Food and organic waste continues to be a major waste challenge for societies around the world, and its association with methane emissions when it comes to the climate change issue. The use of BSFL has, in recent years, attracted attention as a method for dealing with food waste. This study examined the potential of BSFL bioconversion as a circular economy pathway for organic resources. In this thesis, BSFL was analysed with respect to minimising negative environmental effects, particularly from food waste. Its competitive environmental standpoint incorporates many advantages, including the production of valuable by-products (lipids, protein, chitin, and minerals). These products had diverse applications such as food, pharmaceuticals, and in the creation of other valuable by-products, consequently contributing to the circular economy. Additionally, utilising BSFL as a tool for food waste management in the circular economy is highly beneficial for both society and the environment, promoting a closed-loop biological cycle within the circular organic economy. Thus, the circular economy hypothesis can be realised. The research in this thesis indicated that chemical extraction is more cost-effective and yields better results compared to enzymatic extraction, although the BSFL is more environmentally friendly. However, further extensive research is needed to improve the market value of this type of approach. Integrating socio-economic strategies will be crucial in developing this sustainable solution using the biological circular economy of organic waste.

There were only 350 patents available related to "Black Soldier Fly" or "*Hermertia illucens*"; however, only 302 can be considered for this study. The analysis shown that the leading country for patent documents on BSFL is China, followed by South Korea, the United States and Russia. Most patents focused on animal feed or protein, followed by lipids and chitin or

chitosan. Although the technology was promising to solve the circular economy for the biological cycle, the number of patent publications had declined over the last few years since 2018. Based on this analysis, it can be concluded that China will lead the way on patent publication related to the utilisation of BSFL, which was applicable as a biological circular economy for food and agricultural waste. The conclusions for the thesis are as follows:

8.1 Optimising sustainable oil extraction from BSFL using SC-CO2 that was high in Lauric Acid.

BSFL was one of the robust insects that may be utilised in emerging technology to support a circular organics economy due to their efficient waste bioconversion and excellent nutritional supplies. In this work, SC-CO2 extraction was shown to be a successful method for extracting oil from BSFL without using organic solvents. Proteins, chitin, and its derivative chitosan may be extracted from the defatted solid residue sample to increase its value. With the optimum conditions found to be 366 bar, 43 °C and 2.2 hours extraction time of SC-CO2 extraction, the oil recovery was 35.58%, 5.58% higher than solvent extraction. Besides that, with SC-CO2 extraction, the concentration of fatty acid composition, mainly the lauric acid and the SFA ratio, was regulated by adjusting the parameter of the SC-CO2. An optimisation of the maximum oil recovery, maximum lauric acid content and minimum concentration of SFA ratio was formulated, and the optima were found to be 30.1 %, 52.0 g/100 g and 5.0, respectively, with corresponding SC-CO2 optimal conditions of 400 bar, 46.8 º C and 1.4 hours of extraction time. Therefore, based on this study, the ‘green’ process of SC-CO2 extraction along with RSM provides a systematic approach to valorising the BSF, which paves the way for process scale-up for the industry. This offers a proof-of-concept aligned with the circular economy principles and to create new circular organics businesses that may offer marketable products and by-products of BSFL.

8.2 The oil derived from BSFL, rich in Lauric Acid, demonstrates biocompatibility and exhibits non-cytotoxicity towards 3T3 cells.

The selection of BSFLO obtained through SC-CO2 extraction for the in-vitro study was based on its practicality, environmentally friendly nature, and reduced contamination with other chemicals. The SC-CO2 method yielded a higher ratio of saturated fatty acids (SFA) to unsaturated fatty acids (USFA) than solvent extraction. Significantly, BSFLO contained a substantial concentration of lauric acid (54.97%), which is known to stimulate the proliferation of 3T3 cells. The results of this study indicated that BSFLO did not exhibit cytotoxic effects on 3T3 cells. However, at a higher concentration of 7.5 µl/mL and when administered daily, it was found to be toxic, hindering the cells' effective growth. This suggests that the increased concentration of BSFLO oil placed undue stress on the cells, impairing their growth capabilities. Then, the microscopic observations provided evidence of cell spreading from Day 1 to Day 3, confirming the capacity of BSFLO to promote cell proliferation. The wound healing assay demonstrated that BSFLO performed competitively compared to the control group, suggesting its potential application in wound healing. Future research efforts could investigate the effects of varying concentrations of lauric acid and other fatty acids on cell proliferation and differentiation and explore their potential applications in regenerative medicine.

8.3 Chitin and Chitosan extracted from BSFL show more purity compared to prawns.

Chitin and chitosan extracted from BSFL using different types to remove the fat were purified and characterised by their physicochemical. Based on the FTIR analysis, the chitin extracted was α-chitin, which is almost like the commercial chitin extracted from prawns. The spectra' similarity from the FTIR suggests the same chitin quality for both fat extraction

samples except for a sample that did not undergo any fat removal. Nitrogen content shows that both defatting methods are almost similar with 6.19% and 6.60% from solvent extraction and SC-CO2 extraction but had a significantly lower value of nitrogen content with 2.12% for the non-defatted extraction samples. Then, DA values of 123%, 83% and 1169 % for chitin that underwent SC-CO2 extraction, solvent extraction, and no fat extraction, respectively. The DA value of the chitin sample defatted by SC-CO2 is a bit higher than the theoretical value of 100% due to possible water or mineral residues in the extracted chitin. However, the chitin sample that was not treated with any fat extraction procedure had a higher DA value, which was over 1000%; the lipid hindered the deproteinisation process where the lipid holds the protein bond in the sample. Then, chitin and chitosan that underwent fat extraction, SC-CO2 and solvent are thermally stable and more degradable than no fat extraction process. However, the thermal stability of chitin and chitosan obtained from BSFL is slightly lower than that of prawn. A similar result was obtained when the crystalline index (CrI) was analysed among the chitin and chitosan samples, which are more crystalline, stronger, and harder when the samples underwent the fat extraction process and gave almost similar behaviour to the commercial (prawn) chitin and chitosan. Finally, the surface morphology, which is the honeycomb structure, was clearly observed when fat extraction occurred.

Hence, the comprehensive analysis conducted on chitin and chitosan extracted from BSFL underscores the significance of fat removal processes in enhancing purity, thereby rendering them promising for a myriad of applications. The FTIR analysis confirmed the similarity between BSFL and prawn-derived chitin, while nitrogen content and deacetylation (DA) values highlighted the effectiveness of fat extraction in reducing impurities. Furthermore, the thermal stability and crystalline behaviour observed in fat-extracted samples, though

slightly lower than prawn-derived counterparts, position BSFL-extracted chitin and chitosan as thermally stable and degradable materials. These findings not only establish the purity of BSFL-extracted chitin and chitosan in comparison to prawn-derived counterparts but also open avenues for diverse applications. The observed honeycomb structure in samples subjected to fat extraction enhances their appeal for applications ranging from pharmaceuticals to biomedical uses. The consistent quality and purity achieved through fat removal processes suggest that BSFL-derived chitin and chitosan could serve as valuable alternatives in industries where high purity is paramount. The potential applications are indeed myriad, spanning areas such as wound healing, drug delivery, and various other biomedical and industrial uses, making these findings significant in the broader context of material science and technology.

8.4 Chitosan-based hydrogel exhibits promise and suitability for biomedical applications.

In this study, chitosan was successfully extracted from Black Soldier Fly (BSF) larvae, though the yield was slightly lower than a reference study, possibly due to losses during the deproteinisation process. The extensive processing steps, including filtration and washing, likely contributed to a 3% loss of the original sample. Characterisation of the extracted chitosan revealed a lower crystallinity index (CrI) compared to commercial prawn chitosan, indicating potential differences in structural properties. The synthesised chitosan-based hydrogels (CH-G-GA), composed of chitosan, gelatine, and glutaraldehyde as a crosslinker, demonstrated promising properties. Transparent yellow hydrogels were obtained, and gelation occurred at different concentrations of chitosan and gelatine. Fourier Transform Infrared (FTIR) analysis confirmed the presence of essential functional groups involved in

intermolecular bonding within the hydrogels. Thermal analysis (TGA/DTG) demonstrated that higher chitosan concentrations in hydrogels resulted in increased thermal stability.

Swelling tests revealed that hydrogels with higher gelatine concentrations and lower chitosan concentrations exhibited the highest swelling degrees, reaching equilibrium after approximately 2 to 2.5 hours. Additionally, the hydrogels showed controlled biodegradability when exposed to lysozyme enzyme, with faster degradation observed in samples with higher gelatine content. This behavior suggested that the presence of chitosan enhanced crosslinking efficiency and reduced degradability, contributing to improved network stability. Overall, the study provides valuable insights into the extraction and characterisation of chitosan from BSFL and the potential applications of chitosan-based hydrogels in biomedical fields, particularly in areas such as tissue engineering and wound healing. The sustainable sourcing of chitosan from BSFL underscores its potential as a bioresource for diverse biomedical applications, marking a significant contribution to the field of biomaterials research.

8.5 Recommendations for future work.

This thesis has demonstrated that BSFL are crucial in producing various valuable products. Several recommendations have been proposed to further improve the research in this field and harness the full potential of BSFL in the organic circular economy. These recommendations encompass safety, market analysis, product diversification, scaling up, environmental impact assessment, regulatory compliance, waste management integration, and adopting a multi-disciplinary approach. By implementing these suggestions, researchers can unlock the true potential of BSFL and contribute to waste reduction, environmental protection, and the development of valuable by-products for various industries.

1. Microbiological Testing of BSFL Oil and BSFL chitin and chitosan: To ensure the safety and suitability of BSFL oil and chitosan for different applications, rigorous microbiological testing is recommended. This testing should assess the presence of harmful microorganisms, including bacterial and fungal contaminants and potential pathogens. Such testing will establish the quality and safety of BSFL oil and chitosan, particularly in the food and pharmaceutical sectors.
2. Market and Economic Analysis: Conduct a comprehensive market analysis to understand the demand, potential applications, and economic feasibility of products derived from BSFL. Identify potential industries and sectors that can benefit from these products and assess the market competitiveness and potential barriers to adoption.
3. Product Diversification: Explore the development of new and innovative products from BSFL beyond animal feed, protein, lipids, and chitin. Investigate the viability of establishing new applications in industries such as cosmetics, pharmaceuticals, biofuels, and other high-value commodities that can help the circular economy.
4. Scale-up and Commercialisation: Focus on scaling up the SC-CO2 extraction process and other methodologies to industrial levels. This includes improving extraction efficiency, lowering production costs, and maintaining reliable product quality. Collaboration with industry partners may be essential for successful commercialisation.
5. Environmental Impact Assessment: Conduct a comprehensive life cycle assessment (LCA) to determine the environmental impact of adopting BSFL as an organic circular economy tool. Compare its environmental footprint with conventional waste

management methods and other alternative solutions to demonstrate its environmental superiority adequately.

6. Waste Management Integration: Collaborate with local municipalities and waste management authorities to integrate BSFL-based systems into existing waste management infrastructures. Demonstrate the practicality and efficiency of this approach to encourage its adoption on a broader scale.
7. Multi-disciplinary Approach: Encourage interdisciplinary research and collaboration between scientists, engineers, economists, and social scientists. This will help address the complex challenges of integrating BSFL-based technologies into the circular economy and ensure a holistic approach to sustainability.

By implementing these recommendations, researchers can continue to enhance the potential and application of BSFL as a powerful tool in the organic circular economy, contributing to waste reduction, environmental protection, and developing valuable by-products for various industries.

References

1. Ritchie, H. and M. Roser. *Environmental impacts of food production. Published online at OurWorldInData.org.* 2020; Available from: https://ourworldindata.org/environmental-impacts-of-food.
2. Poore, J. and T. Nemecek, *Reducing food's environmental impacts through producers and consumers.* Science, 2018. **360**(6392): p. 987-992.
3. Ahmed, S.F., et al., *Recent developments in physical, biological, chemical, and hybrid treatment techniques for removing emerging contaminants from wastewater.* Journal of Hazardous Materials, 2021. **416**.
4. Bajželj, B., et al., *Importance of food-demand management for climate mitigation.* Nature Climate Change, 2014. **4**(10): p. 924-929.
5. Čičková, H., et al., *The use of fly larvae for organic waste treatment.* Waste Management, 2015. **35**: p. 68-80.
6. Caligiani, A., et al., *Composition of black soldier fly prepupae and systematic approaches for extraction and fractionation of proteins, lipids and chitin.* Food Research International, 2018. **105**: p. 812-820.
7. Gladun, V.V., *The first record of hermetia illucens (Diptera, stratiomyidae) from russia.* Nature Conservation Research, 2019. **4**(4): p. 111-113.
8. Ravi, H.K., et al., *Alternative solvents for lipid extraction and their effect on protein quality in black soldier fly (Hermetia illucens) larvae.* Journal of Cleaner Production, 2019. **238**.
9. Cammack, J.A. and J.K. Tomberlin, *The Impact of Diet Protein and Carbohydrate on Select Life-History Traits of The Black Soldier Fly Hermetia illucens (L.) (Diptera: Stratiomyidae).* Insects, 2017. **8**(2).
10. Europaea, F. *Hermetia illucens (Linnaeus, 1758)*. 2020 [cited 2020 03/09/2020]; Available from: https://fauna-eu.org/cdm_dataportal/taxon/d9ea2161-804d-4ea2-9927-6373081010f1.
11. Diclaro;, J.W. and P.E. Kaufman;. *Featured Creatures: black soldier fly*. 2009 [cited 2020 03/09/2020]; Available from: http://entnemdept.ufl.edu/creatures/livestock/black_soldier_fly.htm.
12. Pieterse, E., et al., *Black soldier fly (Hermetia illucens) pre-pupae meal as a dietary protein source for broiler production ensures a tasty chicken with standard meat quality for every pot.* Journal of the Science of Food and Agriculture, 2019. **99**(2): p. 893-903.
13. Purkayastha, D., et al., *Isolation and morphological study of ecologically-important insect "Hermetia illucens" collected from Roorkee compost plant.* Pollution, 2017. **3**(3): p. 453-459.
14. Ruhnke, I., et al., *Impact of on-range choice feeding with black soldier fly larvae (Hermetia illucens) on flock performance, egg quality, and range use of free-range laying hens.* Animal Nutrition, 2018. **4**(4): p. 452-460.
15. Bruno, D., et al., *The digestive system of the adult Hermetia illucens (Diptera: Stratiomyidae): morphological features and functional properties.* Cell and Tissue Research, 2019. **378**(2): p. 221-238.
16. Holmes, L.A., S.L. Vanlaerhoven, and J.K. Tomberlin, *Substrate effects on pupation and adult emergence of Hermetia illucens (Diptera: Stratiomyidae).* Environmental Entomology, 2013. **42**(2): p. 370-374.

17. Tomberlin, J.K. and D.C. Sheppard, *Factors influencing mating and oviposition of black soldier flies (Diptera: Stratiomyidae) in a colony.* Journal of Entomological Science, 2002. **37**(4): p. 345-352.
18. Nakamura, S., et al., *Small-scale rearing of the black soldier fly, Hermetia illucens (Diptera: Stratiomyidae), in the laboratory: low-cost and year-round rearing.* Applied Entomology and Zoology, 2016. **51**(1): p. 161-166.
19. Sheppard, D.C., et al., *Rearing methods for the black soldier fly (diptera: Stratiomyidae).* Journal of Medical Entomology, 2002. **39**(4): p. 695-698.
20. Wang, Y.-S. and M. Shelomi, *Review of black soldier fly (Hermetia illucens) as animal feed and human food.* Foods, 2017. **6**(10): p. 91.
21. Ravi, H.K., et al., *Larvae mediated valorization of industrial, agriculture and food wastes: Biorefinery concept through bioconversion, processes, procedures, and products.* Processes, 2020. **8**(7).
22. Magee, K., et al., *Valorisation of Organic Waste By-Products Using Black Soldier Fly (Hermetia illucens) as a Bio-Convertor.* Sustainability, 2021. **13**(15): p. 8345.
23. Ewald, N., et al., *Fatty acid composition of black soldier fly larvae (Hermetia illucens) – Possibilities and limitations for modification through diet.* Waste Management, 2020. **102**: p. 40-47.
24. Batish, I., et al., *Effects of Enzymatic Hydrolysis on the Functional Properties, Antioxidant Activity and Protein Structure of Black Soldier Fly (Hermetia illucens) Protein.* Insects, 2020. **11**(12).
25. Leni, G., et al., *Protein hydrolysates from alphitobius diaperinus and hermetia illucens larvae treated with commercial proteases.* Journal of Insects as Food and Feed, 2020. **6**(4): p. 393-404.
26. Giannetto, A., et al., *Waste valorization via hermetia illucens to produce protein-rich biomass for feed: Insight into the critical nutrient taurine.* Animals, 2020. **10**(9): p. 1-17.
27. Lim, J.-W., et al., *Palatability of black soldier fly larvae in valorizing mixed waste coconut endosperm and soybean curd residue into larval lipid and protein sources.* Journal of Environmental Management, 2019. **231**: p. 129-136.
28. Mohd-Noor, S.-N., et al., *Optimization of self-fermented period of waste coconut endosperm destined to feed black soldier fly larvae in enhancing the lipid and protein yields.* Renewable Energy, 2017. **111**: p. 646-654.
29. Somroo, A.A., et al., *Influence of Lactobacillus buchneri on soybean curd residue co-conversion by black soldier fly larvae (Hermetia illucens) for food and feedstock production.* Waste Management, 2019. **86**: p. 114-122.
30. Rosa, R., et al., *Life Cycle Assessment of Chemical vs Enzymatic-Assisted Extraction of Proteins from Black Soldier Fly Prepupae for the Preparation of Biomaterials for Potential Agricultural Use.* ACS Sustainable Chemistry & Engineering, 2020. **8**(39): p. 14752-14764.
31. Benner Jr, B.A., *Supercritical fluid extraction of organics in environmental analysis.* Encyclopedia of Analytical Chemistry: Applications, Theory and Instrumentation, 2006.
32. Park, H., et al., *Pharmaceutical Applications of Supercritical Fluid Extraction of Emulsions for Micro-/Nanoparticle Formation.* Pharmaceutics, 2021. **13**(11).
33. Hoornweg, D., P. Bhada-Tata, and C. Kennedy, *Waste production must peak this century.* Nature, 2013. **502**(7473): p. 615-617.

34. Delicato, C., et al., *Consumers' perception of bakery products with insect fat as partial butter replacement.* Food Quality and Preference, 2020. **79**: p. 103755.
35. Feng, W., et al., *Exploring the potential of lipids from black soldier fly: New paradigm for biodiesel production (II)—Extraction kinetics and thermodynamic.* Renewable Energy, 2018. **119**: p. 12-18.
36. Li, W., et al., *Potential biodiesel and biogas production from corncob by anaerobic fermentation and black soldier fly.* Bioresource Technology, 2015. **194**: p. 276-282.
37. Wang, C., et al., *Exploring the potential of lipids from black soldier fly: New paradigm for biodiesel production (I).* Renewable Energy, 2017. **111**: p. 749-756.
38. Muxika, A., et al., *Chitosan as a bioactive polymer: Processing, properties and applications.* International Journal of Biological Macromolecules, 2017. **105**: p. 1358-1368.
39. Durante, M., et al., *Application of response surface methodology (RSM) for the optimization of supercritical CO2 extraction of oil from patè olive cake: Yield, content of bioactive molecules and biological effects in vivo.* Food Chemistry, 2020. **332**: p. 127405.
40. Sarker, M.Z., et al., *Supercritical carbon dioxide (SC-CO2) extraction and fractionation of palm kernel oil from palm kernel as cocoa butter replacers blend.* Journal of Food Engineering, 2006. **73**: p. 210-216.
41. Friedrich, J.P. and E.H. Pryde, *Supercritical CO<inf>2</inf> extraction of lipid-bearing materials and characterization of the products.* Journal of the American Oil Chemists' Society, 1984. **61**(2): p. 223-228.
42. Wei, Z.-J., et al., *Optimization of supercritical carbon dioxide extraction of silkworm pupal oil applying the response surface methodology.* Bioresource Technology, 2009. **100**(18): p. 4214-4219.
43. Purschke, B., et al., *Pilot-scale supercritical CO2 extraction of edible insect oil from Tenebrio molitor L. larvae – Influence of extraction conditions on kinetics, defatting performance and compositional properties.* European Journal of Lipid Science and Technology, 2017. **119**(2): p. 1600134.
44. Kim, S.W., et al., *Removal of fat from crushed black soldier fly larvae by carbon dioxide supercritical extraction.* Journal of Animal and Feed Sciences, 2019. **28**(1): p. 83-88.
45. Pan, W.-J., et al., *Supercritical carbon dioxide extraction of the Oak Silkworm (Antheraea pernyi) Pupal Oil: process optimization and composition determination.* International journal of molecular sciences, 2012. **13**(2): p. 2354-2367.
46. Purschke, B., et al., *Pilot-scale supercritical CO2 extraction of edible insect oil from Tenebrio molitor L. larvae–Influence of extraction conditions on kinetics, defatting performance and compositional properties.* European Journal of Lipid Science and Technology, 2017. **119**(2): p. 1600134.
47. CHEN, X., Y. FENG, and Z. CHEN, *Common edible insects and their utilization in China.* Entomological Research, 2009. **39**(5): p. 299-303.
48. Rehman, K.U., et al., *Black soldier fly, Hermetia illucens as a potential innovative and environmentally friendly tool for organic waste management: A mini-review.* Waste Management and Research, 2023. **41**(1): p. 81-97.
49. Garcia, D.A., et al., *Climate change mitigation by means of sustainable development of energy, water and environment systems.* Energy Conversion and Management-X, 2023. **17**.

50. Bar-On, Y.M., R. Phillips, and R. Milo, *The biomass distribution on Earth.* Proceedings of the National Academy of Sciences of the United States of America, 2018. **115**(25): p. 6506-6511.
51. Roser, H.R.a.M., *Environmental Impacts of Food Production.* Our World in Data, 2022.
52. Gaugler, T., S. Stoeckl, and A.W. Rathgeber, *Global climate impacts of agriculture: A meta-regression analysis of food production.* Journal of Cleaner Production, 2020. **276**.
53. Gomez-Zavaglia, A., J.C. Mejuto, and J. Simal-Gandara, *Mitigation of emerging implications of climate change on food production systems.* Food Research International, 2020. **134**.
54. Schneider, P. and F. Asch, *Rice production and food security in Asian Mega deltas-A review on characteristics, vulnerabilities and agricultural adaptation options to cope with climate change.* Journal of Agronomy and Crop Science, 2020. **206**(4): p. 491-503.
55. Yang, L.S., et al., *Causality of climate, food production and conflict over the last two millennia in the Hexi Corridor, China.* Science of the Total Environment, 2020. **713**.
56. Gil, J., *Going to waste.* Nature Food, 2020. **1**(4): p. 192-192.
57. Fundation, E.M., *Cities and Circular Economy for Food* 2019.
58. Foundation, E.M. *What is a circular economy?* A framework for an economy that is restorative and regenerative by design 2017 [cited 2021 30/07/2021]; Available from: https://www.ellenmacarthurfoundation.org/circular-economy/concept.
59. Geissdoerfer, M., et al., *The Circular Economy–A new sustainability paradigm?* Journal of cleaner production, 2017. **143**: p. 757-768.
60. Macarthur, E. *The Circular Economy In Detail*. 2021 [cited 2021; Available from: https://www.ellenmacarthurfoundation.org/.
61. Swanepoel, S. *CIRCULAR ECONOMIES: WORKING LIKE NATURE FOR NATURE*. 2019; Available from: https://www.thebeachcoop.org/2019/07/21/circular-economies-working-like-nature-for-nature/.
62. Weenk, E. and R. Henzen, *Mastering the Circular Economy: A Practical Approach to the Circular Business Model Transformation*. 2021: Kogan Page.
63. Allwood, J.M., *Chapter 30 - Squaring the Circular Economy: The Role of Recycling within a Hierarchy of Material Management Strategies*, in *Handbook of Recycling*, E. Worrell and M.A. Reuter, Editors. 2014, Elsevier: Boston. p. 445-477.
64. Kirchherr, J., D. Reike, and M. Hekkert, *Conceptualizing the circular economy: An analysis of 114 definitions.* Resources, conservation and recycling, 2017. **127**: p. 221-232.
65. Thyberg, K.L. and D.J. Tonjes, *Drivers of food waste and their implications for sustainable policy development.* Resources, Conservation and Recycling, 2016. **106**: p. 110-123.
66. Gustavsson;, J., C. Cederberg;, and U. Sonesson;, *Global food losses and food waste – Extent, causes and prevention*. 2011, FAO: Rome.
67. Pang, W.C., et al., *Reducing greenhouse gas emissions and enhancing carbon and nitrogen conversion in food wastes by the black soldier fly.* Journal of Environmental Management, 2020. **260**.
68. Searchinger;, T., et al., *Creating a Sustainable Food Future—A Menu of Solutions to Feed Nearly 10 Billion People by 2050*. 2018, World Resources Institute.

69. Behera, S.K., et al., *Methane production from food waste leachate in laboratory-scale simulated landfill.* Waste Management, 2010. **30**(8-9): p. 1502-1508.
70. Zhang, W.L., L. Zhang, and A.M. Li, *Anaerobic co-digestion of food waste with MSW incineration plant fresh leachate: process performance and synergistic effects.* Chemical Engineering Journal, 2015. **259**: p. 795-805.
71. Adhikari, B.K., et al., *Characterization of food waste and bulking agents for composting.* Waste Management, 2008. **28**(5): p. 795-804.
72. De Marco, M., et al., *Nutritional value of two insect larval meals (Tenebrio molitor and Hermetia illucens) for broiler chickens: Apparent nutrient digestibility, apparent ileal amino acid digestibility and apparent metabolizable energy.* Animal Feed Science and Technology, 2015. **209**: p. 211-218.
73. Danieli, P.P., et al., *The Effects of Diet Formulation on the Yield, Proximate Composition, and Fatty Acid Profile of the Black Soldier Fly (Hermetia illucens L.) Prepupae Intended for Animal Feed.* Animals (Basel), 2019. **9**(4).
74. EPA, N., *Emissions impacts of landfilling food waste*, in *Fact sheet November 202*. 2022, NSW Environment Protection Authority: Australia.
75. Kaza, S., et al., *What a Waste 2.0: A Global Snapshot of Solid Waste Management to 2050*, in *What a Waste 2.0: A Global Snapshot of Solid Waste Management to 2050*. 2018.
76. Wikipedia, *Food waste process*.
77. Nordin, N.H., et al., *Reducing Food Waste: Strategies for Household Waste Management to Minimize the Impact of Climate Change and Contribute to Malaysia's Sustainable Development.* IOP Conference Series: Earth and Environmental Science, 2020. **479**: p. 012035.
78. Lewis, H., et al., *Food waste opportunities within the food wholesale and retail sectors.* 2017.
79. Byrne, D. and W.E. Smith, *Dangers in feeding waste material to livestock.* 2004.
80. Salemdeeb, R., et al., *Environmental and health impacts of using food waste as animal feed: a comparative analysis of food waste management options.* Journal of Cleaner Production, 2017. **140**: p. 871-880.
81. Ojha, S., S. Bußler, and O.K. Schlüter, *Food waste valorisation and circular economy concepts in insect production and processing.* Waste Management, 2020. **118**: p. 600-609.
82. Giannetto, A., et al., *Hermetia illucens (Diptera: Stratiomydae) larvae and prepupae: Biomass production, fatty acid profile and expression of key genes involved in lipid metabolism.* Journal of Biotechnology, 2020. **307**: p. 44-54.
83. Smetana, S., E. Schmitt, and A. Mathys, *Sustainable use of Hermetia illucens insect biomass for feed and food: Attributional and consequential life cycle assessment.* Resources Conservation and Recycling, 2019. **144**: p. 285-296.
84. Wong, C.Y., et al., *In-Situ Yeast Fermentation to Enhance Bioconversion of Coconut Endosperm Waste into Larval Biomass of Hermetia illucens: Statistical Augmentation of Larval Lipid Content.* Sustainability, 2020. **12**(4).
85. Byrne, J., *Report: Black soldier fly market will be worth US$2.57bn in 2030*. 2020, Feed Navigator.com.
86. Ramos-Elorduy, J., *Anthropo-entomophagy: Cultures, evolution and sustainability.* Entomological Research, 2009. **39**(5): p. 271-288.

87. Lensvelt, E.J.S. and L.P.A. Steenbekkers, *Exploring Consumer Acceptance of Entomophagy: A Survey and Experiment in Australia and the Netherlands.* Ecology of Food and Nutrition, 2014. **53**(5): p. 543-561.
88. Rudy Caparros Megido, L.S., Mélodie Geuens, Yves Brostaux, Taofic Alabi, Christophe Blecker, Didier Drugmand, Éric Haubruge, Frédéric Francis, *Edible Insects Acceptance by Belgian Consumers: Promising Attitude for Entomophagy Development.* Journal of Sensory Studies, 2014. **29**(1): p. 14-20.
89. Vane-Wright, R.I., *Why Not Eat Insects?* Bulletin of Entomological Research, 1991. **81**(1): p. 1-4.
90. Kavran, M., et al., *EDIBLE INSECTS - SAFE FOOD FOR HUMANS AND LIVESTOCK*, in *Ecological and Economic Significance of Fauna of Serbia*, R. Petanovic, Editor. 2018. p. 251-300.
91. Gordon, D.G., *The Eat-a-Bug Cookbook, Revised: 40 Ways to Cook Crickets, Grasshoppers, Ants, Water Bugs, Spiders, Centipedes, and Their Kin*. 1998, Berkely, CA, USA: Ten Speed Press.
92. D'Aluisio, F. and P. Menzel, *Man Eating Bugs: The Art and Science of Eating Insects*. 1998, Ten Speed Press: Berkeley, CA, USA.
93. Huis, A.v., H.v. Gurp, and M. Dicke, *The Insect Cookbook: Food for a Sustainable Planet*. 2014, New York, NY, USA: Columbia University Press.
94. Vantomme, P., et al., *Insects to feed the world conference: summary report, FAO/Wageningen University, Wageningen, the Netherlands*. 2014.
95. Halloran, A., R. Flore, and C. Mercier, *Notes from the 'Insects in a gastronomic context'workshop in Bangkok, Thailand.* Journal of Insects as Food and Feed, 2015. **1**(3): p. 241-243.
96. House, J., *Consumer acceptance of insect-based foods in the Netherlands: Academic and commercial implications.* Appetite, 2016. **107**: p. 47-58.
97. IPIFF, *Guide on Good Hygiene Practices for Europen Union (EU) prodicers of insects as food and feed*, IPIFF, Editor. 2020.
98. Oonincx, D.G., et al., *Feed conversion, survival and development, and composition of four insect species on diets composed of food by-products.* PloS one, 2015. **10**(12): p. e0144601.
99. Van Huis, A., *Potential of insects as food and feed in assuring food security.* Annual review of entomology, 2013. **58**: p. 563-583.
100. Costa-Neto, E.M., *Insects as human food: an overview.* Amazônica-Revista de Antropologia, 2014. **5**(3): p. 562-582.
101. Oonincx, D.G., et al., *An exploration on greenhouse gas and ammonia production by insect species suitable for animal or human consumption.* PloS one, 2010. **5**(12): p. e14445.
102. Wikipedia. *Hermetia illucens*. 2020 [cited 2020; Available from: https://en.wikipedia.org/wiki/Hermetia_illucens.
103. Savonen, C., *Big maggots in your compost? They're soldier fly larvae*, in *OSU Extension Service– Gardening*. 2005.
104. Sheppard, C., *House fly and lesser fly control utilizing the black soldier fly in manure management systems for caged laying hens.* Environmental entomology, 1983. **12**(5): p. 1439-1442.
105. Green, T.R. and R. Popa, *Enhanced ammonia content in compost leachate processed by black soldier fly larvae.* Applied biochemistry and biotechnology, 2012. **166**(6): p. 1381-1387.

106. Lalander, C., et al., *Faecal sludge management with the larvae of the black soldier fly (Hermetia illucens)—From a hygiene aspect.* Science of the Total Environment, 2013. **458**: p. 312-318.
107. Bortolini, S., et al., *Hermetia illucens (L.) larvae as chicken manure management tool for circular economy.* Journal of Cleaner Production, 2020. **262**.
108. El-Dakar, M.A., et al., *Bioaccumulation of residual omega-3 fatty acids from industrial Schizochytrium microalgal waste using black soldier fly (Hermetia illucens) larvae.* Journal of Cleaner Production, 2020. **268**.
109. Gao, Z.H., et al., *Bioconversion performance and life table of black soldier fly (Hermetia illucens) on fermented maize straw.* Journal of Cleaner Production, 2019. **230**: p. 974-980.
110. Li, W., et al., *Efficient bioconversion of organic wastes to value-added chemicals by soaking, black soldier fly (Hermetia illucens L.) and anaerobic fermentation.* Journal of Environmental Management, 2018. **227**: p. 267-276.
111. Paz, A.S.P., N.S. Carrejo, and C.H.G. Rodriguez, *Effects of Larval Density and Feeding Rates on the Bioconversion of Vegetable Waste Using Black Soldier Fly Larvae Hermetia illucens (L.), (Diptera: Stratiomyidae).* Waste and Biomass Valorization, 2015. **6**(6): p. 1059-1065.
112. Nguyen, T.T., J.K. Tomberlin, and S. Vanlaerhoven, *Ability of black soldier fly (Diptera: Stratiomyidae) larvae to recycle food waste.* Environmental entomology, 2015. **44**(2): p. 406-410.
113. Kim, W., et al., *Biochemical characterization of digestive enzymes in the black soldier fly, Hermetia illucens (Diptera: Stratiomyidae).* Journal of Asia-Pacific Entomology, 2011. **14**(1): p. 11-14.
114. Li, Q., et al., *Bioconversion of dairy manure by black soldier fly (Diptera: Stratiomyidae) for biodiesel and sugar production.* Waste management, 2011. **31**(6): p. 1316-1320.
115. Nguyen, H.C., et al., *Lipase-catalyzed synthesis of biodiesel from black soldier fly (Hermetica illucens): Optimization by using response surface methodology.* Energy Conversion and Management, 2017. **145**: p. 335-342.
116. Mohd-Noor, S.-N., et al., *Optimization of self-fermented period of waste coconut endosperm destined to feed black soldier fly larvae in enhancing the lipid and protein yields.* Renewable Energy, 2017. **111**: p. 646-654.
117. Sheppard, D.C., et al., *A value added manure management system using the black soldier fly.* Bioresource technology, 1994. **50**(3): p. 275-279.
118. Diener, S., et al., *Biological treatment of municipal organic waste using black soldier fly larvae.* Waste and Biomass Valorization, 2011. **2**(4): p. 357-363.
119. Veldkamp, T. and G. Bosch, *Insects: A protein-rich feed ingredient in pig and poultry diets.* Animal Frontiers, 2015. **5**(2): p. 45-50.
120. Meneguz, M., et al., *Effect of rearing substrate on growth performance, waste reduction efficiency and chemical composition of black soldier fly (Hermetia illucens) larvae.* Journal of the Science of Food and Agriculture, 2018. **98**(15): p. 5776-5784.
121. Smets, R., et al., *Sequential Extraction and Characterisation of Lipids, Proteins, and Chitin from Black Soldier Fly (Hermetia illucens) Larvae, Prepupae, and Pupae.* Waste and Biomass Valorization, 2020. **11**(12): p. 6455-6466.

122. Rabani, V., H. Cheatsazan, and S. Davani, *Proteomics and Lipidomics of Black Soldier Fly (Diptera: Stratiomyidae) and Blow Fly (Diptera: Calliphoridae) Larvae.* Journal of insect science (Online), 2019. **19**(3): p. 29.
123. Barroso, F.G., et al., *Insects as food: Enrichment of larvae of Hermetia illucens with omega 3 fatty acids by means of dietary modifications.* Journal of Food Composition and Analysis, 2017. **62**: p. 8-13.
124. Hoc, B., et al., *About lipid metabolism in Hermetia illucens (L. 1758): on the origin of fatty acids in prepupae.* Scientific Reports, 2020. **10**(1).
125. Mai, H.C., et al., *Purification Process, Physicochemical Properties, and Fatty Acid Composition of Black Soldier Fly (Hermetia illucens Linnaeus) Larvae Oil.* Journal of the American Oil Chemists Society, 2019. **96**(11): p. 1303-1311.
126. Truzzi, C., et al., *Fatty acids profile of black soldier fly (Hermetia illucens): Influence of feeding substrate based on coffee-waste silverskin enriched with microalgae.* Animal Feed Science and Technology, 2020. **259**.
127. Truzzi, C., et al., *Fatty acids profile of black soldier fly (Hermetia illucens): Influence of feeding substrate based on coffee-waste silverskin enriched with microalgae.* Animal Feed Science and Technology, 2020. **259**: p. 114309.
128. Oonincx, D.G.A.B., et al., *Dietary enrichment of edible insects with omega 3 fatty acids.* Insect Science, 2020. **27**(3): p. 500-509.
129. Hoc, B., et al., *About lipid metabolism in Hermetia illucens (L. 1758): on the origin of fatty acids in prepupae.* Scientific Reports, 2020. **10**(1): p. 11916.
130. Liland, N.S., et al., *Modulation of nutrient composition of black soldier fly (Hermetia illucens) larvae by feeding seaweed-enriched media.* PLoS ONE, 2017. **12**(8).
131. Caligiani, A., et al., *Influence of the killing method of the black soldier fly on its lipid composition.* Food Research International, 2019. **116**: p. 276-282.
132. Ravi, H.K., et al., *Effect of devitalization techniques on the lipid, protein, antioxidant, and chitin fractions of black soldier fly (Hermetia illucens) larvae.* European Food Research and Technology, 2020.
133. Matthäus, B., et al., *Renewable Resources from Insects: Exploitation, Properties, and Refining of Fat Obtained by Cold-Pressing from Hermetia illucens (Black Soldier Fly) Larvae.* European Journal of Lipid Science and Technology, 2019. **121**(7).
134. Raksasat, R., et al., *A review of organic waste enrichment for inducing palatability of black soldier fly larvae: Wastes to valuable resources.* Environmental Pollution, 2020: p. 115488.
135. Spranghers, T., et al., *Nutritional composition of black soldier fly (Hermetia illucens) prepupae reared on different organic waste substrates.* Journal of the Science of Food and Agriculture, 2017. **97**(8): p. 2594-2600.
136. Wong, C.Y., et al., *Potential Protein and Biodiesel Sources from Black Soldier Fly Larvae: Insights of Larval Harvesting Instar and Fermented Feeding Medium.* Energies, 2019. **12**(8).
137. Nitbani, F.O., et al., *Antimicrobial Properties of Lauric Acid and Monolaurin in Virgin Coconut Oil: A Review.* ChemBioEng Reviews, 2022. **9**(5): p. 442-461.
138. Kim, Y.B., et al., *Black soldier fly larvae oil as an alternative fat source in broiler nutrition.* Poultry Science, 2020. **99**(6): p. 3133-3143.
139. Fawole, F.J., et al., *Insect (black soldier fly larvae) oil as a potential substitute for fish or soy oil in the fish meal-based diet of juvenile rainbow trout (Oncorhynchus mykiss).* Animal Nutrition, 2021. **7**(4): p. 1360-1370.

140. Dayrit, F.M., *The Properties of Lauric Acid and Their Significance in Coconut Oil.* Journal of the American Oil Chemists' Society, 2015. **92**(1): p. 1-15.
141. Silalahi, J., et al., *The activity of hydrolyzed virgin coconut oil to increase proliferation and cyclooxygenase-2 expression towards on nih 3t3 cell line in wound healing process.* Open Access Macedonian Journal of Medical Sciences, 2019. **7**(19): p. 3164-3168.
142. Cummins, V.C., et al., *Evaluation of black soldier fly (Hermetia illucens) larvae meal as partial or total replacement of marine fish meal in practical diets for Pacific white shrimp (Litopenaeus vannamei).* Aquaculture, 2017. **473**: p. 337-344.
143. Kawasaki, K., et al., *Evaluation of Black Soldier Fly (Hermetia illucens) Larvae and Pre-Pupae Raised on Household Organic Waste, as Potential Ingredients for Poultry Feed.* Animals, 2019. **9**(3).
144. van Heugten, E., et al., *Black soldier fly (Hermetia illucens) larvae oil improves growth performance of nursery pigs.* Journal of Animal Science, 2019. **97**: p. 118-118.
145. Saputra, I. and Y.N. Lee, *Nutrition composition of commercial full-fat and defatted black soldier fly larvae meal (Hermetia illucens) as a potential protein resource for aquafeeds.* Biodiversitas, 2023. **24**(9): p. 4877-4884.
146. Mertenat, A., S. Diener, and C. Zurbrügg, *Black Soldier Fly biowaste treatment – Assessment of global warming potential.* Waste Management, 2019. **84**: p. 173-181.
147. Wasko, A., et al., *The first report of the physicochemical structure of chitin isolated from Hermetia illucens.* International Journal of Biological Macromolecules, 2016. **92**: p. 316-320.
148. Young, V.R. and P.L. Pellett, *Protein Evaluation, Amino Acid Scoring and the Food and Drug Administration's Proposed Food Labeling Regulations.* The Journal of Nutrition, 1991. **121**(1): p. 145-150.
149. Wang, S.Y., et al., *Reproductive Potential and Nutritional Composition of Hermetia illucens (Diptera: Stratiomyidae) Prepupae Reared on Different Organic Wastes.* Journal of Economic Entomology, 2019. **113**(1): p. 527-537.
150. Liu, X., et al., *Dynamic changes of nutrient composition throughout the entire life cycle of black soldier fly.* PLOS ONE, 2017. **12**(8): p. e0182601.
151. Purkayastha, D. and S. Sarkar, *Physicochemical Structure Analysis of Chitin Extracted from Pupa Exuviae and Dead Imago of Wild Black Soldier Fly (Hermetia illucens).* Journal of Polymers and the Environment, 2020. **28**(2): p. 445-457.
152. Ahmadi, F., et al., *Chitosan based hydrogels: Characteristics and pharmaceutical applications.* Research in Pharmaceutical Sciences, 2015. **10**(1): p. 1-16.
153. Hamidi, M., A. Azadi, and P. Rafiei, *Hydrogel nanoparticles in drug delivery.* Advanced drug delivery reviews, 2008. **60**(15): p. 1638-1649.
154. Shi, W., Y.C. Ching, and C.H. Chuah, *Preparation of aerogel beads and microspheres based on chitosan and cellulose for drug delivery: A review.* International Journal of Biological Macromolecules, 2021. **170**: p. 751-767.
155. Javadi, E., et al., *Removal of 4-nonylphenol from Surface Water and Municipal Wastewater Effluent Using Three-Dimensional Graphene Oxide–Chitosan Aerogel Beads.* International Journal of Environmental Research, 2020. **14**(5): p. 513-526.
156. Wikipedia. *Tissue Engineering*. 2021; Available from: https://en.wikipedia.org/wiki/Tissue_engineering.
157. Shin, D., et al., *Scalable variable-index elasto-optic metamaterials for macroscopic optical components and devices.* Nature Communications, 2017. **8**(1): p. 16090.

158. Cao, F., L. Ren, and X. Li, *Synthesis of high strength monolithic alumina aerogels at ambient pressure.* RSC Advances, 2015. **5**(23): p. 18025-18028.
159. Kiselev, G.O., et al., *Upconversion metal (Zr, Hf, and Ta) oxide aerogels.* Chemical Communications, 2019. **55**(56): p. 8174-8177.
160. Kong, Y., X.-D. Shen, and S. Cui, *Direct synthesis of anatase TiO2 aerogel resistant to high temperature under supercritical ethanol.* Materials Letters, 2014. **117**: p. 192-194.
161. Huang, Y.-J., et al., *A Pt-free pristine monolithic carbon aerogel counter electrode for dye-sensitized solar cells: up to 20% under dim light illumination.* Nanoscale, 2019. **11**(26): p. 12507-12516.
162. Zhan, W., et al., *Green synthesis of amino-functionalized carbon nanotube-graphene hybrid aerogels for high performance heavy metal ions removal.* Applied Surface Science, 2019. **467-468**: p. 1122-1133.
163. Jiang, Y., S. Chowdhury, and R. Balasubramanian, *New insights into the role of nitrogen-bonding configurations in enhancing the photocatalytic activity of nitrogen-doped graphene aerogels.* Journal of Colloid and Interface Science, 2019. **534**: p. 574-585.
164. Jiang, Y., et al., *Direct 3D Printing of Ultralight Graphene Oxide Aerogel Microlattices.* Advanced Functional Materials, 2018. **28**(16): p. 1707024.
165. He, S., et al., *Rapid and facile synthesis of a low-cost monolithic polyamide aerogel via sol–gel technology.* Materials Letters, 2015. **144**: p. 82-84.
166. Shinko, A., S.C. Jana, and M.A. Meador, *Crosslinked polyurea-co-polyurethane aerogels with hierarchical structures and low stiffness.* Journal of Non-Crystalline Solids, 2018. **487**: p. 19-27.
167. Wang, C., H. Jeon, and N.-Y. Kim, *A compact spiral-coupled directional coupler for a mobile RFID reader via integrated passive technology.* Microwave and Optical Technology Letters, 2015. **57**(9): p. 2142-2146.
168. El-Zawahry, M.M., et al., *Preparation and use of aqueous solutions magnetic chitosan / nanocellulose aerogels for the sorption of reactive black 5.* Biointerface Research in Applied Chemistry, 2021. **11**(4): p. 12380-12402.
169. Zhu, Y., et al., *An effective, green and mild deproteinization method for polysaccharides of Ruditapes philippinarum by attapulgite-based silk fibroin composite aerogel.* International Journal of Biological Macromolecules, 2021. **182**: p. 343-353.
170. Nyce, G.W., et al., *Synthesis and Characterization of Hierarchical Porous Gold Materials.* Chemistry of Materials, 2007. **19**(3): p. 344-346.
171. Georgi, M., et al., *A versatile ethanolic approach to metal aerogels (Pt, Pd, Au, Ag, Cu and Co).* Materials Chemistry Frontiers, 2019. **3**(8): p. 1586-1592.
172. Rousseas, M., et al., *Synthesis of Highly Crystalline sp2-Bonded Boron Nitride Aerogels.* ACS Nano, 2013. **7**(10): p. 8540-8546.
173. Demirtaş, T.T., G. Irmak, and M. Gümüşderelioğlu, *A bioprintable form of chitosan hydrogel for bone tissue engineering.* Biofabrication, 2017. **9**(3): p. 035003.
174. Bergonzi, C., et al., *Study of 3D-printed chitosan scaffold features after different post-printing gelation processes.* Scientific Reports, 2019. **9**(1).
175. Deng, Z., T. Qian, and F. Hang, *Three-Dimensional Printed Hydrogels with High Elasticity, High Toughness, and Ionic Conductivity for Multifunctional Applications.* ACS Biomaterials Science and Engineering, 2020. **6**(12): p. 7061-7070.

176. Ilhan, E., et al., *Fabrication of tissue-engineered tympanic membrane patches using 3D-Printing technology.* Journal of the Mechanical Behavior of Biomedical Materials, 2021. **114**: p. 104219.
177. Wang, Y., et al., *Preparation, characterization, and 3D printing verification of chitosan/halloysite nanotubes/tea polyphenol nanocomposite films.* International Journal of Biological Macromolecules, 2021. **166**: p. 32-44.
178. Wu, X., et al., *3D printed chitosan-gelatine hydrogel coating on titanium alloy surface as biological fixation interface of artificial joint prosthesis.* International Journal of Biological Macromolecules, 2021. **182**: p. 669-679.
179. Liu, Y., et al., *Dual cure (thermal/photo) composite hydrogel derived from chitosan/collagen for in situ 3D bioprinting.* International Journal of Biological Macromolecules, 2021. **182**: p. 689-700.
180. Cleymand, F., et al., *Development of novel chitosan / guar gum inks for extrusion-based 3D bioprinting: Process, printability and properties.* Bioprinting, 2021. **21**.
181. Sanandiya, N.D., et al., *Circular manufacturing of chitinous bio-composites via bioconversion of urban refuse.* Scientific Reports, 2020. **10**(1): p. 4632.
182. Chia, S.Y., et al., *Nutritional composition of black soldier fly larvae feeding on agro-industrial by-products.* Entomologia Experimentalis et Applicata, 2020. **168**(6-7): p. 472-481.
183. Directive, E., *EC of the European Parliament and of the Council of 7 May 2002 on undesirable substances in animal feed*. 2002, Off. J. Eur. Comm.
184. Finke, M.D., *Complete Nutrient Content of Four Species of Feeder Insects.* Zoo Biology, 2013. **32**(1): p. 27-36.
185. Boykin, K.L. and M.A. Mitchell, *Evaluation of vitamin A gut loading in black soldier fly larvae (Hermetia illucens).* Zoo Biology, 2020.
186. Mohan, K., et al., *Recent insights into the extraction, characterization, and bioactivities of chitin and chitosan from insects.* Trends in Food Science & Technology, 2020. **105**: p. 17-42.
187. Laroche, M., et al., *Comparison of Conventional and Sustainable Lipid Extraction Methods for the Production of Oil and Protein Isolate from Edible Insect Meal.* Foods (Basel, Switzerland), 2019. **8**(11): p. 572.
188. Folch, J., M. Lees, and G.H. Sloane Stanley, *A simple method for the isolation and purification of total lipides from animal tissues.* The Journal of biological chemistry, 1957. **226**(1): p. 497-509.
189. Laitinen, A., *Supercritical fluid extraction of organic compounds from solids and aqueous solutions*. 1999: Technical Research Centre of Finland VTT: Finland.
190. Rao, M.S., J. Muñoz, and W.F. Stevens, *Critical factors in chitin production by fermentation of shrimp biowaste.* Applied Microbiology and Biotechnology, 2000. **54**(6): p. 808-813.
191. Oh, Y.-S., et al., *Protease produced by Pseudomonas aeruginosa K-187 and its application in the deproteinization of shrimp and crab shell wastes.* Enzyme and Microbial Technology, 2000. **27**(1): p. 3-10.
192. Yang, J.-K., et al., *Production and purification of protease from a Bacillus subtilis that can deproteinize crustacean wastes ☆.* Enzyme and Microbial Technology, 2000. **26**(5): p. 406-413.
193. Wang, Y.S. and M. .Shelomi, *Review of Black Soldier Fly (Hermetia illucens) as Animal Feed and Human Food.* Foods, 2017. **6**(10).

194. Oonincx, D.G.A.B., et al., *Feed Conversion, Survival and Development, and Composition of Four Insect Species on Diets Composed of Food By-Products.* PLOS ONE, 2015. **10**(12): p. e0144601.
195. Grubb, G. 2018; Available from: https://gourmetgrubb.com/.
196. Hardy, K. *Hop into a BentSpoke beer made of crickets and flies*. 2019; Available from: https://www.canberratimes.com.au/story/6504715/hop-into-a-beer-made-of-crickets-and-flies/.
197. Sanandiya, N.D., et al., *Circular manufacturing of chitinous bio-composites via bioconversion of urban refuse.* Scientific Reports, 2020. **10**(1).
198. Bix, B. 2019; Available from: https://www.buggybix.com.au/products/buggy-bix.
199. Griopro. *Premium Cricket Powder*. 2016; Available from: https://cricketpowder.com/shop/finely-milled-whole-cricket-powder/.
200. Askew, K. *Bugfoundation's vision: To change the eating habits of a whole continent*. 2018 [cited 2021; Available from: https://www.foodnavigator.com/Article/2018/10/12/Bugfoundation-s-vision-To-change-the-eating-habits-of-a-whole-continent?utm_source=copyright&utm_medium=OnSite&utm_campaign=copyright.
201. Multivone. Available from: https://www.multivores.com/en/edible-insects-united-kingdom/72-pasta-crickets.html.
202. Moher D, L.A., Tetzlaff J, Altman DG, *Preferred reporting items for systematic reviews and meta-analyses: The PRISMA statement.* PLoS Medicine, 2009. **6(7): e1000097. doi:10.1371/journal.pmed.1000097**.
203. AOC, *Official Methods of Analysis of the Association of Official Analytical Chemist*. 15th Edition ed. 1990: Association of Official Analytical Chemistd.Inc.
204. Mosmann, T., *Rapid colorimetric assay for cellular growth and survival: Application to proliferation and cytotoxicity assays.* Journal of Immunological Methods, 1983. **65**(1): p. 55-63.
205. D'Hondt, E., et al., *Simplified determination of the content and average degree of acetylation of chitin in crude black soldier fly larvae samples.* Carbohydrate Research, 2020. **488**.
206. Soetemans, L., M. Uyttebroek, and L. Bastiaens, *Characteristics of chitin extracted from black soldier fly in different life stages.* International Journal of Biological Macromolecules, 2020. **165**: p. 3206-3214.
207. Yang, B., et al., *Preparation and characterization of a novel chitosan scaffold.* Carbohydrate Polymers, 2010. **80**(3): p. 860-865.
208. Porstmann, B., et al., *Measurement of lysozyme in human body fluids: Comparison of various enzyme immunoassay techniques and their diagnostic application.* Clinical Biochemistry, 1989. **22**(5): p. 349-355.
209. Sacks, F.M., et al., *Dietary Fats and Cardiovascular Disease: A Presidential Advisory From the American Heart Association.* Circulation, 2017. **136**(3): p. e1-e23.
210. Roselló-Soto, E., et al., *Evaluating the impact of supercritical-CO2 pressure on the recovery and quality of oil from "horchata" by-products: Fatty acid profile, α-tocopherol, phenolic compounds, and lipid oxidation parameters.* Food Research International, 2019. **120**: p. 888-894.
211. Satyannarayana, S., et al., *Process optimization for the supercritical carbon dioxide (SC-CO<inf>2</inf>) extraction of wheat germ oil with respect to yield, and*

phosphorous and tocol contents using a Box Behnken design. Grasas y Aceites, 2018. **69**(3).
212. Norodin, N.S.M., et al. *Supercritical carbon dioxide (SC-CO2) extraction of essential oil from Swietenia mahagoni seeds*. in *IOP Conference Series: Materials Science and Engineering*. 2016.
213. de Lucas, A., J. Rincón, and I. Gracia, *Influence of operation variables on quality parameters of olive husk oil extracted with CO2: Three-step sequential extraction.* Journal of the American Oil Chemists' Society, 2003. **80**(2): p. 181-188.
214. Nitbani, F.O., et al., *Antimicrobial Properties of Lauric Acid and Monolaurin in Virgin Coconut Oil: A Review.* ChemBioEng Reviews, 2022.
215. Temme, E.H., R.P. Mensink, and G. Hornstra, *Comparison of the effects of diets enriched in lauric, palmitic, or oleic acids on serum lipids and lipoproteins in healthy women and men.* The American Journal of Clinical Nutrition, 1996. **63**(6): p. 897-903.
216. Alves, N.F.B., et al., *Acute Treatment with Lauric Acid Reduces Blood Pressure and Oxidative Stress in Spontaneously Hypertensive Rats.* Basic and Clinical Pharmacology and Toxicology, 2017. **120**(4): p. 348-353.
217. Lappano, R., et al., *The lauric acid-activated signaling prompts apoptosis in cancer cells.* Cell Death Discovery, 2017. **3**(1): p. 17063.
218. Uday Kumar D, C.V., Sobarani D, Nagendra Sastry Y, *Lauric Acid as Potential Natural Product in the Treatment of Cardiovascular Disease: A Review.* Journal of Bioanalysis & Biomedicine, 2014. **6**: p. 037 - 039.
219. DiNicolantonio, J.J. and J.H. O'Keefe, *Effects of dietary fats on blood lipids: a review of direct comparison trials.* Open heart, 2018. **5**(2): p. e000871-e000871.
220. Rozycki, M., et al., *The fate of the primary cilium during myofibroblast transition.* Molecular biology of the cell, 2014. **25**(5): p. 643-657.
221. Rahimi, A.M., M. Cai, and S. Hoyer-Fender, *Heterogeneity of the NIH3T3 Fibroblast Cell Line.* Cells, 2022. **11**(17).
222. Singer, A.J. and R.A. Clark, *Cutaneous wound healing.* New England journal of medicine, 1999. **341**(10): p. 738-746.
223. Mai, H.C., et al., *Purification Process, Physicochemical Properties, and Fatty Acid Composition of Black Soldier Fly (Hermetia illucens Linnaeus) Larvae Oil.* JAOCS, Journal of the American Oil Chemists' Society, 2019. **96**(11): p. 1303-1311.
224. van de Voort, F.R., J. Sedman, and T. Russin, *Lipid analysis by vibrational spectroscopy.* European Journal of Lipid Science and Technology, 2001. **103**(12): p. 815-826.
225. Ramya, V., et al., *Dual Roles of Coconut Oil and Its Major Component Lauric Acid on Redox Nexus: Focus on Cytoprotection and Cancer Cell Death.* Frontiers in Neuroscience, 2022. **16**.
226. Almeida, C., et al., *Characterization of lipid extracts from the Hermetia illucens larvae and their bioactivities for potential use as pharmaceutical and cosmetic ingredients.* Heliyon, 2022. **8**(5).
227. Koh, Y.G., et al., *Efficacy and safety of oral palmitoleic acid supplementation for skin barrier improvement: A 12-week, randomized, double-blinded, placebo-controlled study.* Heliyon, 2023. **9**(6).
228. Lin, T.K., L. Zhong, and J.L. Santiago, *Anti-inflammatory and skin barrier repair effects of topical application of some plant oils.* International Journal of Molecular Sciences, 2018. **19**(1).

229. Almeida, C., et al., *Characterization of lipid extracts from the Hermetia illucens larvae and their bioactivities for potential use as pharmaceutical and cosmetic ingredients.* Heliyon, 2022. **8**(5): p. e09455.
230. Marusich, E., et al., *Fatty Acids from Hermetia illucens Larvae Fat Inhibit the Proliferation and Growth of Actual Phytopathogens.* Microorganisms, 2020. **8**(9): p. 1423.
231. Waśko, A., et al., *The first report of the physicochemical structure of chitin isolated from Hermetia illucens.* International Journal of Biological Macromolecules, 2016. **92**: p. 316-320.
232. Wang, H., et al., *Physicochemical structure of chitin in the developing stages of black soldier fly.* International Journal of Biological Macromolecules, 2020. **149**: p. 901-907.
233. Bastiaens, L., et al., *Sources of Chitin and Chitosan and their Isolation*, in *Chitin and Chitosan: Properties and Application*. 2020, John Wiley & Sons Ltd: UK. p. 1-34.
234. Bhavsar, P.S., G. Dalla Fontana, and M. Zoccola, *Sustainable Superheated Water Hydrolysis of Black Soldier Fly Exuviae for Chitin Extraction and Use of the Obtained Chitosan in the Textile Field.* ACS Omega, 2021. **6**(13): p. 8884-8893.
235. Rinaudo, M., *Chitin and chitosan: Properties and applications.* Progress in Polymer Science, 2006. **31**(7): p. 603-632.
236. Ahmed, S., et al., *A review on chitosan centred scaffolds and their applications in tissue engineering.* International Journal of Biological Macromolecules, 2018. **116**: p. 849-862.
237. Cárdenas, G., et al., *Chitin characterization by SEM, FTIR, XRD, and 13C cross polarization/mass angle spinning NMR.* Journal of Applied Polymer Science, 2004. **93**(4): p. 1876-1885.
238. Ji, Y., et al., *DFT-Calculated IR Spectrum Amide I, II, and III Band Contributions of N-Methylacetamide Fine Components.* ACS Omega, 2020. **5**(15): p. 8572-8578.
239. Moosa, A., A. Ridha, and N. Kadim, *Use of Biopolymer Adsorbent in the Removal of Phenol from Aqueous Solution.* American Journal of Materials Science 2016, 6(4): 95-104, 2016. **2016**: p. 95-104.
240. Varun, T.K., et al., *Extraction of chitosan and its oligomers from shrimp shell waste, their characterization and antimicrobial effect.* Vet World, 2017. **10**(2): p. 170-175.
241. Kaya, M., et al., *Changes in physicochemical properties of chitin at developmental stages (larvae, pupa and adult) of Vespa crabro (wasp).* Carbohydrate Polymers, 2016. **145**: p. 64-70.
242. Sajomsang, W. and P. Gonil, *Preparation and characterization of α-chitin from cicada sloughs.* Materials Science and Engineering C, 2010. **30**(3): p. 357-363.
243. Khayrova, A., S. Lopatin, and V. Varlamov, *Black Soldier Fly Hermetia illucens as a Novel Source of Chitin and Chitosan.* International Journal of Sciences, 2019. **8**(04): p. 81-86.
244. Lee, Y.H., et al., *Chitosan isolated from black soldier flies Hermetia illucens: Structure and enzymatic hydrolysis.* Process Biochemistry, 2022. **118**: p. 171-181.
245. Sadeghianmaryan, A., et al., *Extrusion-based printing of chitosan scaffolds and their in vitro characterization for cartilage tissue engineering.* International Journal of Biological Macromolecules, 2020. **164**: p. 3179-3192.
246. Nieto-Suárez, M., M.A. López-Quintela, and M. Lazzari, *Preparation and characterization of crosslinked chitosan/gelatin scaffolds by ice segregation induced self-assembly.* Carbohydrate Polymers, 2016. **141**: p. 175-183.

247. Du, J.R., et al., *Using genipin as a "green" crosslinker to fabricate chitosan membranes for pervaporative dehydration of isopropanol.* Separation and Purification Technology, 2020. **244**: p. 116843.
248. Peppas, N.A., B.V. Slaughter, and M.A. Kanzelberger, *9.20 - Hydrogels*, in *Polymer Science: A Comprehensive Reference*, K. Matyjaszewski and M. Möller, Editors. 2012, Elsevier: Amsterdam. p. 385-395.
249. Sharma, S., et al., *Biocompatible Polymers and Their Applications*, in *Encyclopedia of Materials: Plastics and Polymers*, M.S.J. Hashmi, Editor. 2022, Elsevier: Oxford. p. 796-819.
250. Ozcelik, B., *7 - Degradable hydrogel systems for biomedical applications*, in *Biosynthetic Polymers for Medical Applications*, L. Poole-Warren, P. Martens, and R. Green, Editors. 2016, Woodhead Publishing. p. 173-188.
251. Tagrida, M., et al., *Fish gelatin/chitosan blend films incorporated with betel (Piper betle L.) leaf ethanolic extracts: Characteristics, antioxidant and antimicrobial properties.* Food Hydrocolloids, 2023. **137**: p. 108316.
252. Qiao, C., et al., *Molecular interactions in gelatin/chitosan composite films.* Food Chemistry, 2017. **235**: p. 45-50.
253. Martínez-Mejía, G., et al., *Synthesis of new chitosan-glutaraldehyde scaffolds for tissue engineering using Schiff reactions.* Colloids and Surfaces A: Physicochemical and Engineering Aspects, 2019. **579**: p. 123658.
254. Pradal, C., et al., *Improvement of the wet tensile properties of nanostructured hydroxyapatite and chitosan biocomposite films through hydrophobic modification.* Journal of Materials Chemistry, 2011. **21**(7): p. 2330-2337.
255. Farris, S., J. Song, and Q. Huang, *Alternative reaction mechanism for the cross-linking of gelatin with glutaraldehyde.* Journal of Agricultural and Food Chemistry, 2010. **58**(2): p. 998-1003.
256. Queiroz, M.F., et al., *Does the use of chitosan contribute to oxalate kidney stone formation?* Marine Drugs, 2015. **13**(1): p. 141-158.
257. Ostrowska-Czubenko, J. and M. Gierszewska-Druzyńska, *Effect of ionic crosslinking on the water state in hydrogel chitosan membranes.* Carbohydrate Polymers, 2009. **77**(3): p. 590-598.
258. Ghosh, T., R. Deveswaran, and S. Bharath, *Copper crosslinked carboxymethyl chitosan–gelatin scaffolds: A potential antibacterial and cytocompatible material for biomedical applications.* Materials Today: Proceedings, 2022. **59**: p. 31-38.
259. Kim, S., et al., *Chitosan–Lysozyme Conjugates for Enzyme-Triggered Hydrogel Degradation in Tissue Engineering Applications.* ACS Applied Materials & Interfaces, 2018. **10**(48): p. 41138-41145.